

**The Role of NSAID-Induced ER Stress and Immunomodulation in the Suppression of  
Colorectal Tumorigenesis**

by

**Rochelle E. Fletcher**

Bachelor of Arts in Biology and Chemistry, Wesleyan College, 2013

Submitted to the Graduate Faculty of  
the School of Medicine in partial fulfillment of  
the requirements for the degree of  
Doctor of Philosophy

University of Pittsburgh

2018

UNIVERSITY OF PITTSBURGH

SCHOOL OF MEDICINE

This dissertation was presented

by

Rochelle E. Fletcher

It was defended on

April 9, 2018

and approved by

Thomas Kensler, PhD, Department of Pharmacology and Chemical Biology

Donna Stolz, PhD, Department of Cell Biology and Molecular Physiology

Roddy O'Sullivan, PhD, Pharmacology and Chemical Biology

Jane Wang, PhD, Pharmacology and Chemical Biology

Dissertation Advisor: Lin Zhang, PhD, Pharmacology and Chemical Biology

Copyright © by Rochelle E. Fletcher

2018

# **The Role of NSAID-Induced ER Stress and Immunomodulation in the Suppression of Colorectal Tumorigenesis**

Rochelle E. Fletcher, PhD

University of Pittsburgh, 2018

Prevention or early detection represents a key approach for reducing the mortality and morbidity of colorectal cancer (CRC). Use of non-steroidal anti-inflammatory drugs (NSAIDs) has been associated with decreased risk of CRC in numerous epidemiological studies, clinical trials, and animal model studies. However, the mechanism by which NSAIDs suppress colorectal tumorigenesis has remained unclear. We previously demonstrated that the chemopreventive effect of NSAIDs is mediated by a synthetic lethal interaction between death receptor signaling and loss of the gatekeeper *APC* tumor suppressor, which is dependent on the BH3-only Bcl-2 family member BID. In this study, we found a critical role of endoplasmic reticulum (ER) stress upstream of death receptor signaling and BID activation. Elevated levels of ER stress and cell death markers were detected in advanced adenomas from patients taking NSAIDs including aspirin. Inhibiting ER stress using a pharmacological approach abolished the apoptotic effect of NSAIDs in CRC cells and normal colonic epithelial cells with *APC* loss and also suppressed the chemopreventive activity of the NSAID sulindac in *APC*<sup>Min/+</sup> mice. Importantly, our results unveiled a critical role of ER stress and BID-dependent cell death in triggering immune-mediated elimination of nascent cells that lose *APC*. Markers of immunogenic cell death (ICD), including plasma membrane translocation of calreticulin and phagocytosis by dendritic cells, were suppressed in cells with *BID* knockout or ER stress inhibition. *BID* knockout or ER stress inhibition also reduced tumor-infiltrating lymphocytes (TILs) in sulindac-treated *APC*<sup>Min/+</sup> mice. Collectively, our results suggest that NSAIDs suppress

colorectal tumorigenesis by enhancing immunosurveillance through ER stress and BID-dependent ICD. These results provide novel insight into the chemopreventive mechanism of NSAIDs, which may help to design more effective chemopreventive strategies and agents.

## TABLE OF CONTENTS

<b>PREFACE.....</b>	<b>XV</b>
<b>1.0 INTRODUCTION.....</b>	<b>1</b>
<b>1.1 COLORECTAL CANCER.....</b>	<b>2</b>
<b>1.2 COLORECTAL CANCER AND PREVENTION .....</b>	<b>2</b>
<b>1.3 CHEMOPREVENTION .....</b>	<b>4</b>
<b>1.4 NSAIDS AND CHEMOPREVENTION.....</b>	<b>5</b>
<b>1.5 EXTRINSIC AND INTRINSIC APOPTOSIS.....</b>	<b>5</b>
<b>2.0 THE ROLE OF ER STRESS IN CHEMOPREVENTION .....</b>	<b>8</b>
<b>2.1 INTRODUCTION .....</b>	<b>8</b>
<b>2.1.1 Mechanisms of ER Stress Induction .....</b>	<b>8</b>
<b>2.1.2 ER Stress and NSAIDs .....</b>	<b>8</b>
<b>2.1.3 Targeting Apoptosis in NSAID-Induced Chemoprevention.....</b>	<b>12</b>
<b>2.2 MATERIALS AND METHODS .....</b>	<b>12</b>
<b>2.2.1 Cell Culture and Drug Treatment.....</b>	<b>12</b>
<b>2.2.2 Western Blotting .....</b>	<b>13</b>
<b>2.2.3 Reverse-Transcriptase (RT) and Quantitative PCR .....</b>	<b>13</b>
<b>2.2.4 Transmission Electron Microscopy (TEM) and Immuno-TEM .....</b>	<b>14</b>
<b>2.2.4.1 Transmission Electron Microscopy (TEM).....</b>	<b>14</b>

2.2.4.2	LR White Resin IEM Method: Immuno-TEM.....	14
2.2.5	Analysis of Patient Colonic Polyp Samples .....	15
2.2.6	Immunofluorescence (IF) .....	15
2.2.6.1	Human Tissues. ....	15
2.2.6.2	Human Cells. ....	16
2.2.7	Statistical Analysis .....	16
2.3	<b>RESULTS</b> .....	17
2.3.1	Sulindac Induces ER Stress .....	17
2.3.2	Several Chemopreventive Agents Induce ER Stress .....	20
2.3.3	Mechanisms of Action Downstream of ER Stress in Response to NSAIDs .....	21
2.4	<b>DISCUSSION</b> .....	22
3.0	<b>MECHANISMS OF ER STRESS-INDUCED APOPTOSIS CAUSED BY NSAID TREATMENT</b> .....	25
3.1	<b>INTRODUCTION</b> .....	25
3.1.1	BID-Mediated Synthetic Lethality .....	25
3.1.2	NSAIDs and ER Stress-Induced Cell Death.....	26
3.2	<b>MATERIALS AND METHODS</b> .....	27
3.2.1	Transfection.....	27
3.2.2	Cell Culture and Drug Treatment.....	27
3.2.3	Reverse-Transcriptase (RT) and Quantitative PCR .....	28
3.2.4	Analysis of Cell Viability and Apoptosis.....	28
3.2.5	Targeting <i>APC</i> in NCM 356 cells.....	28

3.2.6	Mice and Treatment .....	29
3.2.6.1	Short-Term ER Stress Experiments.....	31
3.2.6.2	Long-Term ER Stress Experiments. ....	31
3.2.7	Statistical Analysis .....	31
3.3	RESULTS .....	32
3.3.1	Attenuation of ER Stress Inhibits Sulindac-Induced Death Receptor Signaling and Cell Death .....	32
3.3.2	The Role of ER Stress-Mediated Death Receptor Signaling in Apoptosis Induced by Other Chemopreventive Agents.....	40
3.3.3	NSAID-Induced and ER Stress-Associated-Cell Death is Dependent on the Loss of the Tumor Suppressor <i>APC</i> in Normal Epithelial Cells .....	43
3.3.4	Inhibition of ER Stress by Salubrinal Inhibits NSAID-Mediated Apoptosis of Intestinal Stem Cells and Chemoprevention <i>in Vivo</i> . ....	47
3.4	DISCUSSION.....	52
4.0	IMMUNOMODULATORY EFFECTS OF NSAID-INDUCED ER STRESS AND CELL DEATH .....	56
4.1	INTRODUCTION .....	56
4.1.1	Chemoprevention and Immunoprevention .....	56
4.1.2	Safeguarding Against CRC Development by Immunosurveillance .....	57
4.1.3	Immune-Modulating Effects of NSAIDs.....	60
4.1.4	Restoring Immunosurveillance through Immunogenic Cell Death .....	61
4.2	MATERIALS AND METHODS .....	62
4.2.1	Mice and Treatment .....	62

4.2.2	Immunohistochemistry (IHC) .....	63
4.2.3	Flow Cytometric Analysis of CRT Translocation.....	64
4.2.4	Blood Dendritic Cell Isolation from Peripheral Blood Mononuclear Cells (PBMC) .....	64
4.2.5	Phagocytosis of Tumor Cells by DCs .....	64
4.2.6	Statistical Analysis .....	65
4.3	RESULTS .....	65
4.3.1	ER Stress and BID Inhibition Attenuates NSAID-Mediated Lymphocyte Infiltration.....	65
4.3.2	NSAID-Mediated Apoptosis Plays a Role in Immunogenic Cell Death.	69
4.3.3	Loss of the Tumor Suppressor <i>APC</i> Influences <i>CD47</i> Expression .....	75
4.4	DISCUSSION.....	79
5.0	SUMMARY AND FUTURE DIRECTIONS.....	82
5.1	GENERAL SUMMARY .....	82
5.2	FUTURE DIRECTIONS.....	86
	APPENDIX A .....	90
	APPENDIX B .....	92
	APPENDIX C .....	94
	BIBLIOGRAPHY .....	96

## LIST OF TABLES

Table 1. Top Cancer Statistics 2017 .....	2
Table 2. Primers Used in RT-PCR.....	90
Table 3. siRNAs Used in Study .....	91
Table 4. Log of Lab's Initial PDX Samples .....	93

## LIST OF FIGURES

Figure 1. Adenoma-Carcinoma Progression in CRC Development. ....	4
Figure 2. Extrinsic and Intrinsic Apoptotic Pathways. ....	7
Figure 3. A Simplified Model of the UPR/ER Stress Response.....	10
Figure 4. The Intricate Balance between the ER Stress-Induced Pro-Survival vs Pro-Death Mechanism.....	11
Figure 5. Sulindac Induces ER Stress-Associated Proteins in a Time-Dependent Manner in HCT 116 Cells. ....	17
Figure 6. Sulindac Increases the Expression of CHOP and the Cell Surface Translocation of BiP in HCT 116 cells. ....	18
Figure 7. Sulindac Induces Ultrastructural Changes in the Rough Endoplasmic Reticulum. ....	19
Figure 8. Sulindac Induces ER Stress in Other CRC Cell Lines. ....	20
Figure 9. Several Chemopreventive Agents Induce ER Stress.....	21
Figure 10. NSAID Treatment Activates Caspase 8 Signaling and Induces ER Stress in Human Advanced Adenomas. ....	22
Figure 11. Model of NSAID-Induced Apoptosis in <i>APC</i> Deficient Normal Cells.....	26
Figure 12. Pilot Experiment Showing the Influence of Inhibiting Various ER Stress Associated Proteins on NSAID-Induced Death Receptor Signaling.....	33

Figure 13. Attenuation of ER Stress Pharmacologically along the PERK/EIF2 $\alpha$ /ATF4/CHOP Pathway Significantly Reduces the Sulindac-Induced Death Receptor Signaling and Subsequent Cell Death. ....	34
Figure 14. Attenuation of ER Stress Using siRNAs to Target the PERK/EIF2 $\alpha$ /ATF4/CHOP Pathway Significantly Reduces the Sulindac-Induced Increase of Proteins Associated with the DR5 Signaling Pathway.....	36
Figure 15. PERK/ATF4/CHOP Knockdown in Sulindac-Treated Cells Negatively Impacts the Induction of <i>DR5</i> mRNA.....	37
Figure 16. ATF4/CHOP Inhibition Significantly Decreased Cell Death and Increased Cell Survival upon Sulindac Treatment.....	38
Figure 17. <i>ATF4</i> and <i>CHOP</i> Knockdown Significantly Decreased Apoptosis in RKO and HT-29 Cells. ....	39
Figure 18. ER Stress-Mediated Apoptosis Induced by NSAIDs is Dependent on BID. ....	40
Figure 19. The Role of DR5 in the Apoptotic Response to other CRC Chemopreventive Agents. ....	41
Figure 20. The Role of ER Stress-Mediated Death Receptor Signaling in the Apoptotic Response to Other Chemopreventive Agents. ....	42
Figure 21. Sulindac Induces ER Stress in a Time-Dependent Manner in <i>APC</i> -Deficient NCM 356 Cells. ....	43
Figure 22. NSAID-Induced and ER Stress-Associated Cell Death is Dependent on the Loss of Tumor Suppressor <i>APC</i> in Normal Epithelial Cells. ....	44
Figure 23. CHOP Knockdown Significantly Attenuates NSAID-Induced Death in NCM 356 Cells Deficient in <i>APC</i> .....	45

Figure 24. Pharmacological Inhibition of NSAID-Induced ER Stress Impacts Death Receptor Signaling in NCM 356 Cells Deficient in <i>APC</i> . .....	46
Figure 25. The Role of ER Stress-Mediated Death Receptor Signaling in Stable <i>APC</i> KO NCM 356 Cells. ....	47
Figure 26. NSAID-Induced ER stress is Attenuated by Salubrinal in <i>APC</i> <sup>Min/+</sup> Mice. ....	48
Figure 27. Attenuation of ER Stress by Salubrinal Inhibits NSAID-Mediated Apoptosis <i>in Vivo</i> . .....	49
Figure 28. Attenuation of ER Stress via Salubrinal Inhibits NSAID-Mediated Chemoprevention. ....	51
Figure 29. The Influence <i>CHOP</i> KO on NSAID-Mediated Tumor Prevention in <i>APC</i> <sup>Min/+</sup> Mice. ....	52
Figure 30. Immunoediting and Immunoprevention along the Adenoma-Carcinoma Progression in Colorectal Tumor Development. ....	58
Figure 31. Overview of Antitumor Immune Response. ....	59
Figure 32. NSAIDs Promote Lymphocyte Infiltration into the Adenoma <i>in Vivo</i> . ....	66
Figure 33. Inhibiting NSAID-Induced ER Stress Attenuates Lymphocyte Infiltration into the Adenoma <i>in Vivo</i> . ....	67
Figure 34. Inhibiting NSAID-Induced Cell Death Attenuates Lymphocyte Infiltration into the Adenoma <i>in Vivo</i> . ....	68
Figure 35. NSAID-Induced ER Stress-Associated Cell Death Mediated by BID Promotes Lymphocyte Infiltration into the Adenoma <i>in Vivo</i> . ....	69
Figure 36. NSAID-Mediated ICD is Affected by Caspase 8 and BID Depletion as Highlighted by Cell Surface CRT Translocation. ....	70

Figure 37. NSAID-Mediated ICD is Affected by ER Stress Inhibition as Highlighted by Cell Surface CRT Translocation.....	71
Figure 38. NSAID-Mediated ICD is Affected by BID and ER Stress Inhibition as Highlighted by DC Phagocytosis.....	72
Figure 39. NSAID Treatment Influences CRT Translocation and DC Phagocytosis upon the Loss of APC in a Normal Epithelial Background.....	74
Figure 40. <i>CD47</i> Expression is Upregulated in <i>APC</i> KO NCM 356 cells and is Attenuated upon NSAID Treatment.....	76
Figure 41. <i>CD47</i> Expression is Elevated in Colorectal Adenocarcinomas vs. Normal Tissue. ..	78
Figure 42. The Proposed Mechanism of NSAID-Induced Death Seen Upon the Loss of <i>APC</i> in Normal Epithelial Cells.....	85
Figure 43. Identification of Potential NSAID Binding Proteins Upstream of ER Stress by Mass Spectrometry.....	86
Figure 44. Establishment of PDX Models with NOD SCID Mice.....	92

## **PREFACE**

### **Acknowledgments**

*“Ef yuh waan good yuh nose haffi run.” Wise Jamaican Proverb*

*Meaning: To be successful you must work hard*

*The race is not given to the swift nor the strong but he who endures until the end.  
(Ecclesiastes 9:11)*

This thesis would not have been completed without the effort of many to whom I am forever indebted. These persons have helped with the conception, continuation, and completion of this study. Hence, I owe an enviable gratitude to them all.

I must first and foremost thank the Lord Almighty for instilling in me the strength, wisdom, and patience in order to complete this research project. Wholehearted thanks must then be extended to Dr. Lin Zhang who was a very engaged and helpful mentor. He has been an instrumental figure in the successful completion of this thesis. He would always challenge me, and this has helped in the giving of my best. His wife Dr. Jian Yu also provided wonderful advice, which was always welcomed. Overall, everyone in the Zhang/Yu lab was very helpful and this fostered a good environment to learn.

I must also thank other members of my committee, including: Dr. Thomas Kensler, Dr. Donna Stolz, Dr. Jane Wang, and Dr. Roddy O’Sullivan. A special acknowledgement must be made to Dr. Donna Stolz who provided her expertise on the transmission electron microscope when elements of my research required a cell biologist’s point of view. I truly appreciated her enthusiasm and eagerness to help. Overall, the members of my committee were truly exceptional and pivotal to the progression of my project.

I am also truly appreciative of the support of the Pharmacology Department here at the University of Pittsburgh School of Medicine. The members have helped to guide me along this path and provided not only emotional but also financial support via the fellowships that I was awarded during the program. I have to specifically highlight Dr. Pagano, Dr. Romero and Dr. Freeman who all shaped this program that was conducive to propelling me to think more critically as a scientist.

Lastly, but by no means the least, I wish to extend a heartfelt thanks to my support system. This especially is directed to my mother, Dr. Ivoline Fletcher, who has always supported me and without her I would not have been as successful in my academic quest. Even though she was all the way in Jamaica, she was still able to provide unwavering support from the very commencement of my studies. I could not have asked for a better role model growing up. The rest of my family has also been very supportive throughout this process and it was truly appreciated.

Additionally, I am very grateful to the amazing friends I have made here that have helped me during my time as a graduate student. This includes Dr. Kyle Knickelbein, a past graduate student in the lab, who was very supportive throughout my entire journey in and out of the lab. Additional thanks must be made to my lab’s secretary Mrs. Laurice Vance-Carr who was always

a source of encouragement. I can never forget the life-long friends who may not have been physically here with me but have always been a dependable shoulder to lean on, such as Alexa Serrano-Cruz and Shari and Jamar Salmon.

I was honestly grateful for the opportunity to learn and contribute as a researcher and scholar. This phase of my educational journey has now come to a close. Mission accomplished! However, greater experiences await me, and I shall make the best use of the opportunities presented to advance my depth of knowledge in research.

## **List of Abbreviations**

A1	Bcl-2-related protein A1
ACLY	ATP-Citrate lyase
ACS	American Cancer Society
APC	Adenomatous polyposis coli
ATP	Adenosine triphosphate
ATF	Activating transcription factor
Bak	Bcl-2 homologous antagonist/killer
Bax	Bcl-2-associated X protein
Bcl-2	B-cell lymphoma 2
Bcl-xL	B-cell lymphoma-extra large
BH	Bcl-2 homology domain
BID	BH3-interacting domain death agonist
Bim	Bcl-2-like protein 11
BiP	Binding immunoglobulin protein
BRAF	v-Raf murine sarcoma viral oncogene homolog B
c-Myc	Proto-oncogene c-Myc
DISC	Death-inducing signaling complex
CD3	Cluster of differentiation 3
CD8	Cluster of differentiation 8
CD91	Cluster of differentiation 91
CD47	Cluster of differentiation 47
CETSA	Cellular thermal shift assay

CIN	Chromosome instability
CRC	Colorectal cancer
CRT	Calreticulin
CRISPR/cas9	Clustered Regularly Interspaced Short Palindromic Repeats/CRISPR associated protein 9
CHOP	CCAAT-enhancer-binding protein homologous protein
COX	Cyclooxygenase
CTL	Cytotoxic T cells
CTLA-4	Cytotoxic T lymphocyte associated antigen 4
DAB	3, 3-diaminobenzidine
DAMP	Damage associated molecular pattern
DC	Dendritic cell
DMSO	Dimethyl sulfoxide
DR5	Death receptor 5
EDTA	Ethylenediaminetetraacetic acid
EIF2 $\alpha$	Eukaryotic translation initiation factor 2 $\alpha$
ER	Endoplasmic reticulum
Fas	Tumor necrosis factor receptor superfamily member 6
FBS	Fetal bovine serum
FDA	Food and Drug Administration
HBSS	Hanks' balanced salt solution
HEPES	4-(2-hydroxyethyl)-1-piperazineethanesulfonic acid
HLA-DR	Human Leukocyte Antigen-DR

HMGB1	High mobility group box 1
HSP90	Heat shock protein 90
ICD	Immunogenic cell death
IFN- $\gamma$	Interferon gamma
i.p.	Intraperitoneal
Ig	Immunoglobulin
IP	Immunoprecipitation
IRE1	Inositol-requiring enzyme 1
KO	Knockout
KD	Knockdown
KRAS	v-Ki-ras2 Kirsten rat sarcoma viral oncogene homolog
MEK	Mitogen-activated protein kinase kinase
MOMP	Mitochondrial outer membrane permeabilization
MSI	Microsatellite instability
NCI	National Cancer Institute
NCM	Normal colon mucosa
NF- $\kappa$ B	Nuclear factor kappa-light-chain-enhancer of activated B cells
NSAID	Non-steroidal anti-inflammatory drugs
PARP	Poly (ADP-ribose) polymerase
PDX	Patient derived xenograft
PBMC	Peripheral blood mononuclear cells
PD-1	Programmed death 1
PDI	Protein disulfide isomerase

PD-L1	Programmed death ligand 1
PERK	Protein kinase R-like endoplasmic reticulum kinase
PEG	Polyethylene glycol
PGE	Prostaglandin E
PI	Propidium iodide
PI3K	Phosphatidylinositol-4,5-bisphosphate 3-kinase
PUMA	p53-upregulated modulator of apoptosis
PVDF	Polyvinylidene fluoride
RAF	Rapidly accelerated fibrosarcoma
RAS	Rat sarcoma
RER	Rough endoplasmic reticulum
RNAi	RNA interference
ROS	Reactive oxygen species
RT-PCR	Reverse transcription polymerase chain reaction
s.d.	Standard deviation
SER	Smooth endoplasmic reticulum
siRNA	Small interfering RNA
tBid	Truncated BH3-interacting domain death agonist
TAA	Tumor associated antigens
TCGA	The Cancer Genome Atlas
TH	T helper
TIL	Tumor infiltrating lymphocyte
TEM	Transmission electron microscopy

TNF $\alpha$	Tumor necrosis factor alpha
TP53/p53	Tumor protein p53
TRAIL	TNF-related apoptosis-inducing ligand
UPCI	University of Pittsburgh Cancer Institute
UPR	Unfolded protein response
VEGF	Vascular endothelial growth factor
VEGFR	Vascular endothelial growth factor receptor
WT	Wild-type

## 1.0 INTRODUCTION

According to the National Cancer Institute (NCI), cancer refers to a collection of diseases that produce abnormal cells that uncontrollably divide and can invade nearby tissues. This disease is heavily studied as it is the second leading cause of deaths in the United States [1]. In fact, the American Cancer Society (ACS) states that 609,604 people are projected to die from this disease in 2018. Despite these projections, the ACS estimates that there has been an approximate 26% reduction in cancer-related deaths between 1995 and 2015. This is mostly attributed to the increased awareness of smoking-induced carcinogenesis, earlier intervention/prevention strategies, and improved methods of treatment.

Overall, there are numerous forms of cancers with lung, colon, prostate, and breast having the highest numbers of estimated new cases and deaths in 2017 (Table 1) [1]. This variety significantly impacts the effectiveness of the prevention and treatment strategies implemented in each subtype.

**Table 1. Top Cancer Statistics 2017**

<b>Gender</b>	<b>Males</b>		<b>Females</b>	
	<b>Cancer</b>	<b>%</b>	<b>Cancer</b>	<b>%</b>
<b>Estimated New Cases</b>	Prostate	19	Breast	30
	Lung and Bronchus	14	Lung and Bronchus	12
	Colon and Rectum	9	Colon and Rectum	8
<b>Estimated Deaths</b>	Lung and Bronchus	27	Lung and Bronchus	24
	Colon and Rectum	9	Breast	14
	Prostate	8	Colon and Rectum	8

### **1.1 COLORECTAL CANCER**

Despite recent success in screening, early detection, and treatment, colorectal cancer (CRC) remains the overall second leading cause of cancer-related deaths in the United States (US) [1]. While the incidence and mortality rates of colorectal cancer are decreasing overall, studies from the American Cancer Society show that these rates are increasing among adults  $\leq 50$  in the US [2-4]. Prevention or early detection represents a key approach for reducing the mortality and morbidity of cancers including CRC [5].

### **1.2 COLORECTAL CANCER AND PREVENTION**

CRC development occurs in a stepwise fashion, progressing from a benign pre-neoplastic lesion to metastatic disease that has a survival rate of only 11% [6]. In approximately 85% of CRC cases, tumor development engages the well-established adenoma-carcinoma sequence of events (Fig. 1). The precursor lesion adenoma is initiated by gatekeeper genetic alterations in the *Adenomatous Polyposis Coli (APC)* tumor suppressor pathway through aberrant Wnt signaling,

leading to accumulation and subsequent nuclear translocation of  $\beta$ -catenin and activation of oncogenes such as *c-Myc* and *cyclin D1* [7]. Further tumor development is promoted by oncogenic mutations in *KRAS*, *BRAF*, *PIK3CA*, and loss or mutation of other tumor suppressors such as *Tumor Protein p53 (TP53)* [7] (Fig. 1). CRCs arising following the adenoma-carcinoma sequence are often characterized by chromosome instability (CIN) [7].

This process is driven by a series of well-defined genetic and epigenetic alterations (Fig. 1) that typically take many years or decades to accumulate [7]. This long development process creates a substantial window of opportunity for prevention [4]. CRC also has well-described and readily identifiable precursor lesions in human patients, a process mirrored in animal models [8]. For these reasons, CRC has been extensively evaluated with cancer prevention proof-of-principle studies. Depending on the purpose, CRC prevention can be aimed at suppressing tumor initiation (primary prevention), preventing tumor recurrence or progression (secondary prevention), or management of chronic disease (tertiary prevention) [9]. Many preventative studies focus on primary/secondary prevention targeting the earlier stages of the adenoma to carcinoma model.

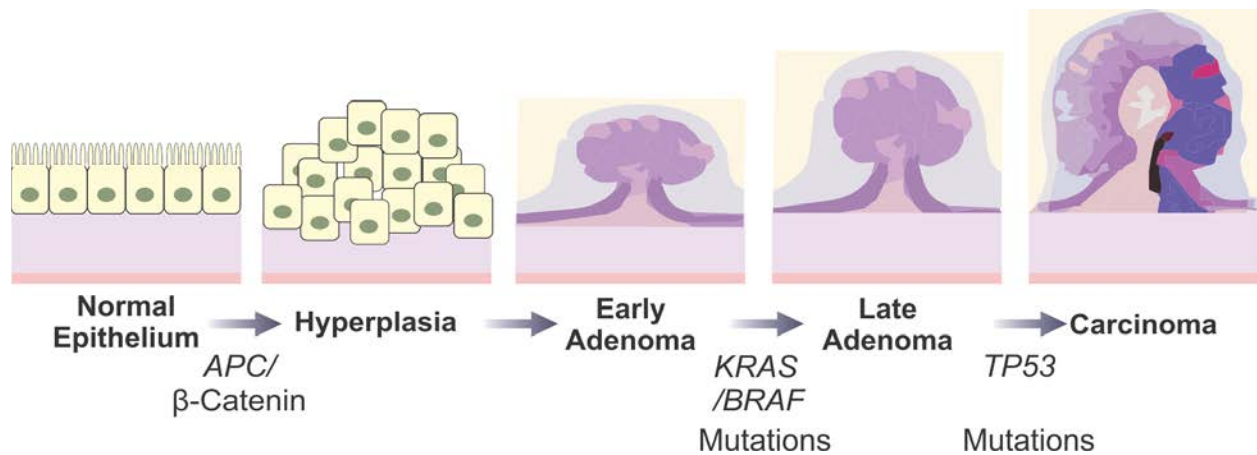


**Figure 1. Adenoma-Carcinoma Progression in CRC Development.** Development of colorectal cancer is driven by genetic alterations in the *APC/β-catenin* pathway, leading to aberrant Wnt signaling and formation of hyperplastic cryptic foci and early adenomas. Accumulation of genetic alterations in oncogenes such as *KRAS/BRAF* and tumor suppressors such as *TP53* results in formation of late adenomas and carcinomas. This figure is adapted from Fletcher et al, BBA Cancer Reviews, 2018 [10].

### 1.3 CHEMOPREVENTION

A promising approach for reducing the mortality and morbidity of CRC is chemoprevention, which refers to the use of natural or pharmacological agents to suppress tumorigenesis. For example, the regular use of aspirin and other non-steroidal anti-inflammatory drugs (NSAIDs) has been consistently associated with a reduced risk of CRC [11, 12]. A number of other agents, such as folic acid, calcium, vitamin D, antioxidants (including vitamin A, vitamin C, vitamin E, selenium, and beta-carotene), and ω-3 polyunsaturated fatty acids (PUFAs), have exhibited chemopreventive activity in epidemiological and/or clinical studies, as well as various preclinical models [13, 14].

## **1.4 NSAIDS AND CHEMOPREVENTION**

NSAIDs are the best and most potent examples of chemopreventive agents which have been shown to reduce CRC incidence in animal models and in human epidemiological studies and clinical trials [15, 16]. This group of drugs includes a variety of over-the-counter or prescription drugs (e.g., aspirin, sulindac, ibuprofen, and indomethacin), which are often used for treating inflammation, pain, or fever.

The chemopreventive properties of NSAIDs have been primarily attributed to inhibition of cyclooxygenase (COX) enzymes, which leads to a reduction in prostaglandin E (PGE) [17]. However, the exact mechanisms of action of these drugs in CRC chemoprevention have yet to be fully delineated. Side effects such as gastrointestinal, cardiac, and renal toxicities have also been reported due to the inhibition of COX enzymes [17] which limits the long-term use of these drugs in chemoprevention. This is a critical issue emphasized by the NCI: potential preventive therapies must meet a higher safety bar than those used to treat cancer.

## **1.5 EXTRINSIC AND INTRINSIC APOPTOSIS**

Apoptosis is one of the most effective mechanisms of defense against cancer as it eradicates abnormal cells. NSAIDs and other chemopreventive agents such as retinoids and vanilloids have also been shown to induce apoptosis [18]. Apoptosis is a tightly regulated mechanism of cell death that typically follows one of two main pathways, namely: extrinsic and intrinsic pathways [19, 20] (Fig. 2). Death receptor (DR) signaling is a major component of the extrinsic apoptotic pathway. Pro-apoptotic ligands bind to death receptors such as DR5 and initiate the formation of the death-

inducing signaling complex (DISC). Members of this complex include pro-caspase 8, which when activated, results in further caspase activation culminating in cell death. Unlike death receptor signaling, the intrinsic apoptotic pathway is primarily regulated by TP53 and Bcl-2 family proteins [19]. In response to stress, the mitochondrial outer membrane becomes permeable, leading to the release of apoptogenic proteins such as cytochrome c and SMAC and activation of executioner caspases. Crosstalk between the two main apoptotic pathways can occur through the caspase-8-dependent cleavage of the Bcl-2 family protein BH3 interacting-domain death agonist (BID) to generate active tBID, which then activates the intrinsic pathway [19, 21].

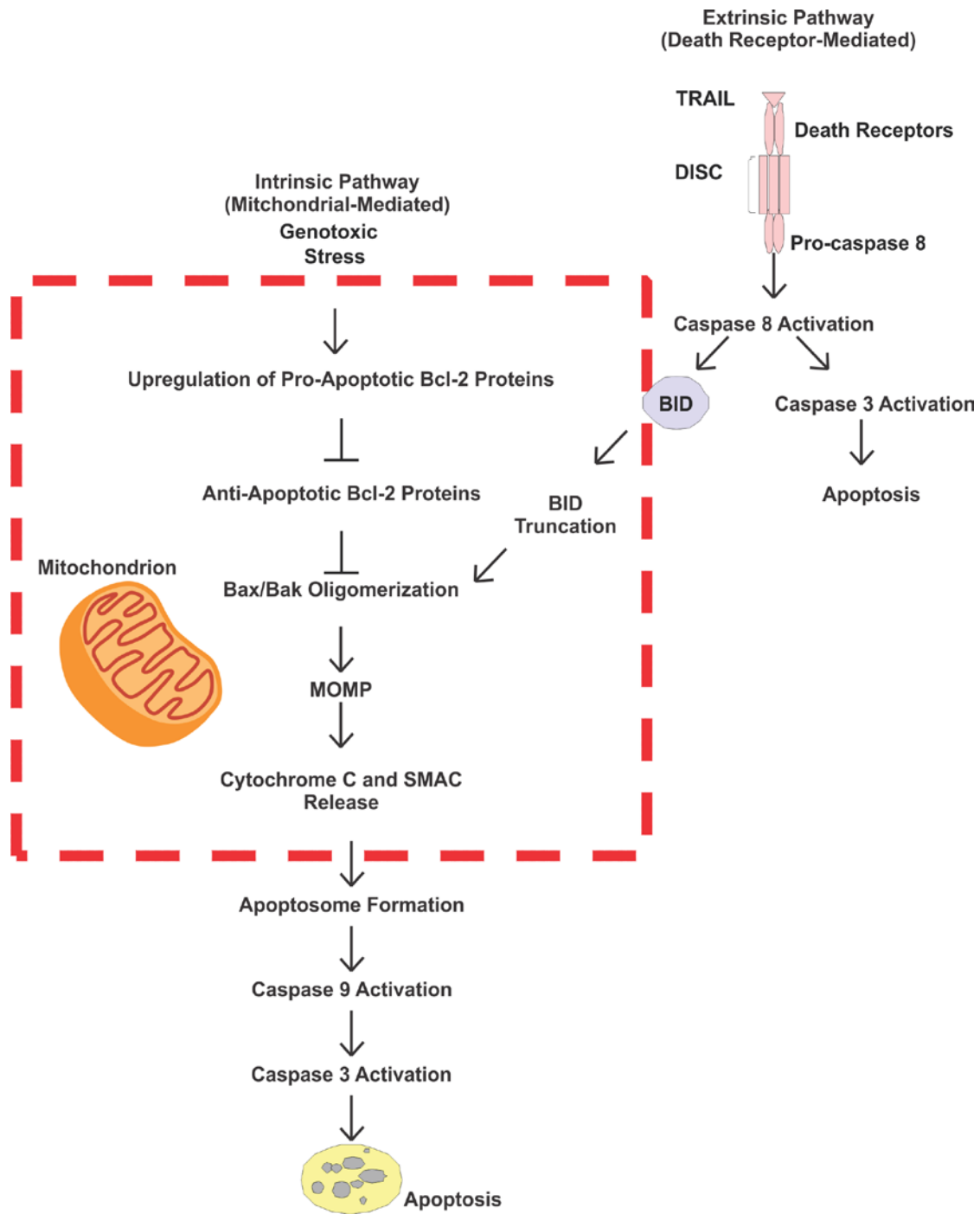


**Figure 2. Extrinsic and Intrinsic Apoptotic Pathways.** There are two main apoptotic pathways: the death receptor driven extrinsic pathway and the mitochondria-mediated intrinsic pathway. Cross talk between these pathways occurs via caspase 8-mediated BID cleavage. This figure is modified from the original artwork in Tait et al., Journal of Cell Science, 2012 [20].

## **2.0 THE ROLE OF ER STRESS IN CHEMOPREVENTION**

### **2.1 INTRODUCTION**

#### **2.1.1 Mechanisms of ER Stress Induction**

The endoplasmic reticulum (ER) is an important organelle that can be further subdivided into the rough ER (RER) and the smooth ER (SER) [22]. The former is studded with ribosomes and located closer to the nucleus and the latter is more tubular in structure and located more distally from the nucleus [22]. Overall, this organelle carries out three main functions including: calcium regulation, lipid biosynthesis and protein folding and assembly [23, 24]. Deregulation of any of these functions can lead to an accumulation of misfolded or unfolded proteins resulting in the induction of the unfolded protein response (UPR)/ER stress [23]. This deregulation can be caused by physiological or pathological attacks such as viral infection, increased protein demand or the accumulation of mutated proteins [23].

#### **2.1.2 ER Stress and NSAIDs**

Three main signaling cascades regulate the UPR/ER stress response. Each cascade is initiated by the activation of one of the three ER-localized prototypical stress sensors: inositol-requiring enzyme 1 $\alpha$  (IRE1 $\alpha$ ), protein kinase-like ER kinase (PERK), and activating transcription factor 6

(ATF6) (Fig. 3) [23]. Under normal conditions, the chaperone protein glucose-regulated protein 78 (GRP 78/BiP) is bound to each of the three sensors. However, upon the accumulation of unfolded proteins, BiP detaches from them and binds to misfolded proteins in an effort to help reduce cellular stress. This detachment allows the activation of each of the three pathways. Stress magnitude and timing play critical roles in the intricate balance between the pro-survival and pro-death mechanisms of the UPR (Fig. 4) [25]. Initially, the response is aimed at reducing the unfolded protein load through multiple pro-survival mechanisms such as the induction of other chaperone proteins [23]. If this does not alleviate the stress, it becomes highly chronic and the UPR switches from a pro-survival to a pro-death signal. Apoptosis is then triggered via several mechanisms such as the activation of C/EBP homologous transcription factor (CHOP) and sometimes activation transcription factor 3 (ATF3). These cascades are important to study as ER stress has been implicated in the pathogenesis of many diseases and also identified as a potential target in cancer therapy [26]. Recent evidence shows that several NSAIDs have the ability to impact the ER homeostasis [27], and the ER stress can stimulate an apoptotic response [28]. However, the exact implications for this phenomenon are still not clear.

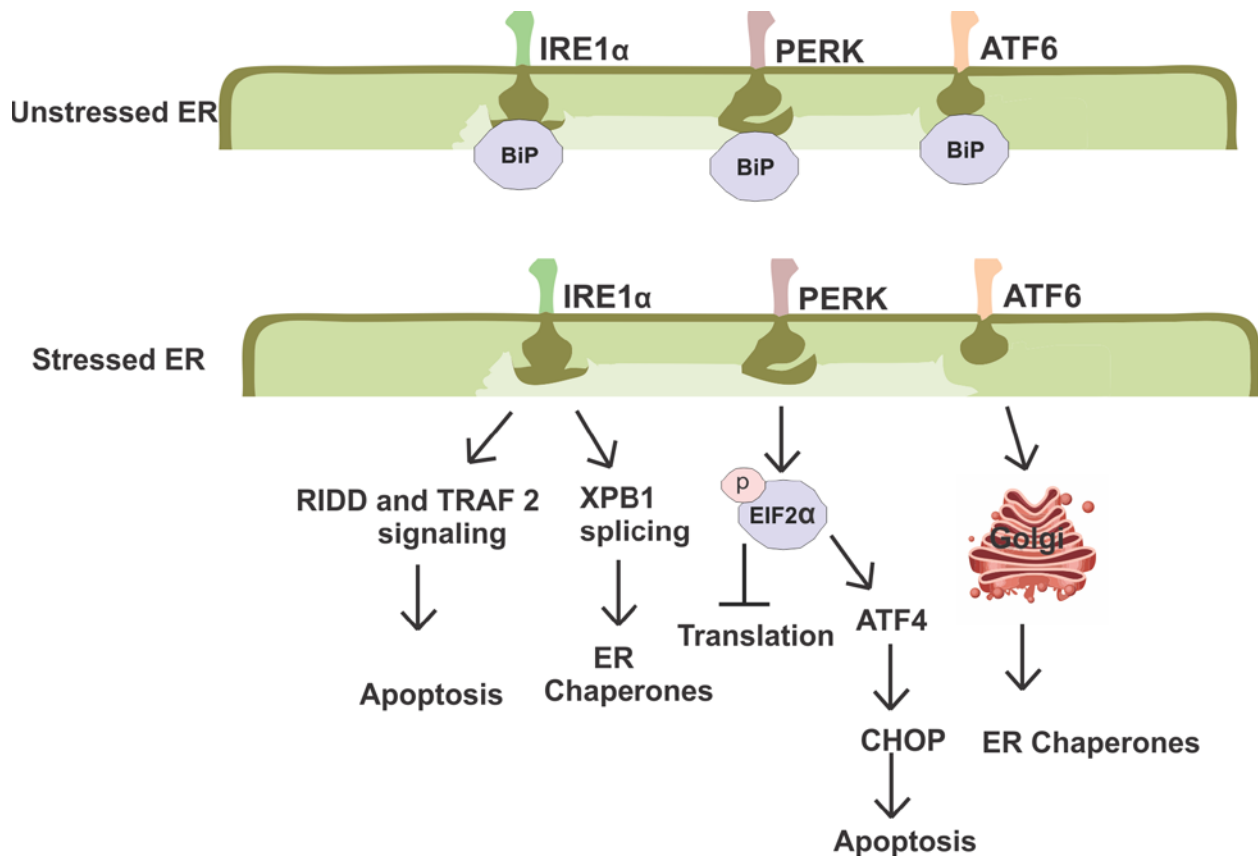


**Figure 3. A Simplified Model of the UPR/ER Stress Response.** BiP is bound to the three main ER stress sensors in an unstressed state. Upon the induction of ER stress, BiP detaches to help with protein folding thereby allowing for the activation of the three signaling cascades (IRE1α, PERK, and ATF6). This figure is modified from the original artwork in Rufo et al., Trends in Cancer, 2017 [29].

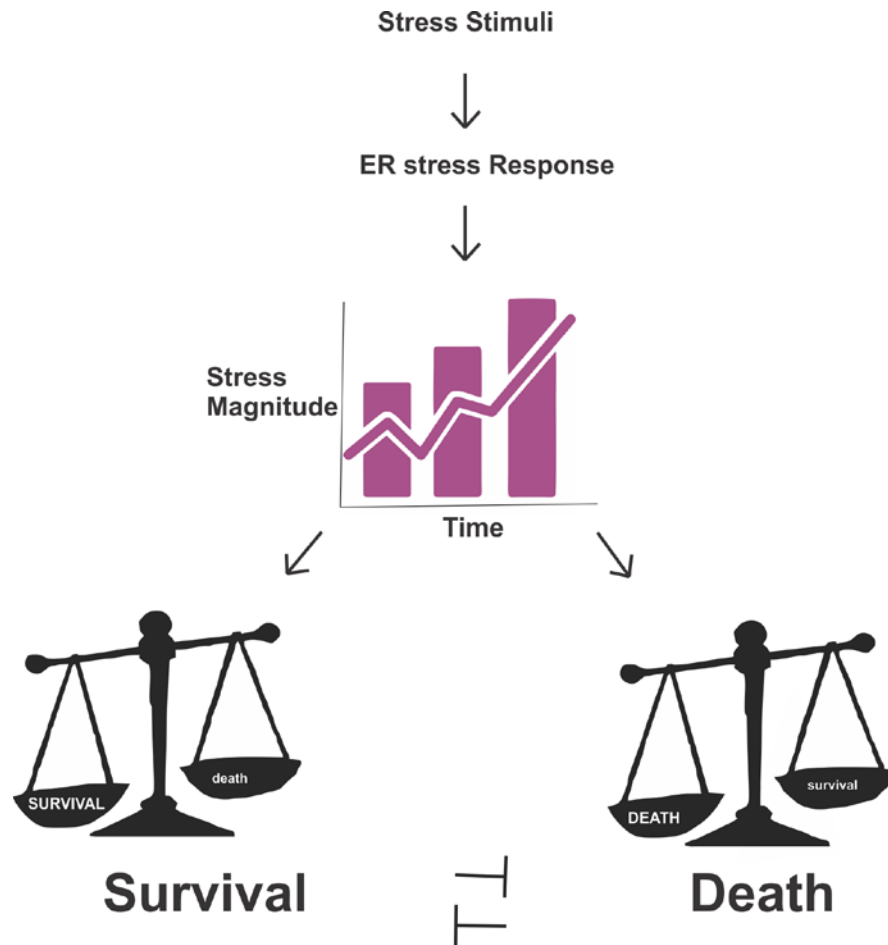


**Figure 4. The Intricate Balance between the ER Stress-Induced Pro-Survival vs Pro-Death Mechanism.** The magnitude and timing of ER stress will influence whether it will promote cell survival or cell death. This figure is modified from the original artwork in Corazzari et al., *Frontiers in Oncology*, 2017 [25].

### **2.1.3 Targeting Apoptosis in NSAID-Induced Chemoprevention**

Many chemopreventive agents including NSAIDs induce apoptosis in carcinogenesis models or in human chemoprevention trials [18]. It was suggested that apoptosis induction is a critical mechanism in chemoprevention [18]. For example, it was shown that sulindac can stimulate apoptosis in the rectal mucosa of FAP patients and in several animal models such as the intestinal mucosa of *APC*<sup>Min/+</sup> mice and in the colorectal carcinomas of carcinogen-treated rats [30-32]. In terms of specificity, it has been shown the loss of *APC* in otherwise normal cells triggers NSAID-induced apoptosis [21]. Furthermore, more recent studies have shown that NSAIDs eliminate stem cells that are improperly activated by oncogenic events via the induction of SMAC dependent apoptosis [33]. Even with all of these data, the exact mechanism via which NSAID-induced cell death is initiated is very obscure.

## **2.2 MATERIALS AND METHODS**

### **2.2.1 Cell Culture and Drug Treatment**

Human CRC cell lines, including HCT 116, HT-29, and RKO (American Type Culture Collection), and their derivatives, were cultured in McCoy's 5A media according the supplier's instructions (Invitrogen). Cells were kept in a non-humidified incubator at 37°C with the addition of 5% CO<sub>2</sub>.

Unless otherwise specified, cells were plated at 20-30% density in 12-well plates for drug treatment. Chemicals utilized include: sulindac sulfide (Merck, active metabolite of sulindac),

indomethacin (Sigma), celecoxib (Sigma), acetaminophen (Sigma), metformin (Cayman Chemical Company), naproxen sodium (Apex Bio), diclofenac (sodium salt) (Cayman Chemical Company), sodium salicylate (Sigma), and Salubrinal (Apex Bio). All agents except for naproxen sodium were diluted in DMSO (Sigma). Naproxen was diluted in distilled water.

### **2.2.2 Western Blotting**

Cell lysate preparation and western blotting were performed as described [34]. Proteins (30  $\mu$ g for each lane) were separated by SDS-PAGE using the Nu-PAGE system (Invitrogen) and transferred to PVDF membranes (Immobilon-P, Millipore). Antibodies for western blotting include those against:  $\beta$ -Actin (Sigma #A5441), cleaved caspase-3 (Cell Signaling #9661), death receptor 5 (Abcam #ab8416), CHOP (Cell Signaling #2895s), CREB-2 (Santa Cruz #sc-200), caspase-8 p18 (Santa Cruz # sc-6136), APC (Calbiochem #OP44), pEIF2 $\alpha$  (Cell Signaling #3398), EIF2 $\alpha$  (Santa Cruz #sc-11386), PERK (Cell Signaling #5683P), pPERK (Santa Cruz #sc-32577), PDI (Cell Signaling #3501P), BiP (Cell Signaling #3177), c-Myc (Santa Cruz #sc-40), BID (Cell Signaling #2002), and IRE1 $\alpha$  (Cell Signaling #3294P). Each western blot is representative of at least two independent experiments.

### **2.2.3 Reverse-Transcriptase (RT) and Quantitative PCR**

Total RNA was isolated using the Mini RNA Isolation II kit (ZYMO Research) according to the manufacturer's protocol. One microgram of total RNA was used to generate cDNA by using SuperScript III reverse transcriptase (Invitrogen). Real-time PCR was performed with previously described conditions [35]. Primers used in this study are listed in Table S2.

## **2.2.4 Transmission Electron Microscopy (TEM) and Immuno-TEM**

**2.2.4.1 Transmission Electron Microscopy (TEM).** TEM was performed as described previously [36]. Cells grown on tissue culture plasticware were fixed in 2.5% glutaraldehyde in 100 mM PBS (8 gm/l NaCl, 0.2 gm/l KCl, 1.15 gm/l Na<sub>2</sub>HPO<sub>4</sub>·7H<sub>2</sub>O, 0.2 gm/l KH<sub>2</sub>PO<sub>4</sub>, pH 7.4) overnight at 4°C. Monolayers were then washed in PBS three times then post-fixed in aqueous 1% osmium tetroxide, 1% Fe<sub>6</sub>CN<sub>3</sub> for 1 hour. Cells were washed 3 times in PBS then dehydrated through a 30-100% ethanol series, followed by several changes of Polybed 812 embedding resin (Polysciences, Warrington, PA). Cultures were embedded by inverting Polybed 812-filled BEEM capsules on top of the cells. Blocks were cured overnight at 37°C, and then cured for two days at 65°C. Monolayers were pulled off the tissue culture plastic and sectioned en face. Ultrathin cross sections (60 nm) of the cells were obtained on a Riechart Ultracut E microtome, post-stained in 4% uranyl acetate for 10 minutes and 1% lead citrate for 7 minutes. Sections were viewed on a JEOL JEM 1011 transmission electron microscope (JEOL, Peabody MA) at 80 KV. Images were taken using a side-mount AMT 2k digital camera (Advanced Microscopy Techniques, Danvers, MA).

**2.2.4.2 LR White Resin IEM Method: Immuno-TEM.** The specimens were fixed in cold 2% paraformaldehyde in 0.01 M PBS (pH 7.4). Specimens were rinsed in PBS, dehydrated through a graded series of ethanol, infiltrated with and embedded in LR White Resin (Electron Microscopy Sciences, Hatfield, PA). Semi-thin (300 nm) sections were cut on a Leica Ultracut 7, stained with 0.5% Toluidine Blue in 1% sodium borate, and examined under the light microscope to determine specific area. Ultrathin sections (65 nm) were picked up on 100 mesh nickel grids, labeled with 1:100 dilution of Rabbit anti-BiP (AbCam) overnight at 4°C, and then

labeled with a 6 nm goat anti-rabbit colloidal gold conjugated secondary at a dilution of 1:10 at room temperature for 1 hour. After rinsing in PBS and dH<sub>2</sub>O, the sections were counterstained with 2% uranyl acetate and examined on JEOL 1011 transmission electron microscope with a side mount AMT 2k digital camera (Advanced Microscopy Techniques, Danvers, MA).

### **2.2.5 Analysis of Patient Colonic Polyp Samples**

Frozen specimens from patients with sporadic colonic adenomas (9 treated with NSAIDs, 7 untreated) were acquired from the Health Sciences Tissue Bank of the University of Pittsburgh. Acquisition of the tissue samples was approved by the Institutional Review Board. Informed consent was received from all participating patients. IF was performed as described below.

### **2.2.6 Immunofluorescence (IF)**

**2.2.6.1 Human Tissues.** Following embedding in paraffin, 5 µm slices of tumor tissue were cut in preparation for staining. IHC/IF was performed as described below using antibodies against: pEIF2α (Cell Signaling #3398S, 1:100) and active caspase 8 (Novus Biologicals #NB100-56116, 1:600). Antigen retrieval was then carried out on rehydrated sections via boiling for 10 minutes in 0.1 M citrate buffer (pH 6.0) with 1 mM EDTA. Non-specific antibody binding was blocked using 20% goat serum at room temperature for 30 minutes. Primary antibody incubations were done in the dark overnight at 4°C with their respective antibodies in a humidified chamber. Sections were then incubated for 1 hour at room temperature with AlexaFluor 594- conjugated goat anti-rabbit secondary antibodies (A11012; 1:250, Invitrogen). They were then washed in PBS and mounted with VectaShield + DAPI (Vector Labs). Images were acquired using an

Olympus BX51 system microscope equipped with SPOT camera and SPOT Advanced 5.1 software.

**2.2.6.2 Human Cells.** HCT 116 cells were seeded onto sterile coverslips and treated the following day. After the 24-hour treatment, cells were fixed with 2% paraformaldehyde in PBS for 1 hour. Samples were then stored in PBS at 4 degrees until staining.

Immunostaining was performed using the antibodies for CHOP (Thermofisher #MA1-250, 1:100) and BiP (Abcam 21685, 1:500). Cells were permeabilized with 0.1% triton X-100 at room temperature for 15 minutes. They were blocked with 5% normal goat serum at room temperature for 45 minutes. Cells were incubated overnight with primary antibodies at 4 °C. Incubation with secondary antibodies was performed at room temperature for 1 hour. Finally, a Hoechst solution was used for staining for 30-45 seconds. Images were acquired on a Nikon A1 confocal microscope.

### **2.2.7 Statistical Analysis**

Statistical analyses were performed by using GraphPad Prism IV software. Differences were considered significant if the probability of the difference occurring by chance was less than 5 in 100 ( $P < 0.05$ ). Multiple comparisons of the responses were analyzed by one-way ANOVA and either Dunnett's or Tukey's post hoc test, whereas those between two groups were made by unpaired t test. All statistical tests were two-tailed.

## 2.3 RESULTS

### 2.3.1 Sulindac Induces ER Stress

In order to delineate the role of ER stress in mediating the anti-cancer effects of NSAIDs, the CRC cell line HCT 116 was treated with sulindac sulfide (the active metabolite of sulindac). Upon treatment, we found the drug induced various proteins associated with ER stress in a time-dependent manner. These proteins include pEIF2 $\alpha$ , ATF4, and CHOP (Fig. 5A). The mRNA levels of these ER stress-associated proteins were also increased (Fig 5B). Furthermore, these proteins were all upregulated in tandem with DR5, a key regulator of the extrinsic apoptotic pathway upstream of caspase 8 [37].

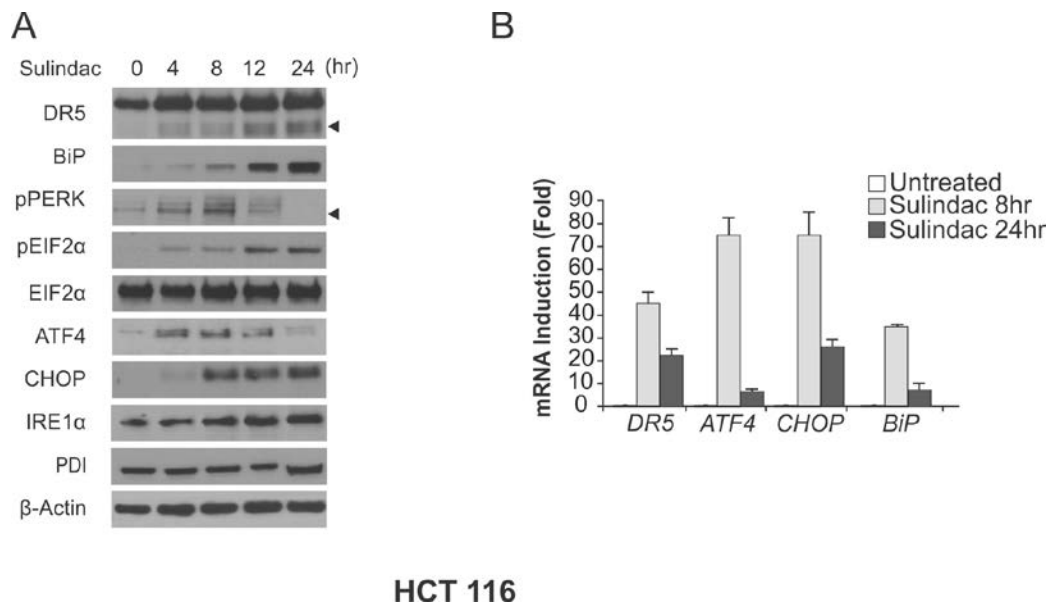


**Figure 5. Sulindac Induces ER Stress-Associated Proteins in a Time-Dependent Manner in HCT 116 Cells.** (A) Western blots showing sulindac-induced (120  $\mu$ M) expression of various proteins indicative of ER stress at different time points. (B) The induction of mRNA of ER stress-associated

factors after indicated treatment times with 120  $\mu$ M sulindac sulfide. Results were expressed as means + s.d. of three independent experiments.

The induction of ER stress associated proteins by NSAIDs was confirmed by IF staining of CHOP and BiP (Fig. 6A). Furthermore, immuno-TEM clearly showed that sulindac treatment increased the cell surface expression of BiP, a downstream effect of general ER stress (Fig. 6B).

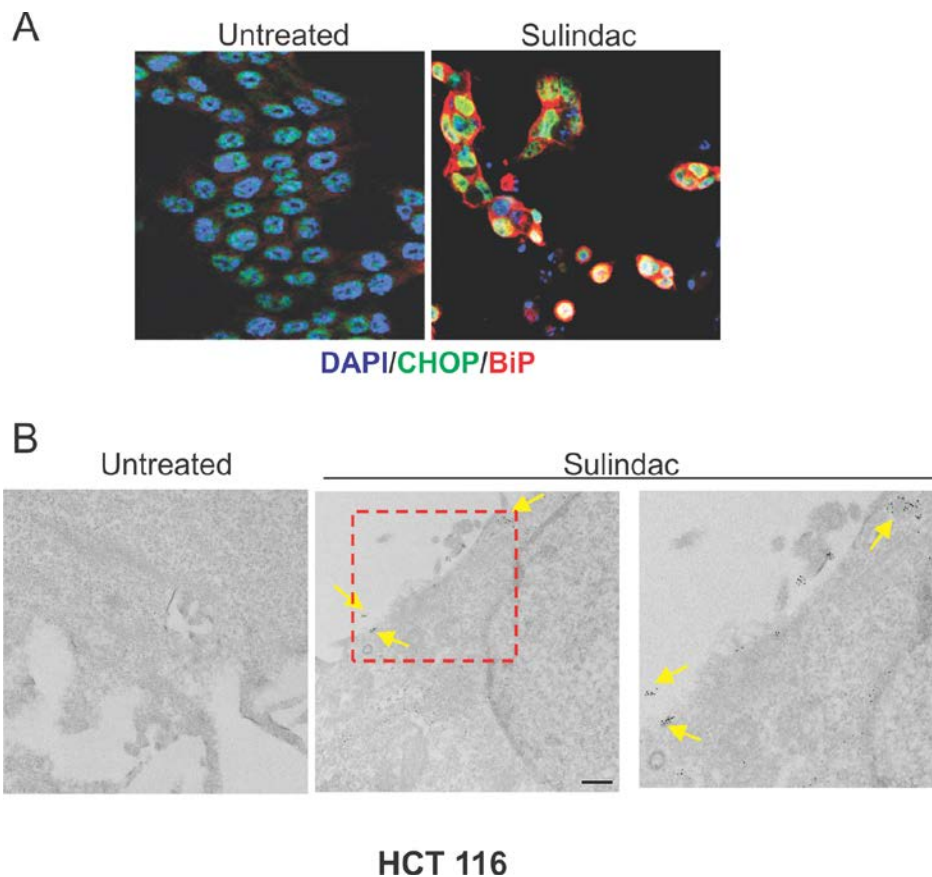


**Figure 6. Sulindac Increases the Expression of CHOP and the Cell Surface Translocation of BiP in HCT 116 cells.** (A) Representative IF staining pictures showing the induction of CHOP and BiP upon treatment with sulindac (120  $\mu$ M). (B) Representative immuno-TEM pictures showing the surface expression of BiP (gold particles, 6 nm, highlighted by yellow arrows) upon treatment with sulindac. All treatment was for 24 hours. Scale bar, 400 nm.

NSAID-induced ultrastructural changes on the RER were then examined via TEM. After 24-hour treatment with sulindac, cells were found to have abnormal ER structures (marked by yellow arrows) with elongated membranes.

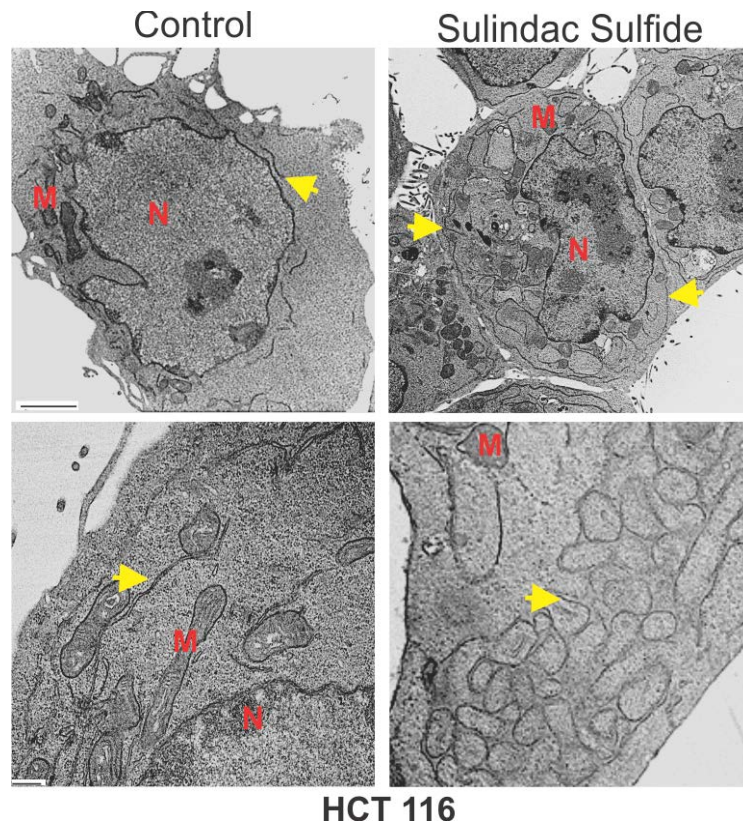


**Figure 7. Sulindac Induces Ultrastructural Changes in the Rough Endoplasmic Reticulum.** TEM pictures showing the cellular ultrastructural differences in the ER upon treatment for 24 hours. Yellow arrows - endoplasmic reticulum, M - mitochondria, N - nucleus. Scale bars for TEM: Upper panel - 2  $\mu$ m, Lower panel - 500 nm.

To confirm that this was not a cell line specific effect, NSAID-induced ER stress was examined in RKO and HT-29 CRC cells. ER stress associated proteins and cell death indicated by caspase 3 activation were induced in both of these cell lines (Fig. 8).

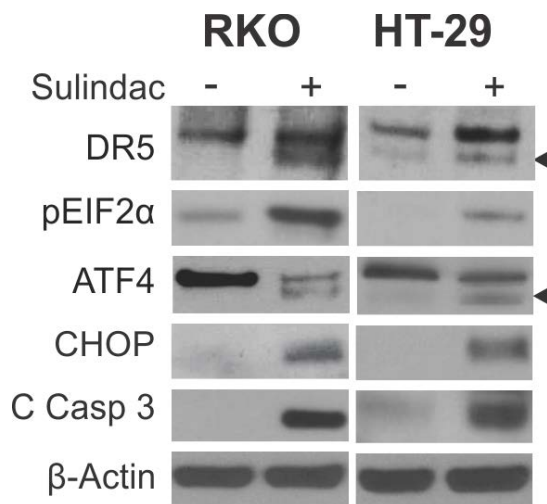


**Figure 8. Sulindac Induces ER Stress in Other CRC Cell Lines.** Western blot showing the induction of proteins associated with ER stress and cell death in RKO and HT-29 cells. RKO cells were treated with 200  $\mu$ M sulindac for 24 hours while HT-29 cells were treated with 200  $\mu$ M sulindac sulfide for 48 hours. C Casp3 - cleaved caspase 3.

### 2.3.2 Several Chemopreventive Agents Induce ER Stress

To investigate whether the ER stress induction is a drug-specific effect, we examined other NSAIDS including indomethacin, celecoxib, naproxen, diclofenac, and sodium (Na) salicylate. Two other chemopreventive agents including acetaminophen and the anti-diabetic drug metformin were also examined. We found that all the agents analyzed induced ER stress. However, the extent to which specific ER stress associated proteins were induced varied depending on the type and dosage of the drug used (Fig. 9).

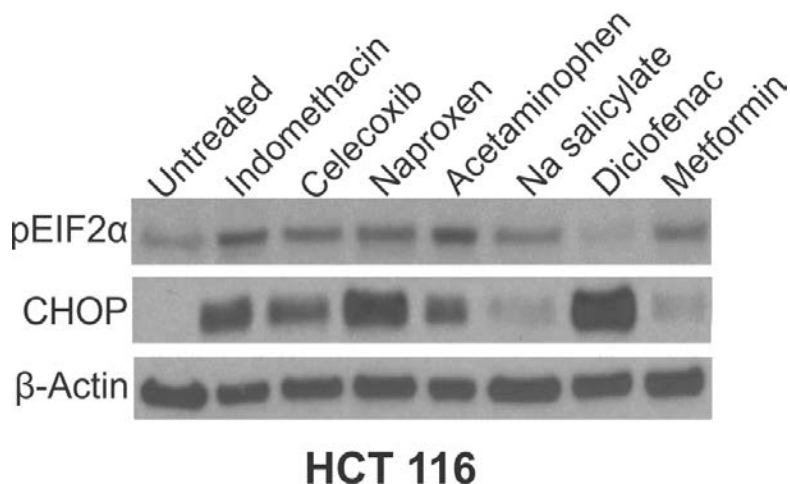


**Figure 9. Several Chemopreventive Agents Induce ER Stress.** Western blot showing the induction of proteins associated with ER stress upon treatment with the indicated chemopreventive agents for 24 hours. Metformin, 500  $\mu$ M, Indomethacin, 500  $\mu$ M, Celecoxib, 80  $\mu$ M, Naproxen, 3 mM, Acetaminophen, 10 mM, Na salicylate, 500  $\mu$ M, Diclofenac, 600  $\mu$ M. Doses were normalized to basal levels required for the induction of apoptosis.

### 2.3.3 Mechanisms of Action Downstream of ER Stress in Response to NSAIDs

We then wanted to examine the mechanisms downstream of NSAID-induced ER stress. Our lab has previously shown that NSAID treatment activates proteins involved in death receptor signaling such as caspase 8 in human advanced adenomas [21]. Several studies by other groups have also shown that some NSAIDs can induce ER stress associated proteins in cell culture and animal models [27]. We therefore wanted to see if there was a correlation between ER stress and death receptor signaling in the same subset of human adenomas described in our previous study [21]. IF staining showed that patients taking NSAIDs had a marked increase in cleaved caspase 8 in their adenomas (Fig. 10A). Subsequently, those adenomas were stained for pEIF2 $\alpha$ , a

common marker for ER stress, and were found to have an increased expression of pEIF2 $\alpha$  (Fig. 10B).

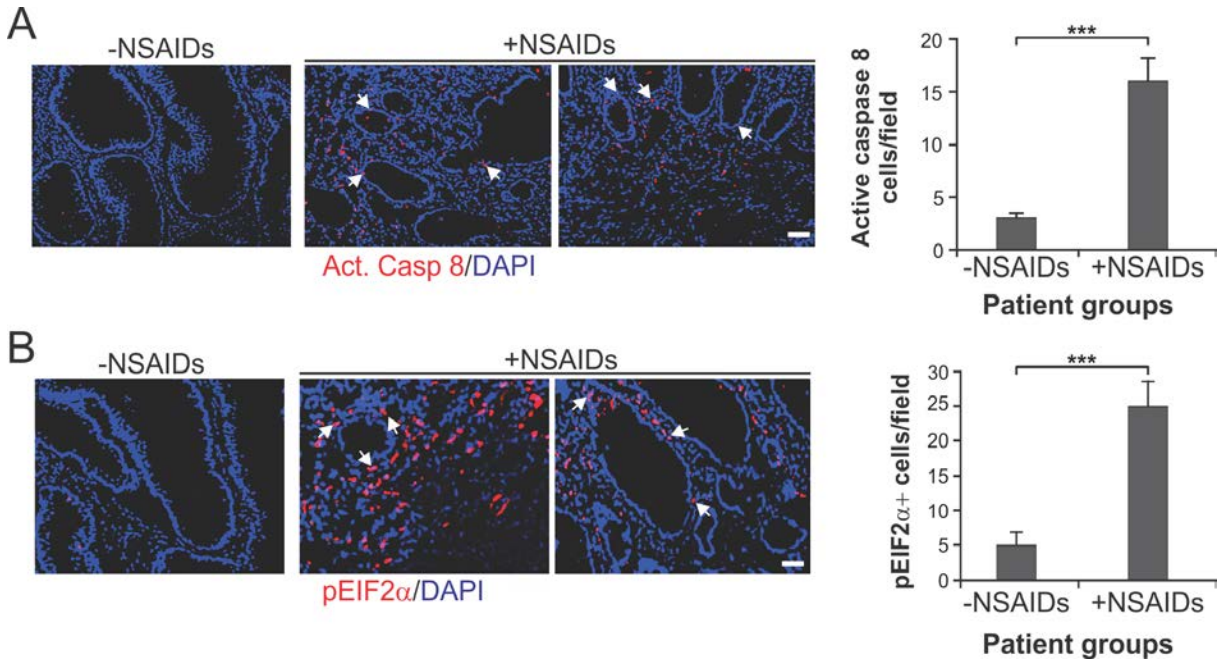


**Figure 10. NSAID Treatment Activates Caspase 8 Signaling and Induces ER Stress in Human Advanced Adenomas.** (A) *Left*, representative pictures of active caspase 8 staining. *Right*, mean numbers + s.d. of positive cells/field. (B) *Left*, representative pictures of pEIF2 $\alpha$  staining. *Right*, mean numbers + s.d. of positive cells/field. n=9 for NSAID treatment, n=7 for untreated. An unpaired t test was used for statistical analysis. \*\*\*P < 0.001.

## 2.4 DISCUSSION

Despite the progress made in cancer prevention research, the mechanisms of action of NSAIDs have still remained obscure [17]. This study aimed to provide novel insight into the molecular mechanisms of action of these drugs in cancer prevention. The main drug used in cell culture

studies is sulindac sulfide, which is the active metabolite of sulindac [17]. Sulindac was shown to have chemopreventive activity against CRC in familial adenomatous polyposis (FAP) patients that are predisposed to developing CRC [17]. There are several classes of NSAIDs, including acetic acid derivatives (sulindac, indomethacin, and diclofenac), salicylates (sodium salicylate and aspirin), and coxibs (celecoxib) among others [27]. These drugs share a common activity of inhibiting COX enzymes. However, COX inhibition does not explain the many COX-independent/downstream effects that have been identified [17].

Some studies have implicated ER stress as a potentially important mechanism in NSAID-mediated chemoprevention in a variety of cell culture and animal models [27, 28]. It has been shown that the induction of the ER stress transcription factor CHOP is not dependent on COX inhibition and prostaglandin production in gastric mucosal cells [28]. Moreover, the addition of prostaglandin did not influence CHOP-induced apoptosis in that model [28]. However, it must be noted that the main cell line model used in our study, HCT 116, does not express the COX-2 enzyme [38]. Therefore, the induction of ER stress seen in those cells was not dependent upon COX-2 inhibition.

We initially examined the protein induction of multiple ER stress markers over 1-24 hours and also verified the changes at the mRNA level. Other methods were also used to confirm these changes in ER stress such as IF and immuno-TEM. Analysis with immuno-TEM revealed a novel finding of the translocation of BiP to the cell surface, which has not been shown in previous studies using this technique. We also confirmed this ER stress induction with other chemopreventive agents. The dosages of these drugs were normalized to the levels needed for induction of apoptosis and are also consistent with those described in the literature and our subsequent pilot experiments.

Although NSAID-induced increases in ER stress associated proteins have been shown before, few studies have looked at the changes in the ultrastructure of the RER. It was found by TEM analysis that the RER becomes swollen (up to five times the volume) during ER stress [23]. This is due to coping mechanisms employed by the cell to deal with the increased protein load. This increased volume creates more space to increase protein folding during the UPR [23]. However, this was not the case in our cells where there was an accumulation of atypical RER with an elongated membrane. Even though the membranes were not swollen, the accumulation of atypical RER would still increase the space available for protein folding during the UPR.

Based on results from a previous study with human adenomas, we decided to look at the correlation between ER stress and cell death in those samples and found a positive correlation. This is a positive indication that will be further delineated to determine the specific mechanisms of ER stress-induced cell death caused by NSAID treatment.

### **3.0 MECHANISMS OF ER STRESS-INDUCED APOPTOSIS CAUSED BY NSAID TREATMENT**

#### **3.1 INTRODUCTION**

##### **3.1.1 BID-Mediated Synthetic Lethality**

Figuring out the specific mechanisms of NSAID-mediated apoptosis would be very helpful for overcoming the main challenges in the field of chemoprevention. In general, apoptosis is activated through the death receptor-mediated extrinsic pathway, the mitochondrial-mediated intrinsic pathway, or both [19]. Recent work from our lab demonstrated that a novel synthetic lethal interaction between DR signaling and alterations in the *APC* tumor suppressor mediated the anti-tumorigenic activity of NSAIDs [21]. Induction of DR5 and subsequent BID-mediated crosstalk between the two apoptotic pathways can kill cancer cells but are not sufficient to induce apoptosis and caspase activation in normal cells [21]. Loss of *APC* in otherwise normal cells triggers NSAID-induced apoptosis [21]. These findings suggested that the induction of DR5 by NSAIDs is critical for these drugs to kill cells with oncogenic alterations. However, how DR5 is upregulated in this system is still unknown.

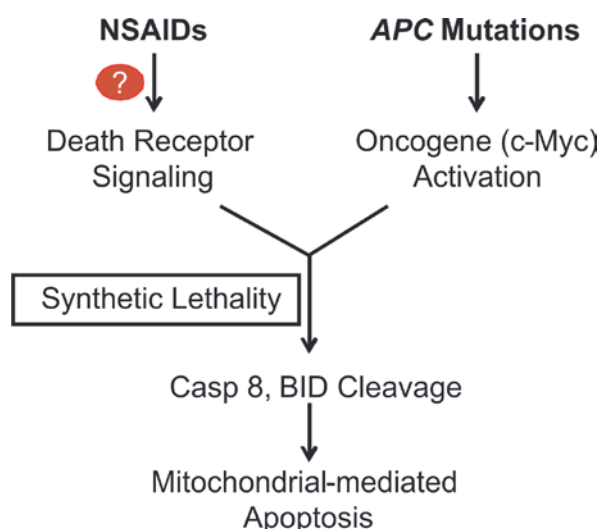


**Figure 11. Model of NSAID-Induced Apoptosis in APC Deficient Normal Cells.** A synthetic lethal interaction is observed with the loss of *APC* and NSAID-induced death receptor signaling in normal colon mucosal cells. Ambiguity remains on how DR5 is upregulated. This figure is modified from the original artwork in Leibowitz et al, PNAS, 2014 [21].

### 3.1.2 NSAIDs and ER Stress-Induced Cell Death

NSAIDs such as indomethacin have been shown to utilize ER stress response-related proteins, particularly CHOP, to induce apoptosis [39]. However, the specific role of ER stress in NSAID-induced cell death is still unclear. Studies have shown that CHOP can suppress the pro-survival protein Bcl-2 and induce pro-apoptotic molecules, such as DR5, PUMA (p53 upregulated modulator of apoptosis), and Bim (Bcl-2-like protein 11) among others depending on the context [37, 40]. Many studies have indicated the induction of DR5 via ER stress proteins as a key mechanism of cell death in CRC cell line models [41]. Furthermore, other anti-cancer drugs were found to induce the transcription factors CHOP and ATF3, resulting in the upregulation of pro-apoptotic proteins such as DR5 [42, 43]. We therefore investigated whether NSAID-induced DR5 expression is mediated through the ER stress response.

## 3.2 MATERIALS AND METHODS

### 3.2.1 Transfection

Cells were seeded in 12-well plates at a confluency of 20-30% 24 hours prior to the transfection of small-interfering RNA (siRNA) duplexes. Cells were transfected with Lipofectamine 2000 according to the manufacturer's instructions. Briefly, siRNAs were transfected in 1X Opti-MEM (Gibco) with 200-400pmol of siRNA (*CHOP*, *ATF4*, *PERK*, *ATF3*, *APC*, and Scrambled) per well of a 12-well plate for 4 hours before the addition of McCoy's 5A or M3 Media (dependent upon cell type). Approximately 24 hours post transfection, drug treatments were performed. The sequences utilized for each siRNA are listed in Table 3.

### 3.2.2 Cell Culture and Drug Treatment

Human CRC cell lines, including HCT 116 (American Type Culture Collection), and their derivatives, were cultured in McCoy's 5A media according the supplier's instructions (Invitrogen). NCM 356 cells and their derivatives were described [44] and cultured in M3 Media according to the supplier's instructions (Incell). Cells were kept in a non-humidified incubator at 37°C with the addition of 5% CO<sub>2</sub>.

Unless otherwise specified, cells were plated at 20-30% density in 12-well plates for drug treatment. Chemicals utilized included: sulindac sulfide (Merck), indomethacin (Sigma), celecoxib (Sigma), acetaminophen (Sigma), metformin (Cayman Chemical Company), naproxen sodium (Apex Bio), diclofenac (sodium salt) (Cayman Chemical Company), sodium salicylate

(Sigma), and Salubrinal (Apex Bio). All agents except for naproxen sodium were diluted in DMSO (Sigma). Naproxen was diluted in distilled water.

### **3.2.3 Reverse-Transcriptase (RT) and Quantitative PCR**

Total RNA was isolated using the Mini RNA Isolation II kit (ZYMO Research) according to the manufacturer's protocol. One microgram of total RNA was used to generate cDNA by using SuperScript III reverse transcriptase (Invitrogen). Real-time PCR was performed using previously described conditions [35]. Primers used in this study are listed in Table 2.

### **3.2.4 Analysis of Cell Viability and Apoptosis**

For crystal violet staining, attached cells were washed with HBSS and stained by incubation at room temperature with a 0.05% crystal violet solution containing 3.7% paraformaldehyde prepared in distilled water. Apoptosis was analyzed by staining floating and attached cells with a solution containing 3.7% formaldehyde, 0.5% Nonidet P-40, and 10 µg/ml Hoechst 33258 (Molecular Probes) in PBS. Condensed and fragmented nuclei were counted via microscopic visualization as previously described [34]. Each sample was analyzed in duplicate with at least 300 cells counted per sample. Results were obtained from at least three independent experiments.

### **3.2.5 Targeting *APC* in NCM 356 cells**

For CRISPR/Cas9-based gene editing, the following sequences were cloned into pSpCas9(BB)-

2A-GFP (Addgene, 48138): human *APC*:

(*APC* Transcript Variant 1 Exon3)

<sup>464</sup>AGCTTAACTTAGATAGCAGTAATTTCCCTGGAGTAAAACTGCGGTCAAAAA  
TGTCCCCTCCGTTCTTATGGAAGCCGGGAAGGATCTGTATCAAGCCGTTCTGGAG  
AGTGCAGTCCTGTTCCCTATGGGTTCAATTTCCAAGAAGAGGGTTTGTAATGGAAGCA  
GAGAAAGTACTGGATATTTAGAAGAAGCTTGAGAAAGAGAG<sup>665</sup>.

CRISPR/Cas9 knock out of *APC* was performed as previously described [45].

### 3.2.6 Mice and Treatment

The procedures for all animal experiments were approved by the Institutional Animal Care and Use Committee of the University of Pittsburgh. C57BL6J *BID*<sup>-/-</sup> (*BID* KO) mice, which were described [46], were crossed with *APC*<sup>Min/+</sup> mice (Jackson Laboratory) to generate *APC*<sup>Min/+</sup> mice with different *BID* genotypes. Female *BID* KO mice were crossed with male *APC*<sup>Min/+</sup> mice (Jackson Laboratory) to generate *APC*<sup>Min/+</sup>/*BID*<sup>+/-</sup> mice. Male *APC*<sup>Min/+</sup>/*BID*<sup>+/-</sup> mice were then crossed to *BID* KO females to generate *APC*<sup>Min/+</sup> littermates with null (-/-) *BID* alleles. Genotyping of *APC* alleles was performed according to the Jackson Laboratory protocol, and genotyping of *BID* alleles was performed as described [46]. All strains were on the C57BL/6 background for more than 10 generations (F10). Mice were housed in micro-isolator cages in a room illuminated from 07:00 to 19:00 hours (12:12-hour light-dark cycle) with access to water and chow *ad libitum*. A similar methodology was used to create *APC*<sup>Min/+</sup>/*CHOP* KO (Jackson Laboratory) mice.

For NSAID treatment, mice were fed AIN-93G diets (Dyets) with or without 200 ppm

sulindac (Sigma) for 1 week for apoptosis analysis or for 2 months for tumor phenotype analysis. After sacrifice of the mice, the small intestinal and colonic tissues were carefully excised and rinsed with saline. The tissue was opened longitudinally and tacked to a foam board for fixation overnight in 10% formalin. Tissues were then rolled up into “swiss rolls” and embedded in paraffin.

**3.2.6.1 Short-Term ER Stress Experiments.** 4-week-old mice were placed into four groups: control, Salubrinal, sulindac, and Salubrinal/sulindac. I.p. injections of 1mg/kg/day of Salubrinal (Apex Bio) were given two days before the mice were put on their respective diets. Salubrinal (10mg/ml) was freshly diluted in 50/50 Polyethylene glycol (PEG)/saline solution before administration. Following this, i.p. injection of salubrinal at 1 mg/kg was given every day for 7 days. Tissues from the small intestine and colon were collected for staining as described previously [21]. Additionally, mucosal scrapings were collected from small intestinal tissue for western blotting.

**3.2.6.2 Long-Term ER Stress Experiments.** Mice were placed in the above mentioned groups in 3.2.6.1. At 4-6 weeks of age, they were placed under the same conditions as those in the short-term experiment. They were then placed back on normal diet and injections stopped until they were 10 weeks of age. Then the treatment was re-initiated for a week. Mice were sacrificed at 11 weeks when intestinal polyps were visible. Tissues were collected for staining and adenoma numbers were counted under a dissecting microscope.

### **3.2.7 Statistical Analysis**

Statistical analyses were performed by using GraphPad Prism IV software. Differences were considered significant if the probability of the difference occurring by chance was less than 5 in 100 ( $P < 0.05$ ). Multiple comparisons of the responses were analyzed by one-way ANOVA and either Dunnett's or Tukey's post hoc test, whereas those between two groups were made by unpaired t test. All statistical tests were two-tailed.

### 3.3 RESULTS

#### 3.3.1 Attenuation of ER Stress Inhibits Sulindac-Induced Death Receptor Signaling and Cell Death

Based on the correlation seen between the death receptor pathway and ER stress in the patient samples in chapter two (Fig. 10), pilot experiments were conducted by examining NSAID-induced death receptor signaling upon knockdown of BiP, ATF3, and CHOP (Fig. 12). As shown in the previous chapter, these proteins were strongly upregulated in the treated cells without knockdown. We found that inhibition of the transcription factor CHOP had the greatest influence on death receptor signaling (Fig. 12B-C). This directed us to focus on the PERK/EIF2 $\alpha$ /CHOP pathway.

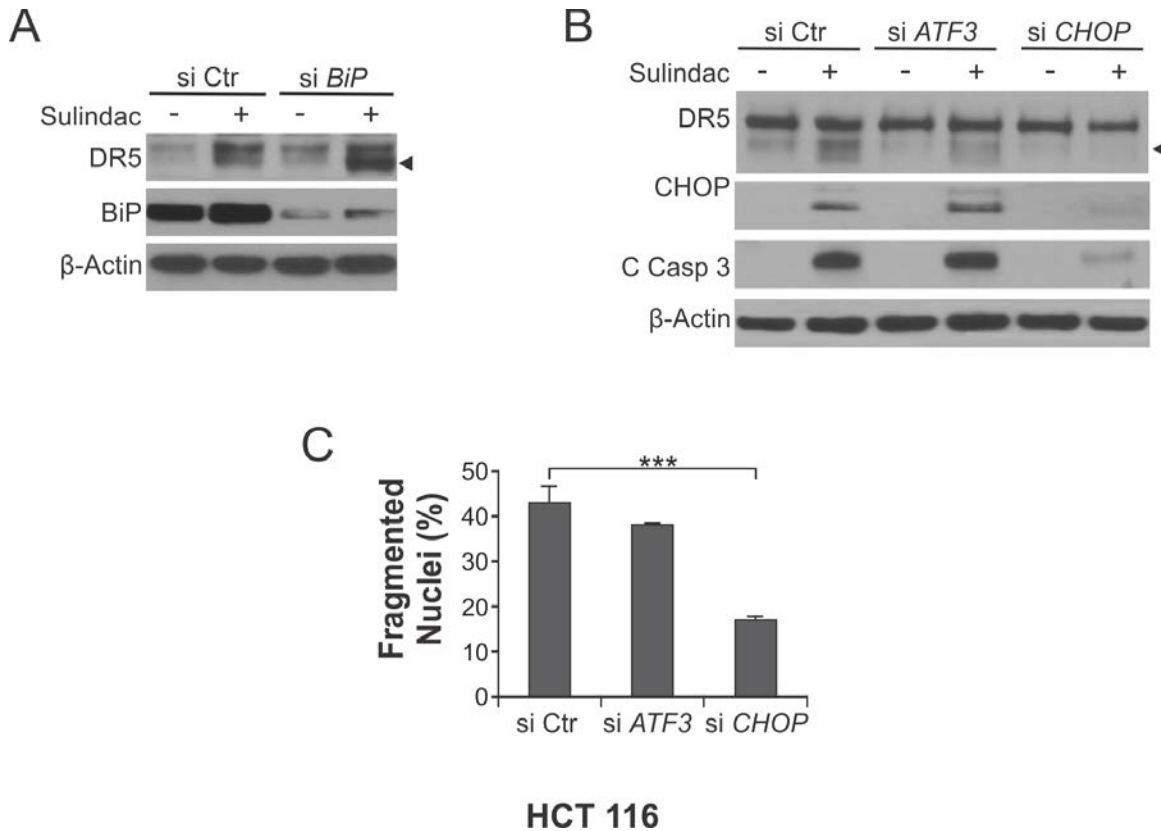


**Figure 12. Pilot Experiment Showing the Influence of Inhibiting Various ER Stress Associated Proteins on NSAID-Induced Death Receptor Signaling.** (A) Western blots showing the influence of BiP knockdown on sulindac-induced death receptor signaling. (B) Western blots for comparing the influence of ATF3 and CHOP knockdown on sulindac-induced cell death. (C) Influence of ATF3 and CHOP inhibition on NSAID-induced cell death as examined by counting condensed and fragmented nuclei after staining with Hoechst 33258. All cells were treated with 120  $\mu$ M sulindac for 24 hours. Error bars represent the s.d. of three independent experiments. ANOVA and Dunnett's post hoc test were used for statistical analysis. \*\*\*P < 0.001.

Initially, ER stress was inhibited pharmacologically with the inhibitor Salubrinal (Sal). This is a selective eIF2 $\alpha$  de-phosphorylation inhibitor, and it is known to protect cells from ER stress-induced apoptosis [47]. Upon pretreatment with Sal, there was a significant reduction seen in death receptor-mediated cell death. There was also a decreased expression of CHOP,

indicating a reduction in ER stress (Fig. 13A). Furthermore, there was a lower expression of cleaved caspase 3 (C Casp 3) and DR5 (Fig. 13A). The inhibition of apoptosis was further confirmed with Hoechst staining (Fig. 13B).

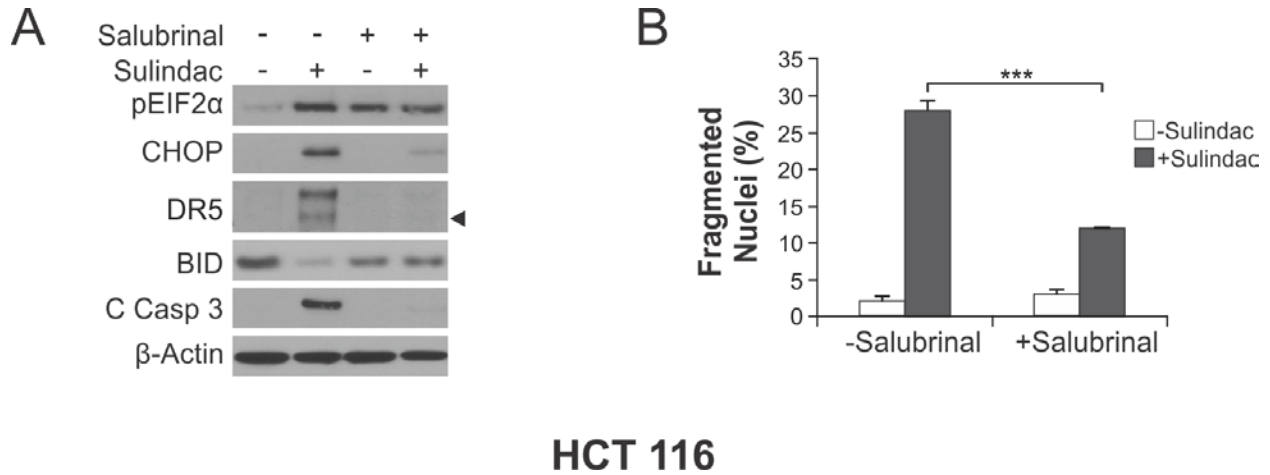


**Figure 13. Attenuation of ER Stress Pharmacologically along the PERK/EIF2 $\alpha$ /ATF4/CHOP Pathway Significantly Reduces the Sulindac-Induced Death Receptor Signaling and Subsequent Cell Death.** ER stress was inhibited chemically with 1  $\mu$ M Salubrinal for 1.5 hours, followed by treatment with 120  $\mu$ M sulindac sulfide for 24 hours. (A) Western blot showing changes in the induction of proteins involved in ER stress-associated cell death. (B) Changes in apoptosis as analyzed by counting condensed and fragmented nuclei after nuclear staining with Hoechst 33258. Results were expressed as means + s.d. of three independent experiments. An unpaired t test was used for statistical analysis. \*\*\*P < 0.001.

ER stress was then inhibited with *PERK*, *ATF4*, and *CHOP* siRNA, which target proteins acting along the PERK signaling pathway (Fig. 14A-C). These siRNAs were selected based on the results of the pilot study (Fig. 12). Similar results as seen with Salubrinal were obtained upon siRNA knockdown (Fig. 14). CHOP inhibition had the most significant influence on death

receptor-mediated cell death. This is attributed to CHOP's ability to bind to the promoter of *DR5* and directly regulate its expression [39]. Knockdown of *ATF4* (directly upstream of CHOP) also had a substantial impact on cell death while *PERK* (the most upstream of the three) had the least significant effect on cell death. This difference was likely due to CHOP/*DR5* induction by alternative pathways such as that mediated by ATF6 induction [26].

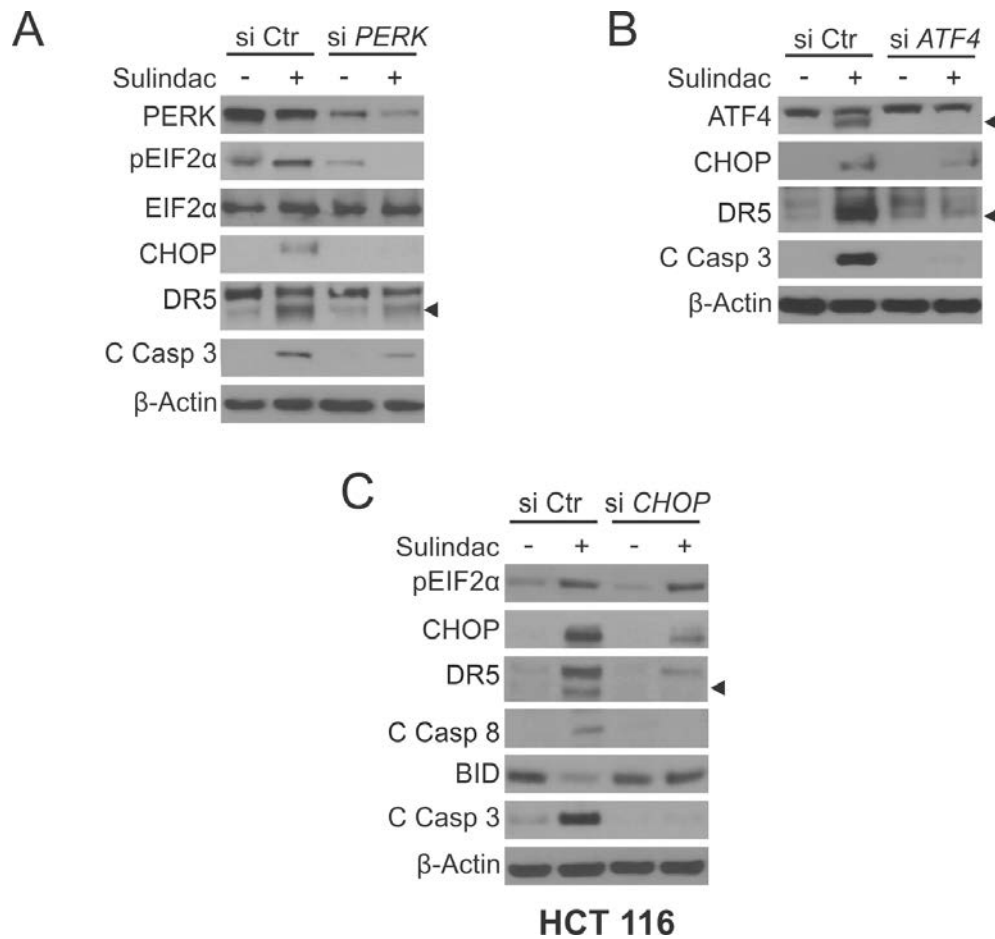


**Figure 14. Attenuation of ER Stress Using siRNAs to Target the PERK/EIF2 $\alpha$ /ATF4/CHOP Pathway Significantly Reduces the Sulindac-Induced Increase of Proteins Associated with the DR5 Signaling Pathway.** ER stress was inhibited using siRNAs to decrease (A) PERK, (B) ATF4, and (C) CHOP protein expression. Cells were then treated with 120  $\mu$ M sulindac sulfide for 24 hours. Western blots were used to examine the changes in protein expression.

These changes were not only observed at the protein level but also at the mRNA level (Fig. 15).

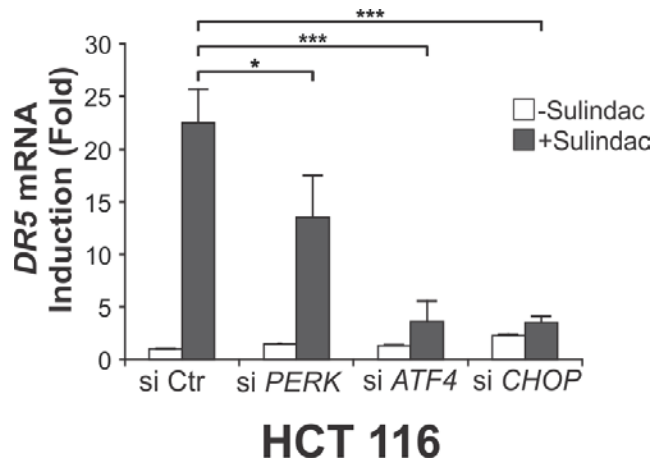
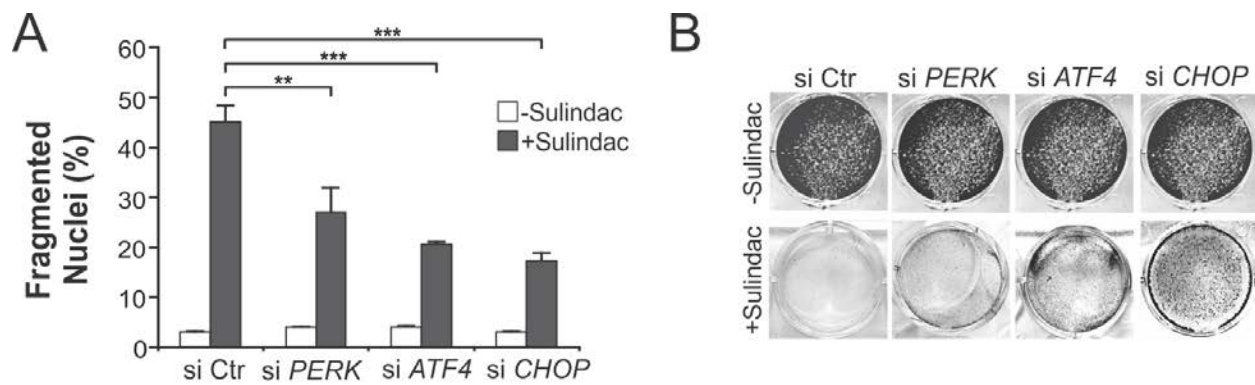


**Figure 15. PERK/ATF4/CHOP Knockdown in Sulindac-Treated Cells Negatively Impacts the Induction of *DR5* mRNA.** ER stress was inhibited with PERK/ATF4/CHOP siRNAs, and cells were then treated with 120  $\mu$ M sulindac sulfide for 24 hours. Changes in mRNA induction were examined via RT-PCR. Results were expressed as means + s.d. of three independent experiments. ANOVA and Dunnett's post hoc test were used for statistical analysis. \* $P < 0.05$ , \*\* $P < 0.01$ , \*\*\* $P < 0.001$ .

Upon the inhibition of ER stress, changes in sulindac-induced apoptosis were also examined. As expected, we found that there was a significant reduction of condensed and fragmented nuclei observed following Hoechst staining (Fig. 16A). This highlighted the importance of the PERK/ATF4/CHOP pathway to ER stress-induced apoptosis. Additionally, cellular viability was rescued the most upon CHOP knockdown, and also modestly with its upstream regulators ATF4 and PERK (Fig. 16B).



## HCT 116

**Figure 16. ATF4/CHOP Inhibition Significantly Decreased Cell Death and Increased Cell Survival upon Sulindac Treatment.** ER stress was inhibited with siRNA against *PERK*, *ATF4*, or *CHOP*, and cells were then treated with 120  $\mu$ M sulindac sulfide. (A) After 24-hour treatment, apoptosis was analyzed by counting condensed and fragmented nuclei after nuclear staining with Hoechst 33258. (B) Crystal violet staining was used to observe cellular viability following the respective knockdowns and treatments. Results in (A) were expressed as means + s.d. of three independent experiments. ANOVA and Dunnett's post hoc test were used for statistical analysis. \*\* $P < 0.01$ , \*\*\* $P < 0.001$ .

We then examined the influence of *ATF4* and *CHOP* knockdown on sulindac treatment in two other cell lines, HT-29 and RKO. Decreased apoptosis was also observed in these cell lines (Fig. 17).

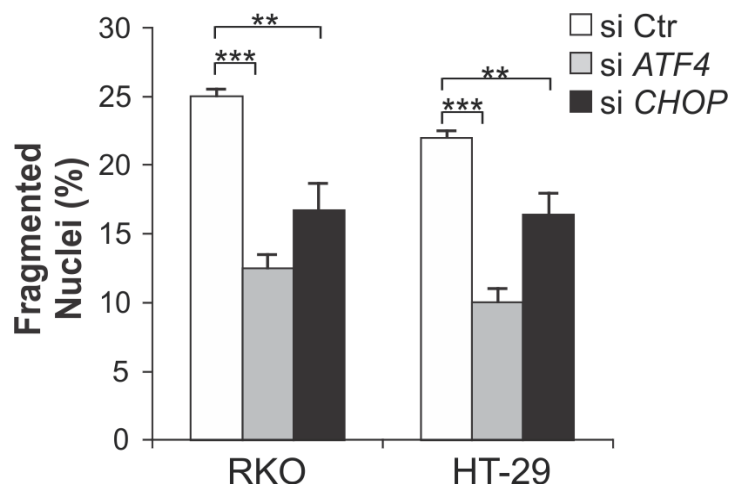


**Figure 17. *ATF4* and *CHOP* Knockdown Significantly Decreased Apoptosis in RKO and HT-29 Cells.** ER stress in RKO and HT-29 cells was inhibited with siRNA against *ATF4* or *CHOP*. RKO cells were treated with 200  $\mu$ M sulindac sulfide for 24 hours while HT-29 cells were treated with 200  $\mu$ M sulindac sulfide for 48 hours. Apoptosis was analyzed by counting condensed and fragmented nuclei after nuclear staining with Hoechst 33258. Results were expressed as means + s.d. of three independent experiments. ANOVA and Dunnett's post hoc test were used for statistical analysis. \*\* $P < 0.01$ , \*\*\* $P < 0.001$ .

As mentioned previously, our earlier work had underscored the importance of BID in NSAID-induced apoptosis [21]. In order to determine the role of BID, wild-type (WT) and *BID* knockout (KO) HCT 116 cells were compared for NSAID-induced ER stress, death receptor signaling, and apoptosis. Even though CHOP and DR5 were still induced, there was a significant reduction in apoptosis observed in *BID* KO cells (Fig. 18), highlighting the pivotal role of BID downstream of ER stress and death receptor signaling in apoptosis induction.

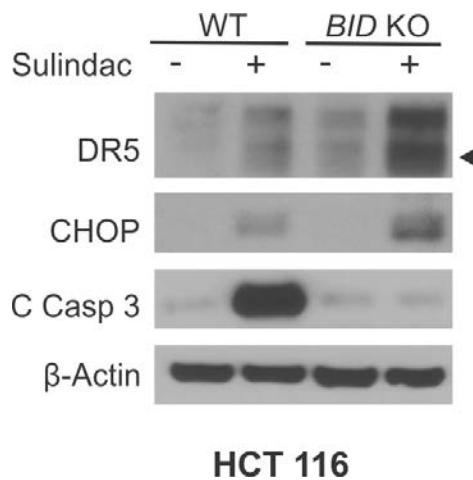


**Figure 18. ER Stress-Mediated Apoptosis Induced by NSAIDs is Dependent on BID.** Western blot showing the influence of *BID* KO on NSAID-induced ER stress and death receptor signaling after 24-hour sulindac treatment (120  $\mu$ M).

### 3.3.2 The Role of ER Stress-Mediated Death Receptor Signaling in Apoptosis Induced by Other Chemopreventive Agents

The proposed mechanism of action of NSAIDs (ER stress and DR5-mediated cell death) was also examined using other chemopreventive agents, such as indomethacin, celecoxib, diclofenac, and sodium salicylate, as well as acetaminophen and the anti-diabetic drug metformin. It was found that death receptor signaling also played a crucial role in apoptosis induced by these other chemopreventive agents (Fig. 19).

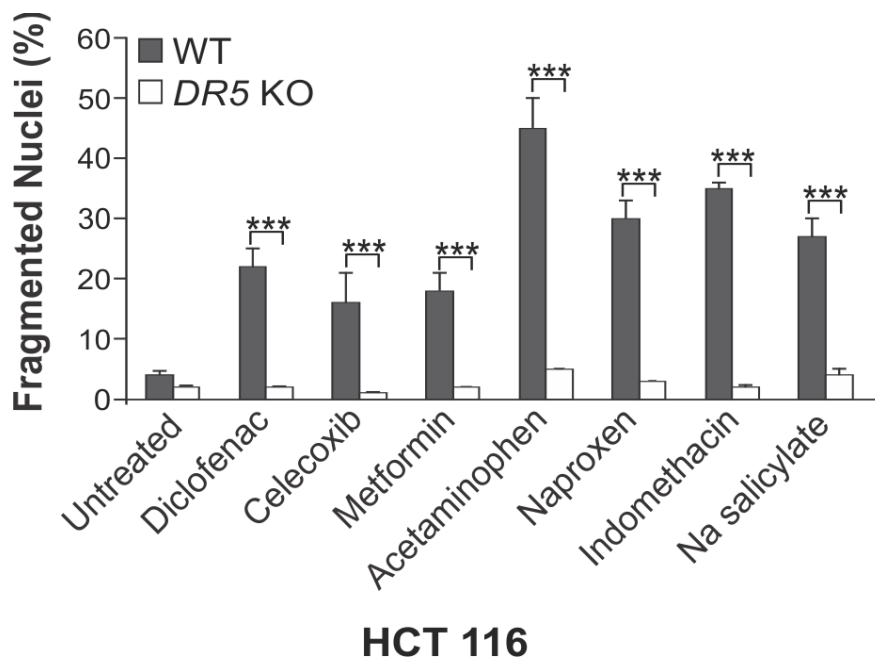


**Figure 19. The Role of DR5 in the Apoptotic Response to other CRC Chemopreventive Agents.**

Influence of *DR5* KO on NSAID-induced cell death as examined by counting condensed and fragmented nuclei after staining with Hoechst 33258 after treating WT and *DR5* KO HCT 116 cells for 24 hours. Metformin 500  $\mu$ M, indomethacin 500  $\mu$ M, celecoxib 80  $\mu$ M, naproxen 3mM, acetaminophen 10 mM, Na salicylate 500  $\mu$ M, diclofenac 600  $\mu$ M. Means are reported + s.d. of three independent experiments. ANOVA and Tukey's post hoc test were used for statistical analysis. \*\*\*P < 0.001.

Furthermore, knockdown of *CHOP* more dramatically reduced apoptosis induced by the drugs that stimulated CHOP protein expression at higher levels, such as naproxen and diclofenac (Fig. 20B).

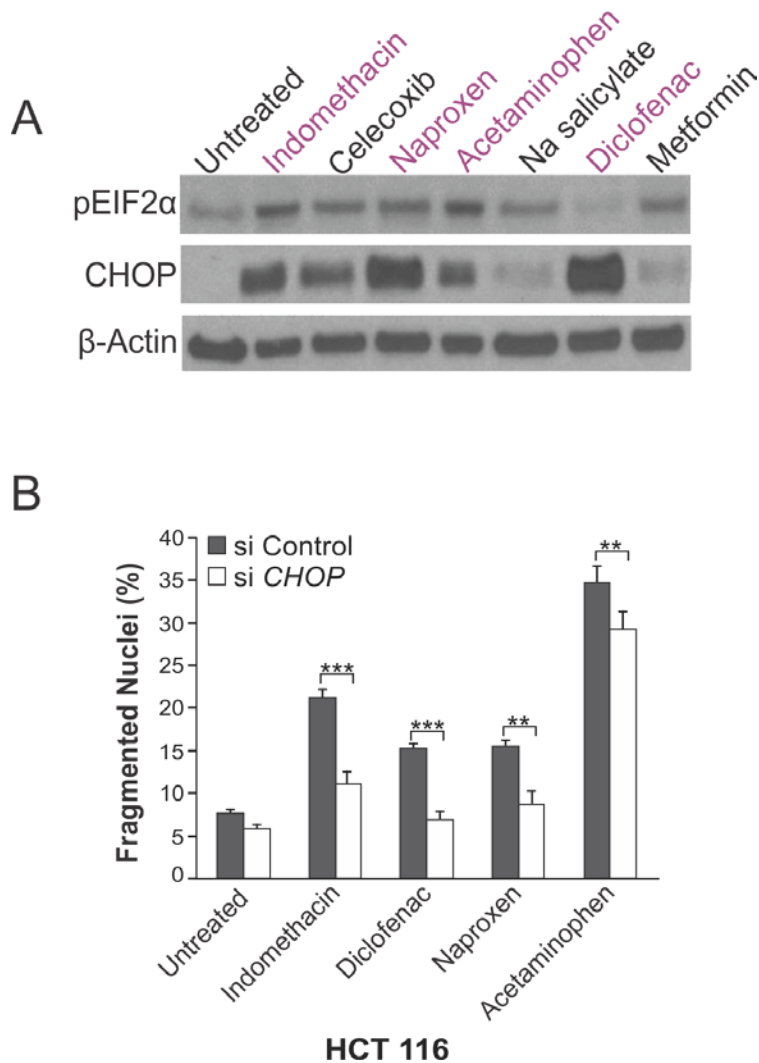
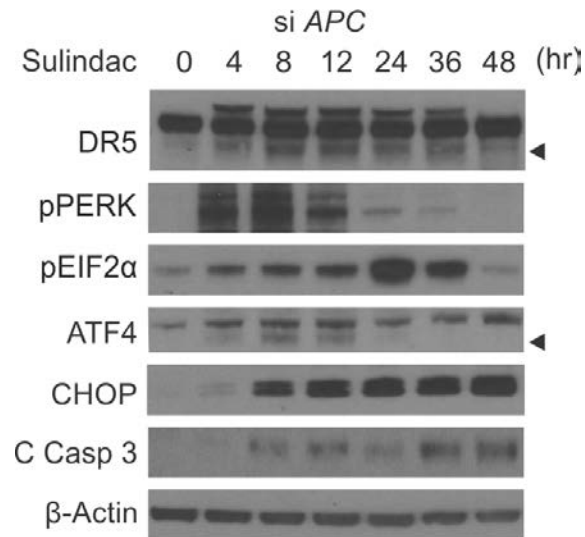


**Figure 20. The Role of ER Stress-Mediated Death Receptor Signaling in the Apoptotic Response to Other Chemopreventive Agents.** (A) Western blots of indicated proteins in HCT 116 cells upon 24-hour treatment with the indicated chemopreventive agents. (B) Influence of *CHOP* knockdown on NSAID-induced cell death analyzed by counting condensed and fragmented nuclei after staining with Hoechst 33258 after 16 hours of treatment. Metformin, 500  $\mu$ M, Indomethacin, 500  $\mu$ M, Celecoxib, 80  $\mu$ M, Naproxen, 3 mM, Acetaminophen, 10 mM, NA Salicylate, 500  $\mu$ M, Diclofenac, 600  $\mu$ M. Means are reported with s.d. of three independent experiments. ANOVA and Tukey's post hoc test were used for statistical analysis. \*\* $P < 0.01$ , \*\*\* $P < 0.001$ .

### 3.3.3 NSAID-Induced and ER Stress-Associated-Cell Death is Dependent on the Loss of the Tumor Suppressor *APC* in Normal Epithelial Cells

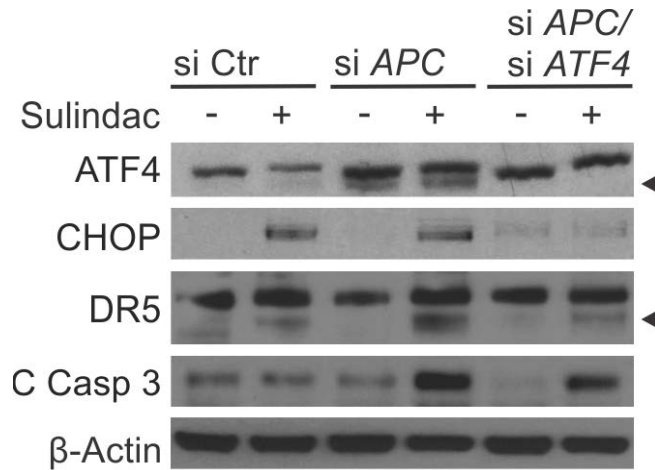
NSAIDs employ their anticancer effect by selectively killing pre-neoplastic cells [21]. Our previous studies have used NCM 356 cells to examine this effect. NCM 356 cells are normal intestinal epithelial cells that are known to have a functional *APC* pathway [48]. In our previous work, a synthetic lethal interaction was found between death receptor signaling (mediated by BID truncation) and the loss of *APC* [21]. Even though NSAID-induced death receptor signaling was initiated in the NCM 356 cells, significant cell death only occurred upon subsequent loss of *APC*. We examined the influence of ER stress and found that transient *APC* depletion in NCM 356 cells significantly induced ER stress-associated proteins (Fig. 21).



### NCM 356

**Figure 21. Sulindac Induces ER Stress in a Time-Dependent Manner in *APC*-Deficient NCM 356 Cells.** Western blot showing the induction of ER stress-associated proteins in transiently *APC*-deficient NCM 356 cells using siRNA and treated with 120 μM sulindac over the indicated time points.

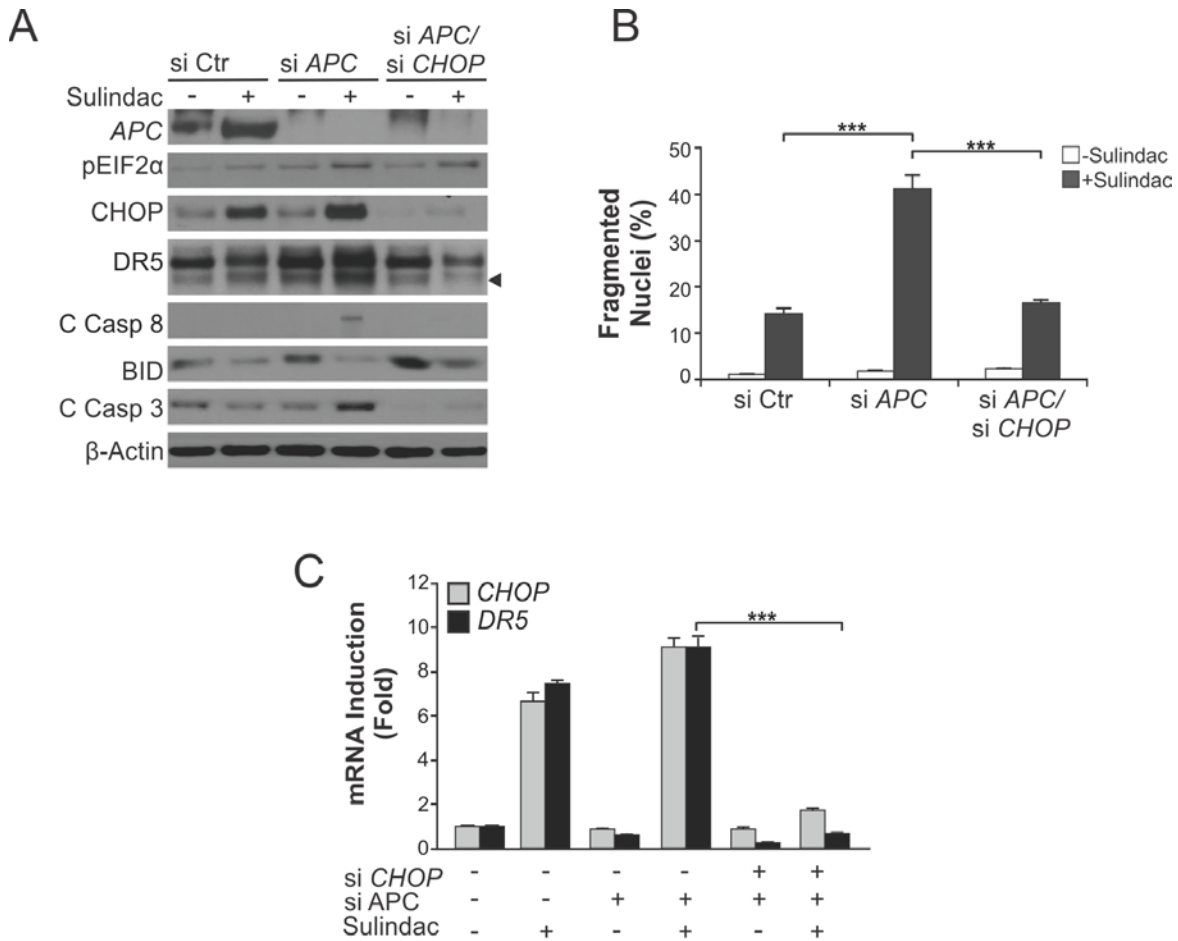
We found that sulindac treatment also induced ER stress in *APC*-competent NCM 356 cells, but little cell death was detected (Fig. 22). Upon the loss of *APC*, there was an increase in ER stress (*ATF4* expression) and a significant increase in apoptosis. ER stress was then inhibited using *ATF4* siRNA, which caused a significant drop in death receptor signaling and cell death (Fig. 22).



## NCM 356

**Figure 22. NSAID-Induced and ER Stress-Associated Cell Death is Dependent on the Loss of Tumor Suppressor *APC* in Normal Epithelial Cells.** NCM 356 cells transfected with indicated siRNA were then treated with 120  $\mu$ M sulindac sulfide for 48 hours. Protein expression was analyzed by Western blotting.

CHOP inhibition led to a greater reduction in DR5 signaling at both the protein and mRNA levels and in subsequent apoptosis in NCM 356 cells with *APC* knockdown (Fig. 23). This indicates that ER stress, specifically CHOP, was important to the second arm (death receptor signaling) of this synthetic lethal interaction.



### NCM 356

**Figure 23. CHOP Knockdown Significantly Attenuates NSAID-Induced Death in NCM 356 Cells Deficient in APC.** NCM 356 cells transfected with the indicated siRNAs were then treated with 120  $\mu$ M sulindac sulfide for 48 hours. (A) Protein expression was analyzed by Western blotting. (B) Apoptosis was analyzed by counting condensed and fragmented nuclei after Hoechst 33258 staining. (C) *CHOP* and *DR5* mRNA expression was analyzed by RT-PCR. Results in (B) and (C) were expressed as means + s.d. of three independent experiments. ANOVA (Tukey's post hoc test) and unpaired t tests were used for statistical analysis. \*\*\* $P < 0.001$ .

Pharmacological inhibition of ER stress by Salubrinal pretreatment similarly suppressed sulindac-induced death receptor signaling and apoptosis (Fig. 24).

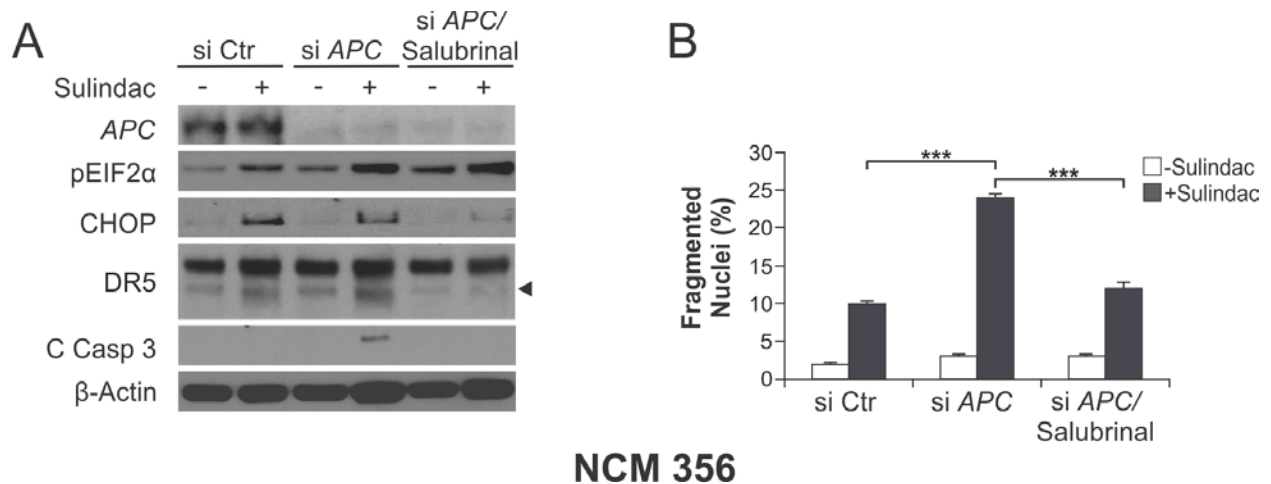


**Figure 24. Pharmacological Inhibition of NSAID-Induced ER Stress Impacts Death Receptor Signaling in NCM 356 Cells Deficient in APC.** NCM 356 cells transfected with indicated the siRNAs with or without Salubrinol pretreatment were treated with 120  $\mu$ M sulindac sulfide for 48 hours. (A) Western blots of the indicated proteins. (B) Apoptosis analyzed by counting condensed and fragmented nuclei after Hoechst 33258 staining. Results were expressed as means + s.d. of three independent experiments. ANOVA and Tukey's post hoc test were used for statistical analysis. \*\*\*P < 0.001.

We also wanted to create a stable system of APC KO NCM 356 cells that could be used in later studies. CRISPR/cas9 was used to generate three single clones. To confirm knockouts, RT-PCR and western blotting were performed (Fig. 25A-B). The influence of ER stress inhibition was also examined in these cells to ensure that results were similar to those in APC knockdown cells (Fig. 25C).

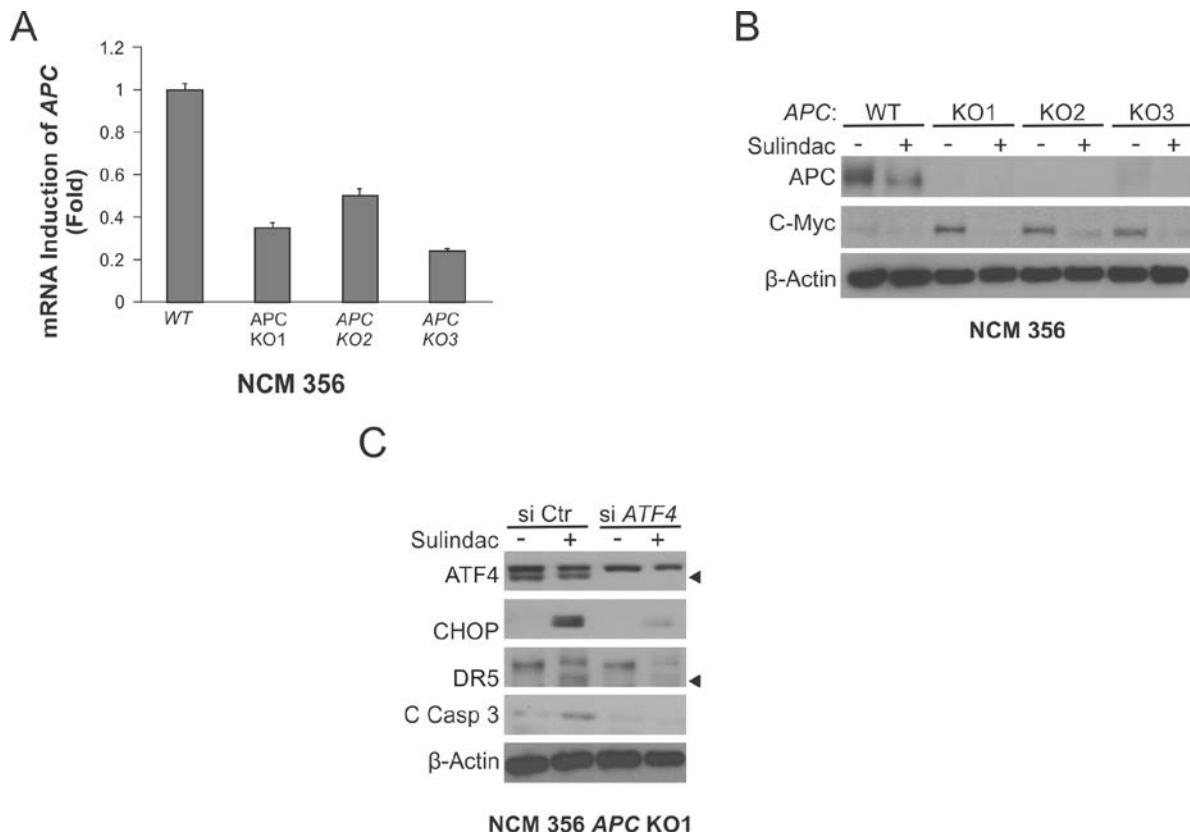


**Figure 25. The Role of ER Stress-Mediated Death Receptor Signaling in Stable APC KO NCM 356 Cells.** (A) RT-PCR confirming *APC* reduction in KO NCM 356 cells. (B) Western blot showing the influence of *APC* KO in NCM 356 cells upon treatment with 120  $\mu$ M sulindac sulfide for 48 hours. (C) ER stress was inhibited genetically via *ATF4* siRNA in *APC* KO NCM 356 cells (clone 1). Results in (A) were expressed as means + s.d. of three independent experiments.

### 3.3.4 Inhibition of ER Stress by Salubrinal Inhibits NSAID-Mediated Apoptosis of Intestinal Stem Cells and Chemoprevention *in Vivo*.

To determine the effect of ER stress inhibition on the *in vivo* activity of sulindac, 4-week-old *APC*<sup>Min/+</sup> mice were treated with sulindac alone, or in combination with the ER stress inhibitor

Salubrinal for 1 week. Changes in ER stress were examined via the protein expression of CHOP in the small intestine (Fig. 26).

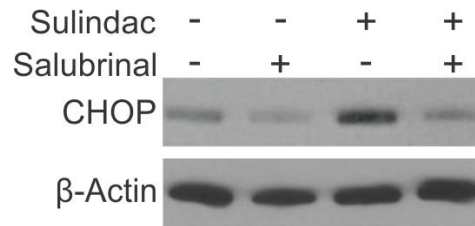


**Figure 26. NSAID-Induced ER stress is Attenuated by Salubrinal in  $APC^{Min/+}$  Mice.** 4-week-old  $APC^{Min/+}$  mice were treated with Sulindac (200 ppm) alone, or in combination with the ER stress inhibitor Salubrinal (1 mg/kg/24 hours) for 1 week. Changes in the expression of CHOP were examined on mucosal scrapings of the small intestinal tissues of control and treated mice. N=3 per group.

We found that sulindac induced a significant increase in cleaved caspase 3, indicative of apoptosis, in the small intestinal crypts of these mice (Fig. 27A-B). Inhibition of ER stress significantly reduced the level of cleaved caspase 3 (Fig. 27A). Similar observations as in Fig. 27B were made in the colon (Fig. 27C).

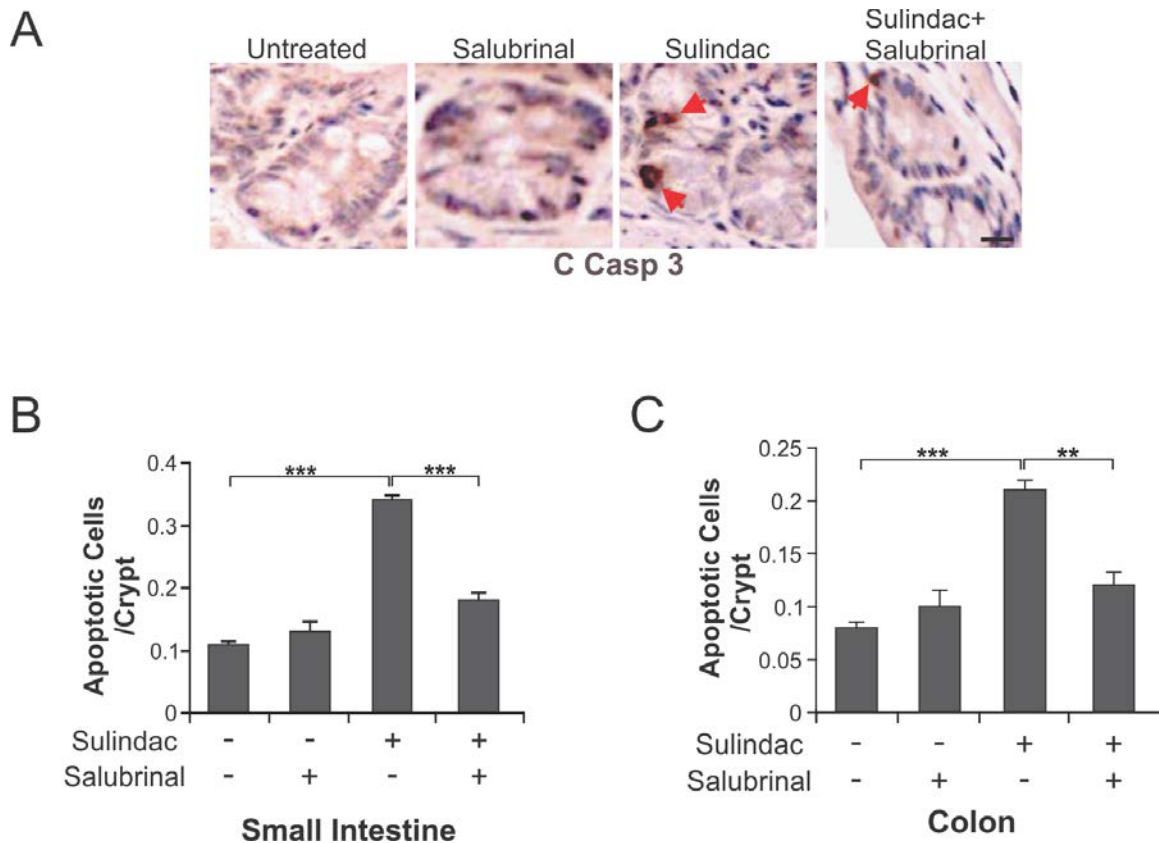


**Figure 27. Attenuation of ER Stress by Salubrinal Inhibits NSAID-Mediated Apoptosis *in Vivo*.** 4-week-old  $APC^{Min/+}$  mice were treated with sulindac (200 ppm) alone, or in combination with the ER stress inhibitor Salubrinal (1 mg/kg/24 hours) for 1 week. (A) Representative staining pictures of small intestinal sections, with arrows indicating example cells with positive staining. (B) Mean + s.d. of positive signals in the small intestinal crypts. (C) Mean + s.d. of positive signals in the colonic crypts. Scale bars, 25  $\mu$ m. N=3 per group. ANOVA and Tukey's post hoc test were used for statistical analysis. \*\*P < 0.01 \*\*\*P < 0.001.

Long-term experiments were then conducted to examine general changes in chemoprevention. Four-week-old  $APC^{Min/+}$  mice were treated with sulindac alone, or in combination with Salubrinal for 2 weeks. After a 4-week break, the treatment schedule was reinitiated for 1 week before mice were sacrificed (week 11). As expected, the administration of

sulindac resulted in a drastic reduction in tumor phenotype in the small intestine of the treated mice (Fig. 28A-B). Upon the introduction of Salubrinal, this reduction was significantly attenuated (Fig. 28A-B). Similar changes were observed in the colon (Fig. 28C).

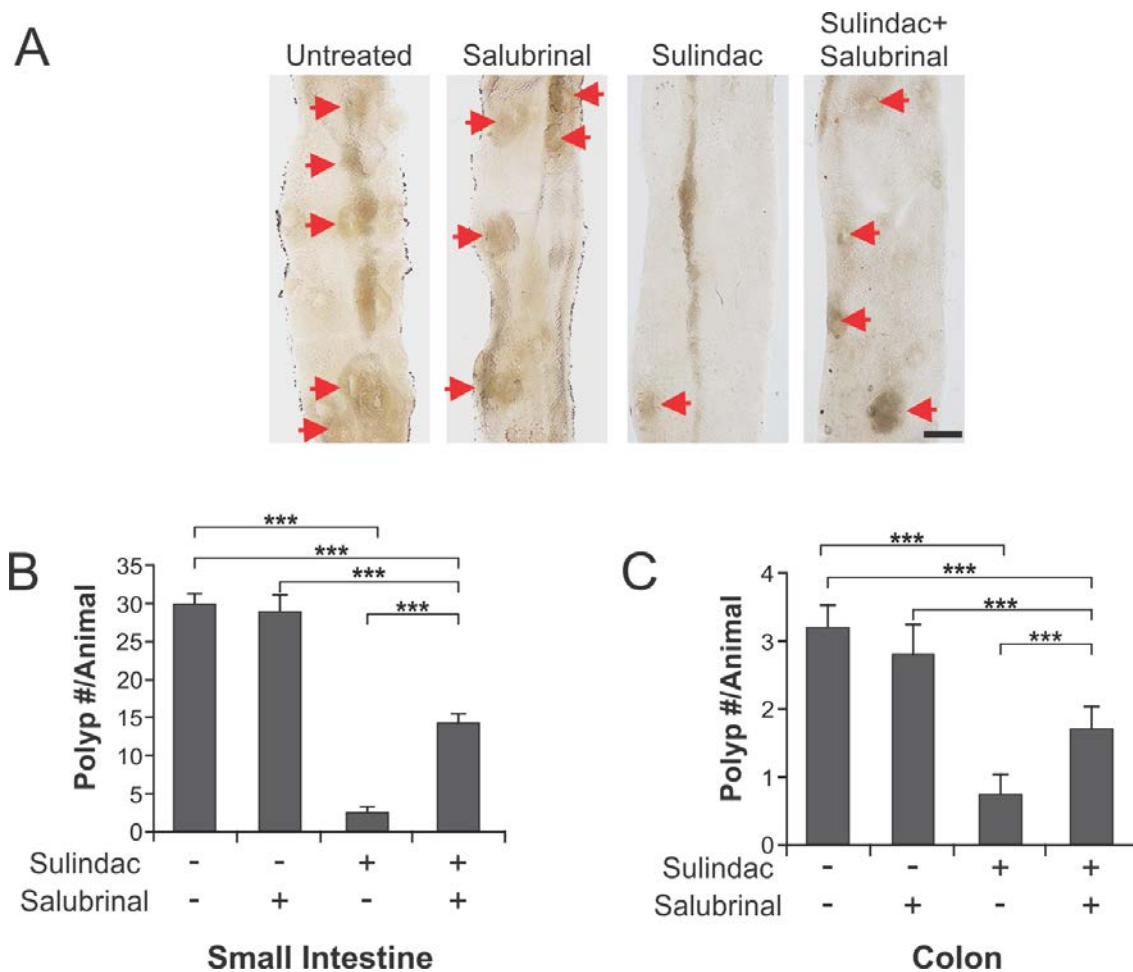


**Figure 28. Attenuation of ER Stress via Salubrinal Inhibits NSAID-Mediated Chemoprevention.**

4-week-old  $APC^{Min/+}$  mice were treated with sulindac (200 ppm) alone, or in combination with Salubrinal (1 mg/kg/24 hours) for 2 weeks. 4 weeks later, treatment was reinitiated for 1 week before sacrificing mice at week 11. (A) Representative images of the small intestine of control and treated mice, with arrows indicating microscopic lesions (polyps/adenomas). (B) Mean numbers + s.d. of small intestinal adenomas (>0.5 mm in diameter). (C) Mean numbers + s.d. of colonic adenomas (>0.5 mm in diameter). Scale bars, 2 mm. N=4 per group. ANOVA and Tukey's post hoc test were used for statistical analysis. \*\*P < 0.01 \*\*\*P < 0.001.

We also tried to inhibit ER stress genetically in the animal models via the creation of a genetically-engineered mouse model (GEMM). We crossed  $APC^{Min/+}$  mice with  $CHOP$  KO mice

to create  $APC^{Min/+}/CHOP$  KO mice. Deletion of  $CHOP$  caused the  $APC^{Min/+}$  mice to develop fewer tumors (Fig. 29A). Although a significant reduction in tumors upon NSAID treatment was observed (Fig. 29A), the overall chemopreventive effects of sulindac were still significantly attenuated in  $APC^{Min/+}/CHOP$  KO mice than in  $APC^{Min/+}$  mice (Fig. 29B).

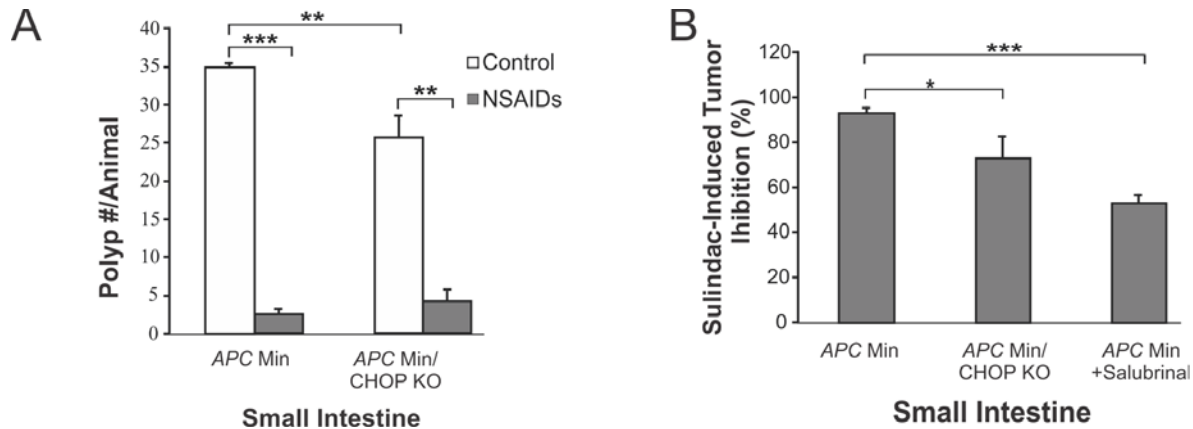


**Figure 29. The Influence  $CHOP$  KO on NSAID-Mediated Tumor Prevention in  $APC^{Min/+}$  Mice.** (A) Mean numbers + s.d. of small intestinal adenomas (>0.5 mm in diameter) in the control and NSAID-treated  $APC^{Min/+}$  and  $APC^{Min/+}/CHOP$  KO mice. (B) Mean numbers + s.d. of tumor inhibition caused by sulindac in  $APC^{Min/+}$ ,  $APC^{Min/+}/CHOP$  KO, and  $APC^{Min/+}$  + Salubrinal-treated mice. (Percent Inhibition was calculated by examining the fraction of tumors eliminated in treatment groups compared to the total number of tumors in control groups). N=4 per group. ANOVA and Tukey's (A) Dunnett's (B) post hoc test were used for statistical analysis. \*P < 0.05, \*\*P < 0.01, \*\*\*P < 0.001.

### 3.4 DISCUSSION

Our previous work highlighted the importance of death receptor signaling and BID in NSAID-induced apoptosis [21]. However, there was still much uncertainty in the mechanisms via which

DR5 was upregulated. ER stress was a potential candidate as it had been implicated in death receptor signaling [37, 41]. Furthermore, our results from the analysis of human advanced adenomas clearly showed that there was a correlation between death receptor signaling mediated by caspase 8/BID and ER stress. Moreover, the NSAID-induced upregulation of ER stress seen in chapter two was in tandem with DR5 induction, which prompted us to examine the specific mechanisms regulating DR signaling.

Based on the substantial induction of BiP, ATF3, and CHOP after NSAID treatment, we knocked down these proteins to determine their role in ER stress induction. Once again, sulindac greatly induced DR5, and the most significant downregulation was seen upon the knockdown of CHOP. This highlighted the importance of the PERK/EIF2 $\alpha$ /ATF4/CHOP pathway. Therefore we focused on this pathway via pharmacological (Salubrinal) and genetic inhibition (*PERK/ATF4/CHOP* siRNAs). In both cases, attenuated ER stress resulted in a significant reduction in DR5 expression and BID cleavage. Furthermore, the importance of BID in relation to this ER stress-induced cell death was confirmed.

We also found that these mechanisms were neither cell line-specific nor sulindac-specific, although different drug concentrations and time periods had to be used to treat HCT 116, RKO, and HT-29 cells. Different CRC cell lines have a different set of mutations that can influence their drug responses [49]. We also expanded our analysis to other chemopreventive agents and found a broad functional role of ER stress-induced death receptor signaling in apoptosis induction.

We then examined these mechanisms in a model with normal colon mucosal cells with a transient or stable loss of *APC*. Colon cancer cell lines have many mutations present and are often used for treatment analysis [49]. However, they are also great models for simply looking at

the mechanisms of action for chemopreventive drugs. On the other hand, these *APC* KO/KD NCM 356 cells more closely mirrored the initial CRC development as approximately 85% of sporadic cases initiate with the loss or mutation of *APC* [6]. Upon treatment, ER stress was also found to be an important factor in the upregulation of DR5 in the BID-mediated synthetic lethality model proposed by our labs' previous work [21].

The role of NSAID-induced ER stress in chemoprevention was further analyzed in an *in vivo* (*APC*<sup>Min/+</sup>) mouse model. These mice carry a heterozygous nonsense mutation in the *APC* gene (the mouse homologue of human *APC* on mouse chromosome 18) resulting in the development more than 30 polyps (adenomas) in the small intestine [50]. In order to test our hypothesis, short-term and long-term treatments were carried out. Our previous work showed that NSAID-induced apoptosis could be clearly seen as early as one week after treatment in the intestinal and colonic tissues of 4 week old *APC*<sup>Min/+</sup> mice [21]. Therefore, we sought to examine the influence of ER stress inhibition on this process. Our results showed that the administration of Salubrinal indeed caused a significant reduction in NSAID-induced apoptosis. These results provided a good rationale to move on to long-term studies. Once again, the administration of Salubrinal negatively impacted the chemopreventive properties of NSAIDs as there were more tumors in the sulindac/Salubrinal group versus the sulindac-only group. This was seen in both the colonic and small intestinal tissues.

Due to the positive results seen with the pharmacological inhibition, we decided to look at the tumor phenotype in an *APC*<sup>Min/+</sup>/*CHOP* KO mouse model. *CHOP* KO mice homozygous for the targeted mutation were commercially available and were crossed with our *APC*<sup>Min/+</sup> mouse model. This *CHOP* KO model was used as the mouse embryonic fibroblasts obtained from these mice have been shown to be resistant to ER stress-induced apoptosis [39]. After

analyzing these mice, we found that control mice developed fewer tumors than their  $APC^{Min/+}$  counterpart. This could be explained by the tumor-promoting effect of basal ER stress [24, 25]. The UPR has both pro-survival and pro-death effects (Fig. 4). Basal and short-term exposure to ER stress activates pro-survival pathways, while an above-threshold and long-term ER stress activates pro-death pathways [25]. Perhaps the impaired ER stress in this  $APC^{Min/+}/CHOP$  KO mice caused them to not effectively reach the basal levels needed to significantly drive tumorigenesis. As a result, the tumor phenotype was different between the two models. Consequently, changes in NSAID-induced tumor inhibition were not on the same scale and were difficult to compare. Sulindac was still effective in reducing the tumor burden in this new model, and this was modestly but significantly less than in the  $APC^{Min/+}$  mouse model.

Overall, genetically targeting ER stress for cancer prevention/therapy may be difficult to achieve [26]. There are many proteins involved in this pathway and timing/threshold levels are of key importance to tumor inhibition. Furthermore, this duality in survival vs. death results in tissue specific changes that are difficult to study in animal models with a total knockout of *CHOP*. For example, studies have shown that *CHOP* expression in macrophages is capable of regulating the magnitude and expression of pro-tumorigenic IL-6 in the Dextran Sodium Sulfate Colitis model [51], which may explain the difference in observed tumor phenotypes. As a result, an inducible and tissue specific *CHOP* KO system could be a potentially better *in vivo* model for future studies. For our experiments, pharmacological inhibition of ER stress *in vivo* proved to be a more useful approach than the genetic inhibition.

## **4.0 IMMUNOMODULATORY EFFECTS OF NSAID-INDUCED ER STRESS AND CELL DEATH**

### **4.1 INTRODUCTION**

#### **4.1.1 Chemoprevention and Immunoprevention**

Directly modulating the immune system for cancer prevention, known as “immunoprevention,” through approaches such as vaccines has been successful against malignancies caused by viral infection, such as human papilloma virus (HPV)-induced cervical cancer [52, 53]. However, similar approaches have yet to be applied for the prevention of non-viral cancers including CRC.

Chemo/dietary prevention and immunoprevention used to be considered as two different prevention approaches. These approaches have increasingly merged with each other, as accumulating evidence indicates that chemopreventive agents also have immunomodulatory effects [54]. Recent success of using antibodies against various immune checkpoints such as Program Death 1 (PD-1), Programmed Death Ligand 1 (PD-L1), and cytotoxic T lymphocyte associated antigen 4 (CTLA-4) for cancer immunotherapy provides indisputable evidence that modulating the immune system is a sound approach for cancer treatment. These recent advances have led to a dramatic increase in prevention studies involving combinations of chemopreventive agents and immune-based biological agents [55].

#### **4.1.2 Safeguarding Against CRC Development by Immunosurveillance**

The original theory of immunosurveillance postulates that a normal cell acquiring oncogenic mutations can be eliminated by the immune system which functions as a major initial barrier to tumor progression [56, 57]. However, the interplays of tumor cells and the immune system are much more complicated than originally thought. It is clear now that the immune response has dual roles in CRC development, with cytotoxic lymphocytes activated by tumorigenic alterations restraining tumor growth, while chronic inflammation creates a microenvironment that fosters tumor cell growth and invasion [58].

The concept of immunosurveillance has now evolved into that of immunoediting [59], which incorporates the influence of the immuno-suppressive tumor microenvironment [60]. Immunoediting includes three phases (Fig. 30): (1) Elimination, (2) Equilibrium, and (3) Escape. Potential tumor cells accumulate neo-antigens or tumor associated antigens (TAAs), which can be recognized by the immune system and removed (elimination) [59, 60]. During this anti-tumor response, cell-mediated and humoral responses are of key importance (Fig. 31). Upon failure of this, the constant immune selection pressure promotes the tumor cell variants with an increased ability to endure an attack by the immune system (equilibrium) [59, 60]. Finally the tumor expands in an unrestrained manner and grows uncontrollably with assistance of several immune suppressing pathways and cells (escape) [59, 60].

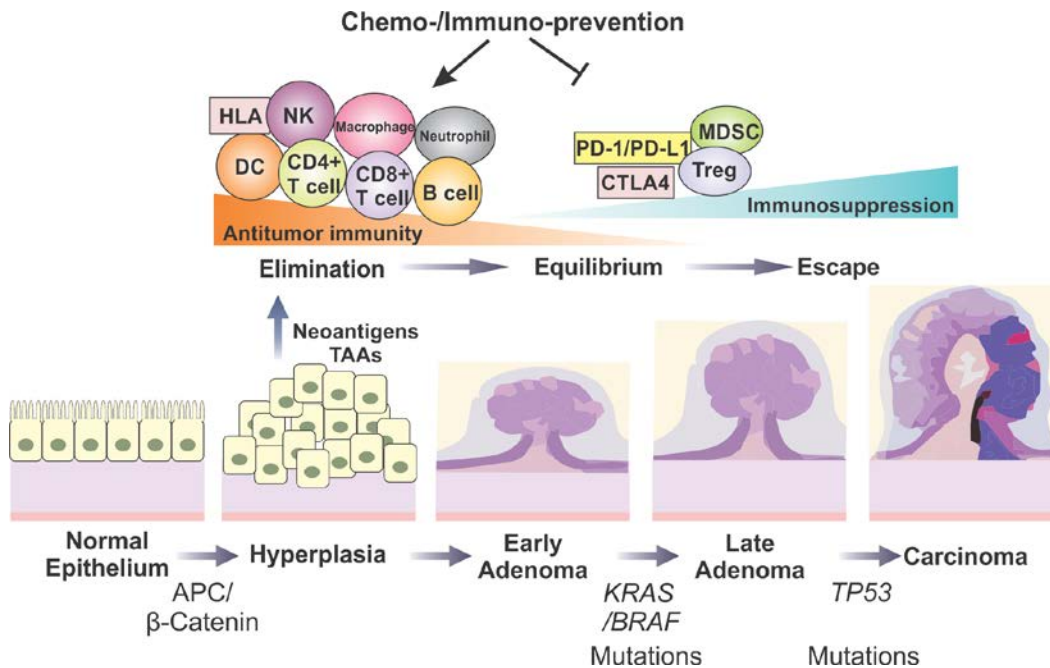


**Figure 30. Immunoeediting and Immunoprevention along the Adenoma-Carcinoma Progression in Colorectal Tumor Development.** Development of colorectal cancer is driven by genetic alterations in the APC/  $\beta$ -catenin pathway, leading to aberrant Wnt signaling and formation of hyperplastic cryptic foci and early adenomas. Accumulation of genetic alterations in oncogenes such as *KRAS/BRAF* and tumor suppressors such as *TP53* results in formation of late adenomas and carcinomas. Emerging tumor cells generate mutated neo-antigens or tumor associated antigens (TAAs) that can trigger antitumor immune response initiated by dendritic cells (DCs) and mediated by CD8+ T cells, CD4+ T cells, and other immune cells as indicated. This process selects for tumor cell variants that are capable of enduring the attack by the immune system, and also creates an immunosuppressive microenvironment due to activation of the PD-1/PD-L1 and CTLA-4 pathways, as well as immunosuppressive cells such as regulatory T cells (Tregs) and myeloid-derived suppressor cells (MDSCs). During this process, antitumor immune response and immunosuppression reach equilibrium, and eventually allow tumor cells to escape from immunosurveillance. Both chemoprevention and immunoprevention modulate the antitumor immune response and restore immunosurveillance through various effects on immune cells and effector molecules

and pathways. This figure is taken from the original artwork in Fletcher et al., BBA Cancer Reviews, 2018 [10].

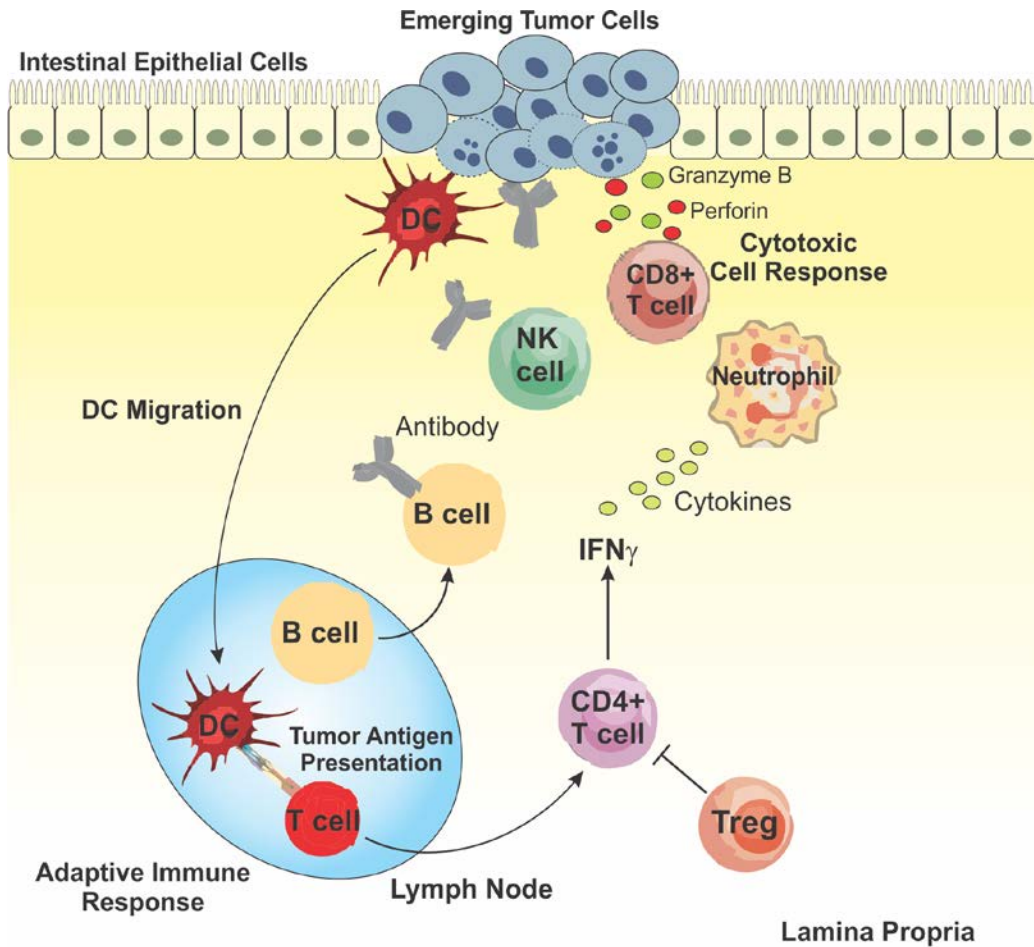


**Figure 31. Overview of Antitumor Immune Response.** Tumor antigens are captured by dendritic cells (DCs) and B cells and presented to T cells in the draining lymph nodes. This will lead to priming of humoral (antibody) and cellular responses (helper and cytotoxic T cells). Interferon- $\gamma$  (IFN- $\gamma$ )-producing CD4+ T cells, cytotoxic CD8+ T cells, and natural killer (NK) cells are the main effectors for this antitumor response. These effects can be attenuated via the actions of regulatory T cells (Tregs). This figure is taken from Fletcher et al, BBA Cancer Reviews, 2018 [10].

### 4.1.3 Immune-Modulating Effects of NSAIDs

Accumulating evidence suggests that immunosurveillance functions as a critical barrier for CRC development, including at the early and premalignant stages, and represents an attractive target for early intervention and prevention [10]. In fact, further evidence suggests that the chemopreventive effect of NSAIDs is mediated, in part, by restoring immunosurveillance and reversing the immune evasive mechanisms that pre-malignant lesions utilize [54]. Recent epidemiological studies in large cohorts show that regular use of aspirin is associated with a reduced risk of CRCs with low-levels of tumor infiltrating lymphocytes (TILs) (CD8+, CD3+, and CD45RO T cells), but not those with medium- or high-levels of TILs [61]. The association of aspirin use with CRC survival was found to be stronger in patients with PD-L1-low tumors than PD-L1-high tumors [62]. Significant associations were found between aspirin/NSAID use, CRC patient survival, and single nucleotide polymorphisms (SNPs) in immune modulators, such as the components of the JAK/STAT suppressors of cytokine signaling (SOCS), interferon, and interleukin-8 (IL-8) signaling pathways [63-65]. In a pilot clinical study, short-term pre-operative treatment of CRC patients with the NSAID celecoxib or indomethacin led to increased levels of active TILs and reduced immunosuppressive Tregs in the stroma and tumor tissues [66].

A number of *in vitro* and *in vivo* studies also showed that the antitumor effect of NSAIDs is acting through restoration of antitumor immune response. Genetic ablation of cyclooxygenase 2 (*COX2*), the target of NSAIDs, or its pharmacological inhibition by aspirin in CRC cells promotes immune-dependent tumor suppression [67]. Aspirin and aspirin-like drugs induce Human Leukocyte Antigen-DR (HLA-DR) expression in CRC cells [68], and alter the balance between pro- and anti-inflammatory cytokines generated by the interaction between CRC cells and immune cells [69]. Tumor suppression by the NSAID sulindac was shown to require CD8+ T

cells, and is accompanied with significantly diminished M2 macrophage recruitment [70]. The NSAIDs celecoxib and indomethacin affect the expression of PD-L1 and PD-L2 in specific bone marrow cells [71, 72]. Additionally, NSAIDs have been shown to alter the phenotype of tumor-associated macrophages (TAMs) from the pro-tumor M2 phenotype to the antitumor M1 phenotype in *APC*<sup>Min/+</sup> mice [73]. The stimulatory effect of NSAIDs on antitumor immunity could also be working by suppression of COX2-mediated production of prostaglandin E2 (PGE2) in tumor and stromal cells, the latter of which induce immunosuppression through their inhibitory effects on DCs, macrophages, neutrophils, cytotoxic T cells (CTLs), type I T helper cells (TH1), and NK cells, as well as its stimulatory effects on MDSCs, Tregs, and type II T helper cells (TH2) [74, 75].

#### **4.1.4 Restoring Immunosurveillance through Immunogenic Cell Death**

ER stress can also contribute to immunomodulation via its close association with Immunogenic Cell Death (ICD). ICD restores the immunosurveillance and antitumor immunity, ultimately leading to a favorable therapeutic response [76-79]. Tumor cells killed by ICD release damage-associated molecular patterns (DAMPs) as immunogenic signals [80, 81]. These DAMPs only stimulate the immune response under stressful circumstances when they are in the extracellular area (exposed at the cell surface or secreted from cells). They include calreticulin (CRT), ATP, high mobility group box 1 (HMGB1), heat shock protein 90 (HSP90), and other chaperokines [82-84]. These molecules elicit antitumor immune response by binding to various receptors. Different drugs/therapies have been screened in a variety of cancer types including CRC for ICD properties. The list is inclusive of anthracyclines, radiotherapy, photodynamic therapy, oxaliplatin, and bortezomib [76, 83-86].

Upon the initiation of an ICD response, production of reactive oxygen species (ROS) is one of the major pathways that can induce ER stress [87, 88]. This stress involves the PKR-like ER Kinase (PERK) mediated phosphorylation of EIF2 $\alpha$  [83, 87, 88]. It has been postulated that this phosphorylation could be used as a marker for this type of cell death [80, 89]. However, pEIF2 $\alpha$  as a biomarker has mixed reviews as some drugs such as thapsigargin have been shown to induce phosphorylation of EIF2 $\alpha$  but fail to influence the translocation of CRT to the cell surface [80, 83, 88, 90]. This translocation is the best-characterized indicator of ICD associated with ER stress [91]. Upon the initiation of ICD, tumor cell surface-exposed CRT binds to CD91 that is expressed on the surface of DCs [92]. This process functions as an “eat me” signal aiding in the tumor’s recognition by the immune system [93].

## 4.2 MATERIALS AND METHODS

### 4.2.1 Mice and Treatment

The procedures for all animal experiments were approved by the Institutional Animal Care and Use Committee of the University of Pittsburgh. C57BL6J *BID*<sup>-/-</sup> (*BID* KO) mice, which were described [46], were crossed with *APC*<sup>Min/+</sup> mice (Jackson Laboratory) to generate *APC*<sup>Min/+</sup> mice with different *BID* genotypes. Female *BID* KO mice were crossed with male *APC*<sup>Min/+</sup> mice (Jackson Laboratory) to generate *APC*<sup>Min/+</sup>/*BID*<sup>+/-</sup> mice. Male *APC*<sup>Min/+</sup>/*BID*<sup>+/-</sup> mice were then crossed to *BID* KO females to generate *APC*<sup>Min/+</sup> littermates with null (-/-) *BID* alleles. Genotyping of *APC* alleles was performed according to the Jackson Laboratory protocol, and genotyping of *BID* alleles was performed as described [46]. All strains were on the C57BL/6

background for more than 10 generations (F10). Mice were housed in micro-isolator cages in a room illuminated from 07:00 to 19:00 hours (12:12-hour light-dark cycle) with access to water and chow *ad libitum*. A similar methodology was used to create *APC<sup>Min/+</sup>/CHOP* KO (Jackson Laboratory) mice.

10-week-old mice were placed on diets with or without 200 ppm sulindac for 7 days. After sacrificing the mice, the small intestinal and colonic tissues were carefully excised and rinsed with saline. The tissues were opened longitudinally and tacked to a foam board for fixation overnight in 10% formalin. Tissues were then rolled up into “swiss rolls” and embedded in paraffin. Following this, embedded tissues were stained via IHC for CD3/CD8 (TIL) and adenomas were counted under a dissecting microscope.

#### **4.2.2 Immunohistochemistry (IHC)**

Following embedding in paraffin, 5  $\mu$ m slices of tumor tissue were cut in preparation for staining. IHC/IF was performed as described below using antibodies against: CD3-mouse (Novus Biologicals #NB600-1441, 1:100) and CD8-mouse (eBioscience #14-0195-82, 1:50).

Rehydrated sections were treated with 3% hydrogen peroxide (IHC only), followed by antigen retrieval for 10 minutes in boiling 0.1 M citrate buffer (pH 6.0) with 1 mM EDTA. Non-specific antibody binding was blocked using 20% goat serum at room temperature for 30 minutes. Primary antibody incubations were done overnight at 4°C with their respective antibodies in a humidified chamber in the dark.

Sections were then incubated for 1 hour at room temperature with either biotinylated goat anti-rabbit or anti-rat secondary antibody (Pierce #31822, Pierce #31830). They were then developed with an ABC kit and DAB (Vector Laboratories, Burlingame, CA).

The images were acquired using an Olympus BX51 system microscope equipped with a SPOT camera and SPOT Advanced 5.1 software.

#### **4.2.3 Flow Cytometric Analysis of CRT Translocation**

Cells were seeded in 12-well plates ( $3 \times 10^5$  cells/well). After incubation at 37°C for 24 hours, cells were treated with the indicated drugs for 12 hours. Cells were stained with primary rabbit antibody anti-CRT (1:1000, ab2907, Abcam) and secondary antibody Alexa Fluor 488 anti-rabbit (1:1000, A11008, Invitrogen). More details have been previously described [94]. Each sample was then analyzed by an ACCURI C6 flow cytometer (BD Biosciences) to identify the cell surface CRT. Isotype-matched IgG antibodies were used as a control, and the fluorescence intensity of stained cells was gated on propidium iodide-negative cells.

#### **4.2.4 Blood Dendritic Cell Isolation from Peripheral Blood Mononuclear Cells (PBMC)**

Venous blood from healthy donors (Central Blood Bank, Pittsburgh, PA) was drawn into heparinized tubes and centrifuged on Ficoll-Hypaque gradients (GE Health Life Sciences). PBMCs were recovered and washed in RPMI-1640 medium. Dendritic cells (DCs) were isolated as previously described [95].

#### **4.2.5 Phagocytosis of Tumor Cells by DCs**

Tumor cells were stained with 5  $\mu$ M Cell Trace Far Red dye (Invitrogen) and seeded in 48-well plates ( $1 \times 10^5$  cells/well) for flow cytometry or in a 4-well Nunc Lab-Tek Chamber Slide

System for immunofluorescence. After 24 hours of incubation, cells were treated with the indicated drugs for 12 hours. DCs were stained with 2  $\mu$ M CFSE (Invitrogen), incubated with hIgG (20  $\mu$ g/ $1 \times 10^6$  cells) for 30 minutes, and afterwards co-cultured with tumor cells for 2 hours in a 1:1 ratio. Cells were collected and then analyzed by an ACCURI C6 flow cytometer (BD Biosciences). Confocal microscopy was performed on a Lecia TSC SP5 laser confocal scanner mounted on a Leica DMI 6000B inverted microscope. More details have been previously described [96]. Transfections were carried out 24 hours after staining and seeding as previously described in chapter three.

#### **4.2.6 Statistical Analysis**

Statistical analyses were performed by using GraphPad Prism IV software. Differences were considered significant if the probability of the difference occurring by chance was less than 5 in 100 ( $P < 0.05$ ). Multiple comparisons of the responses were analyzed by one-way ANOVA and either Dunnett's or Tukey's post hoc test, whereas those between two groups were made by unpaired t test. All statistical tests were two-tailed.

### **4.3 RESULTS**

#### **4.3.1 ER Stress and BID Inhibition Attenuates NSAID-Mediated Lymphocyte Infiltration**

Previous correlative studies have shown that the induction of ER stress could be a mechanism of influx of Tumor Infiltrating Lymphocytes (TILs) [89, 97]. This was especially true for the

induction of proteins associated with PERK/pEIF2 $\alpha$  axis [97]. The influence of ER stress and cell death on this influx was thus examined *in vivo*. We first showed the NSAID treatment indeed promoted lymphocyte infiltration into the mouse polyps. This was highlighted via CD3/CD8 staining (Fig. 32A-B). In these experiments, 10 week-old  $APC^{Min/+}$  mice were treated with sulindac (200 ppm) for 1 week.

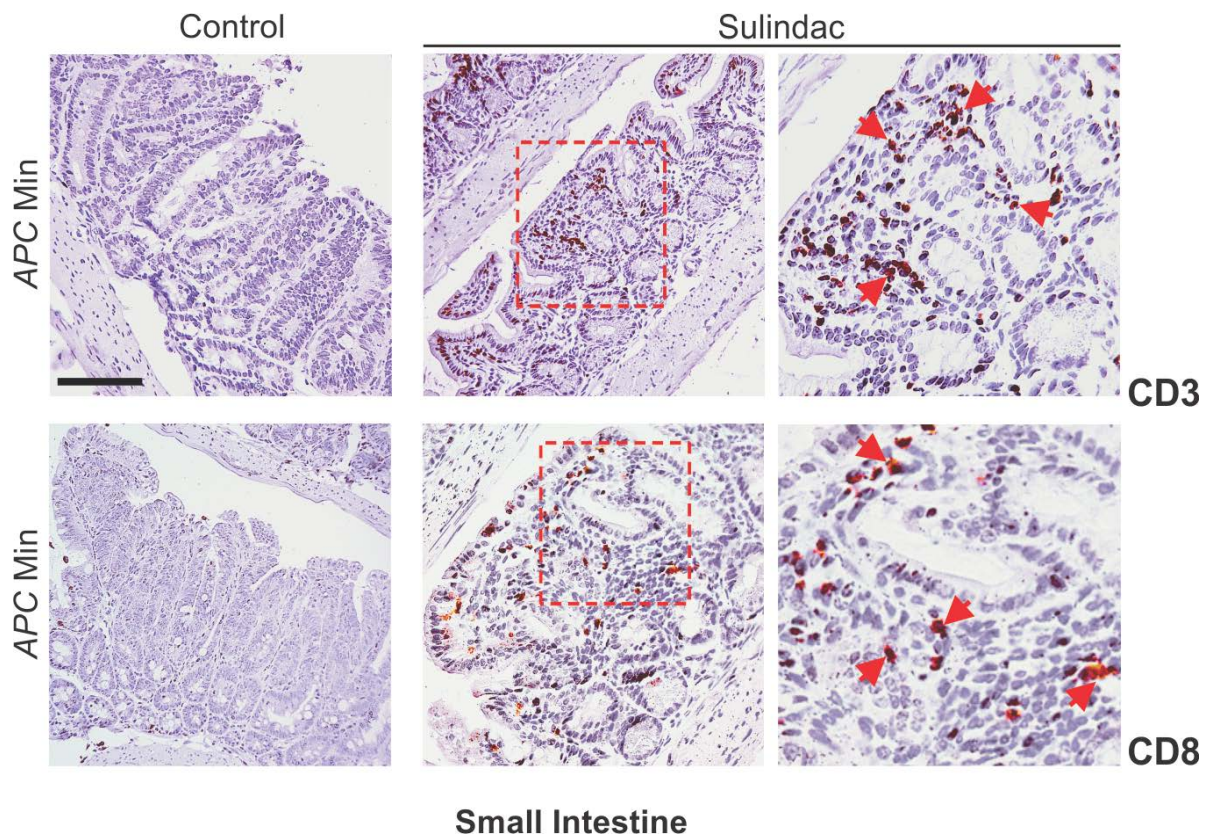


**Figure 32. NSAIDs Promote Lymphocyte Infiltration into the Adenoma *in Vivo*.** 10 week-old  $APC^{Min/+}$  mice were treated with 200 ppm sulindac for 1 week. The small intestines were stained as follows. Upper panel: Representative IHC stains of small intestinal polyps, with arrows indicating example cells with positive CD3 staining. Lower panel: Representative IHC stains of small intestinal polyps, with arrows indicating example cells with positive CD8 staining. Scale bars, 100  $\mu$ m. Magnification, 200X. N=5 per group.

We next examined the influence of ER stress on TIL. We stained the polyps of mice that were given NSAIDs in combination with the ER stress inhibitor Salubrinal. The results showed that lymphocyte infiltration was attenuated by the inhibition of ER stress (Fig. 33).

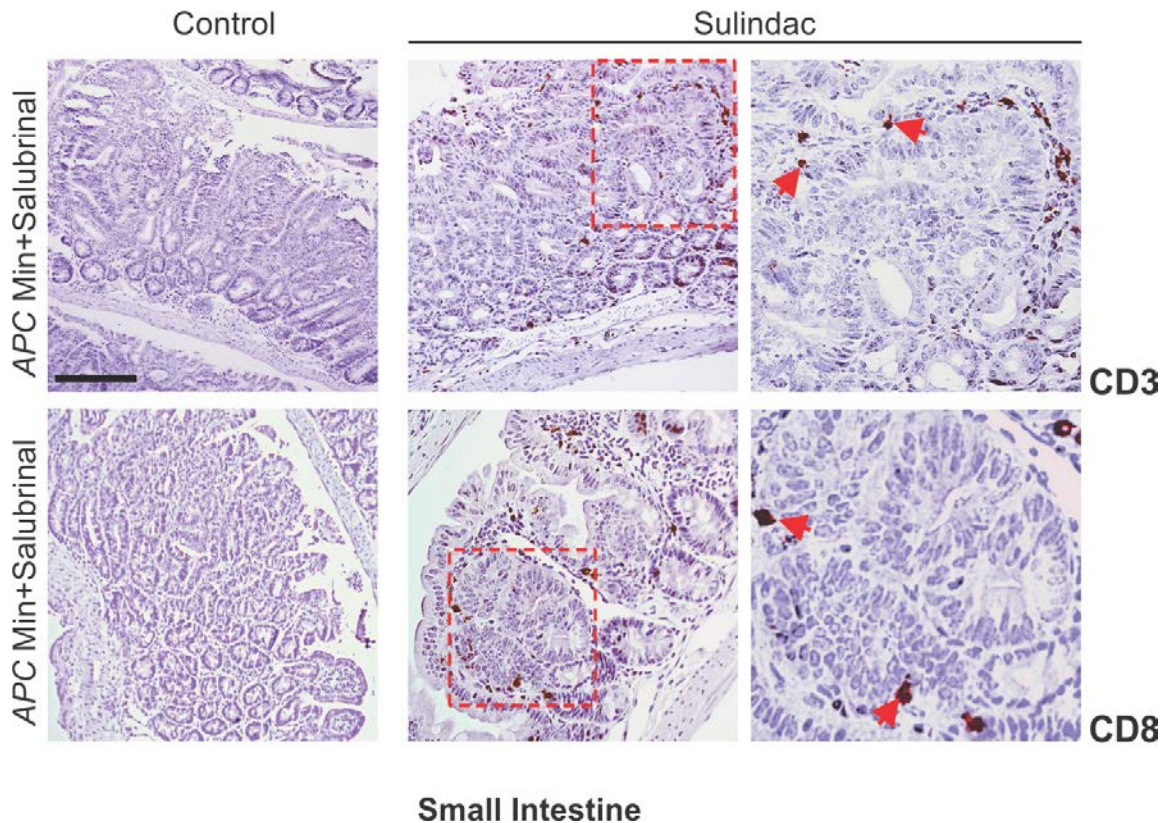


**Figure 33. Inhibiting NSAID-Induced ER Stress Attenuates Lymphocyte Infiltration into the Adenoma *in Vivo*.** 10 week-old  $APC^{Min/+}$  mice were treated with 200 ppm sulindac in combination with 1 mg/kg/day Salubrinal for 1 week. The small intestines were stained as follows. Upper panel: Representative IHC stains of small intestinal polyps, with arrows indicating example cells with positive CD3 staining. Lower panel: Representative IHC stains of small intestinal polyps, with arrows indicating example cells with positive CD8 staining. N=5 per group.

In order to evaluate the influence of apoptosis in this system, similar experiments were conducted with C57BL6J  $BID^{-/-}$  ( $BID$  KO)  $APC^{Min/+}$  mice. Lymphocyte infiltration caused by sulindac was attenuated in this  $BID$  KO group and even more so than the previous groups with Sal injections (Fig. 34).

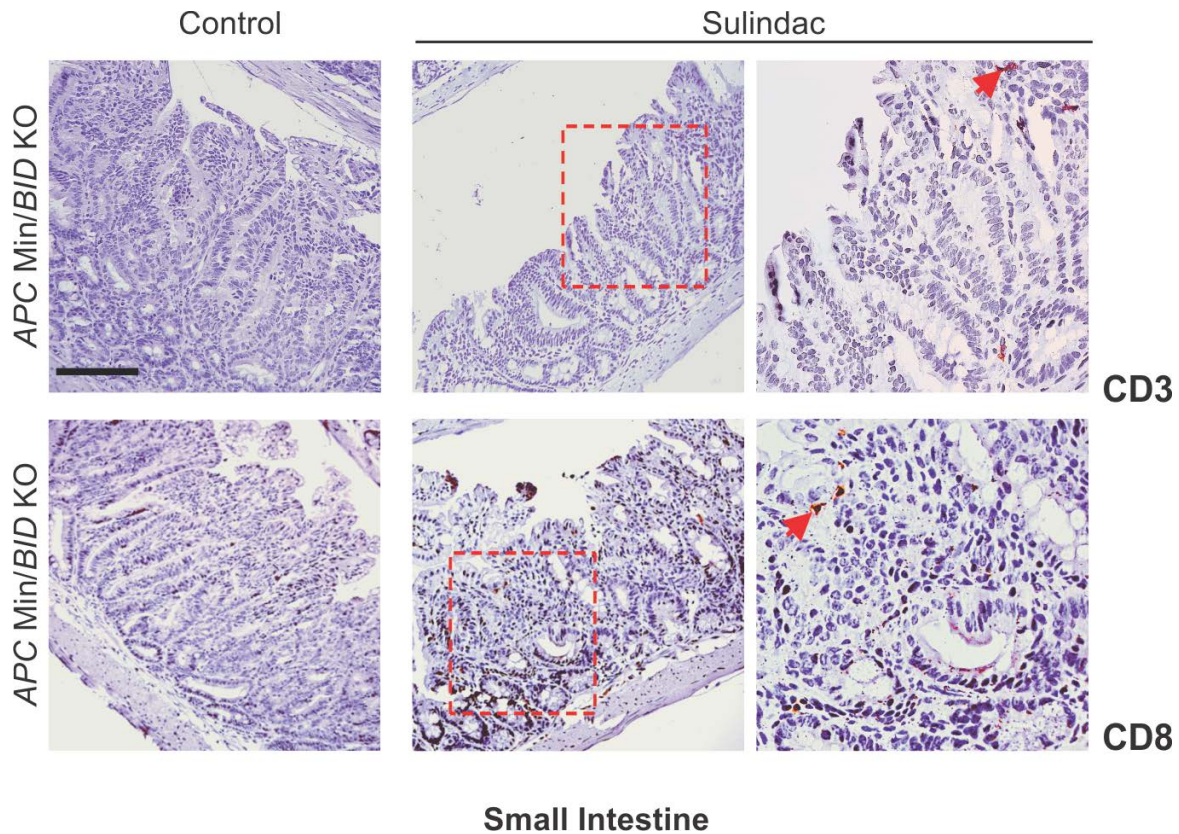


**Figure 34. Inhibiting NSAID-Induced Cell Death Attenuates Lymphocyte Infiltration into the Adenoma *in Vivo*.** 10 week-old  $APC^{Min/+}/BID$  KO mice were treated with 200 ppm sulindac for 1 week. The small intestines were stained as follows. Upper panel: Representative IHC stains of small intestinal polyps, with arrows indicating example cells with positive CD3 staining. Lower panel: Representative IHC stains of small intestinal polyps, with arrows indicating example cells with positive CD8 staining. N=5 per group.

When a comparison was made, both inhibition of ER stress and BID-mediated apoptosis significantly attenuated NSAID-induced TIL infiltration as highlighted by the quantification of the staining shown previously (Fig. 35).

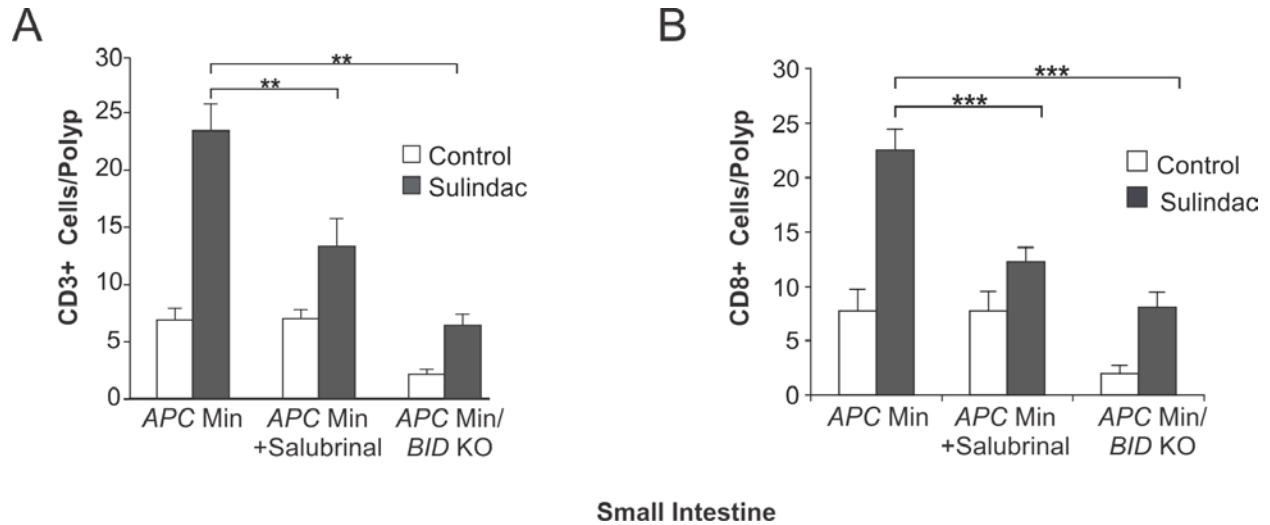


**Figure 35. NSAID-Induced ER Stress-Associated Cell Death Mediated by BID Promotes Lymphocyte Infiltration into the Adenoma *in Vivo*.** 10 week-old  $APC^{Min/+}$  mice were treated with 200 ppm sulindac alone, or in combination with 1 mg/kg/day of the ER stress inhibitor Salubrinol for 1 week. Similar experiments were conducted with  $APC^{Min/+}$  mice with the knockout (KO) of *BID*. Results in Figs, 33-34 were quantified as the Mean numbers + s.d. of positive cells/polyp for CD3 (A) and CD8 (B). N=5 per group. ANOVA and Dunnett's post hoc test were used for statistical analysis. \*\*P < 0.01 \*\*\*P < 0.001.

#### 4.3.2 NSAID-Mediated Apoptosis Plays a Role in Immunogenic Cell Death

To further examine the mechanism of action of this immune response to NSAIDs, in particular, the role of ER stress and cell death, several experiments for analyzing ICD were performed. ER

stress acting along the PERK/pEIF2 $\alpha$ /ATF4 axis has been linked to ICD [83]. We analyzed a classic indication of ICD by examining changes in CRT translocation to the cell surface upon treatment. Sulindac sulfide indeed induced CRT translocation in HCT 116 cells as examined by flow cytometry (Fig. 36). Apoptosis through the extrinsic pathway was essential to this process as there was a significant reduction in CRT translocation in HCT 116 cells with stable knockdown of caspase 8 or knockout of *BID* (Fig. 36).

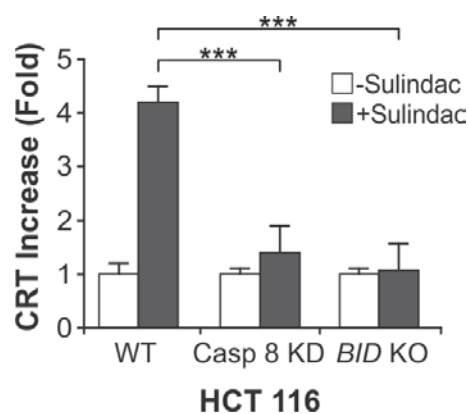


**Figure 36. NSAID-Mediated ICD is Affected by Caspase 8 and BID Depletion as Highlighted by Cell Surface CRT Translocation.** CRT translocation was examined by immunostaining followed by flow cytometry in HCT 116 WT, caspase 8 knockdown, and *BID* KO cells that were treated for 12 hours with sulindac sulfide (120  $\mu$ M). Results were expressed as means + s.d. of three independent experiments. ANOVA and Dunnett's post hoc test were used for statistical analysis. \*\*\* $P < 0.001$ .

The influence of ER stress inhibition on NSAID-induced CRT translocation was then examined in this system. Upon genetic (*PERK/CHOP* siRNA) and pharmacological (Salubrinal) inhibition, a substantial reduction in CRT translocation was seen (Fig. 37A-B).

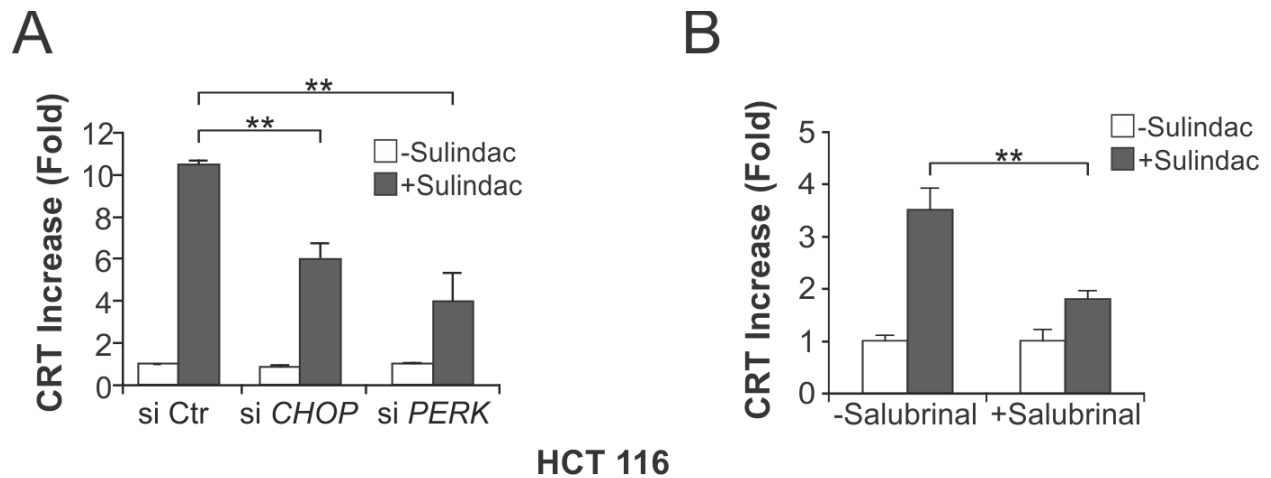


**Figure 37. NSAID-Mediated ICD is Affected by ER Stress Inhibition as Highlighted by Cell Surface CRT Translocation.** ER stress was inhibited genetically (siRNA, 24 hours prior) in (A) and chemically (Salubrinal, 1.5 hour pretreatment) in HCT 116 cells in (B). CRT translocation was then examined by immunostaining followed by flow cytometry in cells that were treated for 12 hours with sulindac sulfide (120  $\mu$ M). Results were expressed as means + s.d. of three independent experiments. ANOVA and Dunnett's post hoc test were used for statistical analysis. **\*\*P < 0.01.**

Subsequently, the influence of sulindac on the DC phagocytosis of tumor cells was examined. We treated tumor cells with sulindac sulfide for 12 hours. Then we co-cultured these tumor cells with DCs for 2 hours. We observed a significant increase in phagocytosis (Fig. 38A), which was attenuated with *CHOP/ATF4* siRNA and by *BID* knockout in HCT 116 cells (Fig. 38B).

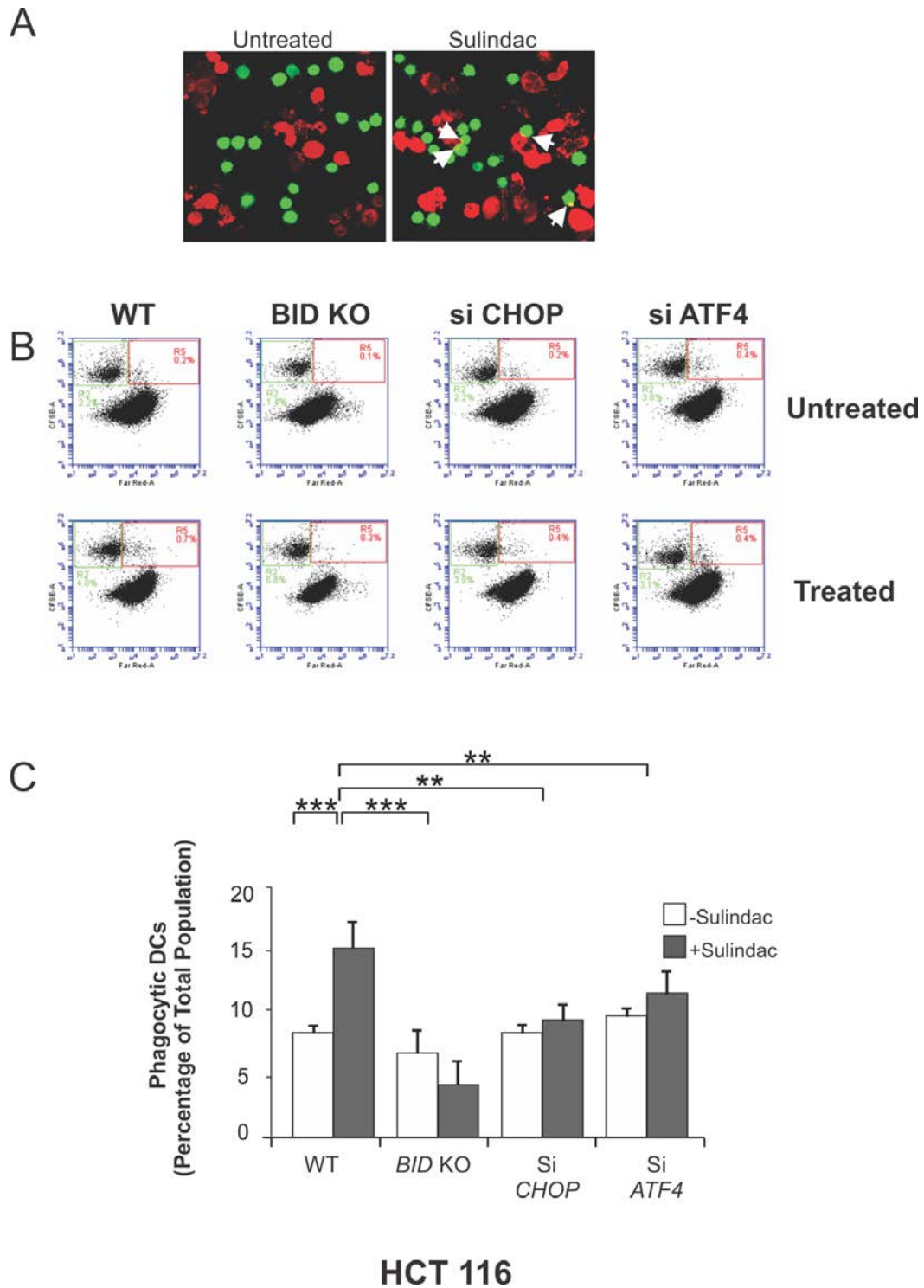


**Figure 38. NSAID-Mediated ICD is Affected by BID and ER Stress Inhibition as Highlighted by DC Phagocytosis.** Dendritic cells stained with CSFE were co-cultured for 2 hours with tumor cells stained with Far Red that were previously treated with sulindac for 12 hours. Phagocytosis was examined

by the presence of double-stained cells identified by microscopy (A) and by flow cytometry (B-C) in HCT 116 cells. (B-C) Flow cytometry allowed for the quantification of the levels of phagocytosis. The red box represented phagocytic DCs, and the green box represented total DCs. Experiments were performed in HCT 116 WT, *BID* KO, and *CHOP/ATF4* knockdown HCT 116 cells.. Results were expressed as means + s.d. of three independent experiments. ANOVA and Tukey's post hoc test were used for statistical analysis. \*\*P < 0.01, \*\*\*P < 0.001.

Furthermore, the influence of sulindac on CRT translocation and DC phagocytosis was observed in stable *APC* KO NCM 356 cells (Fig. 39A-B).

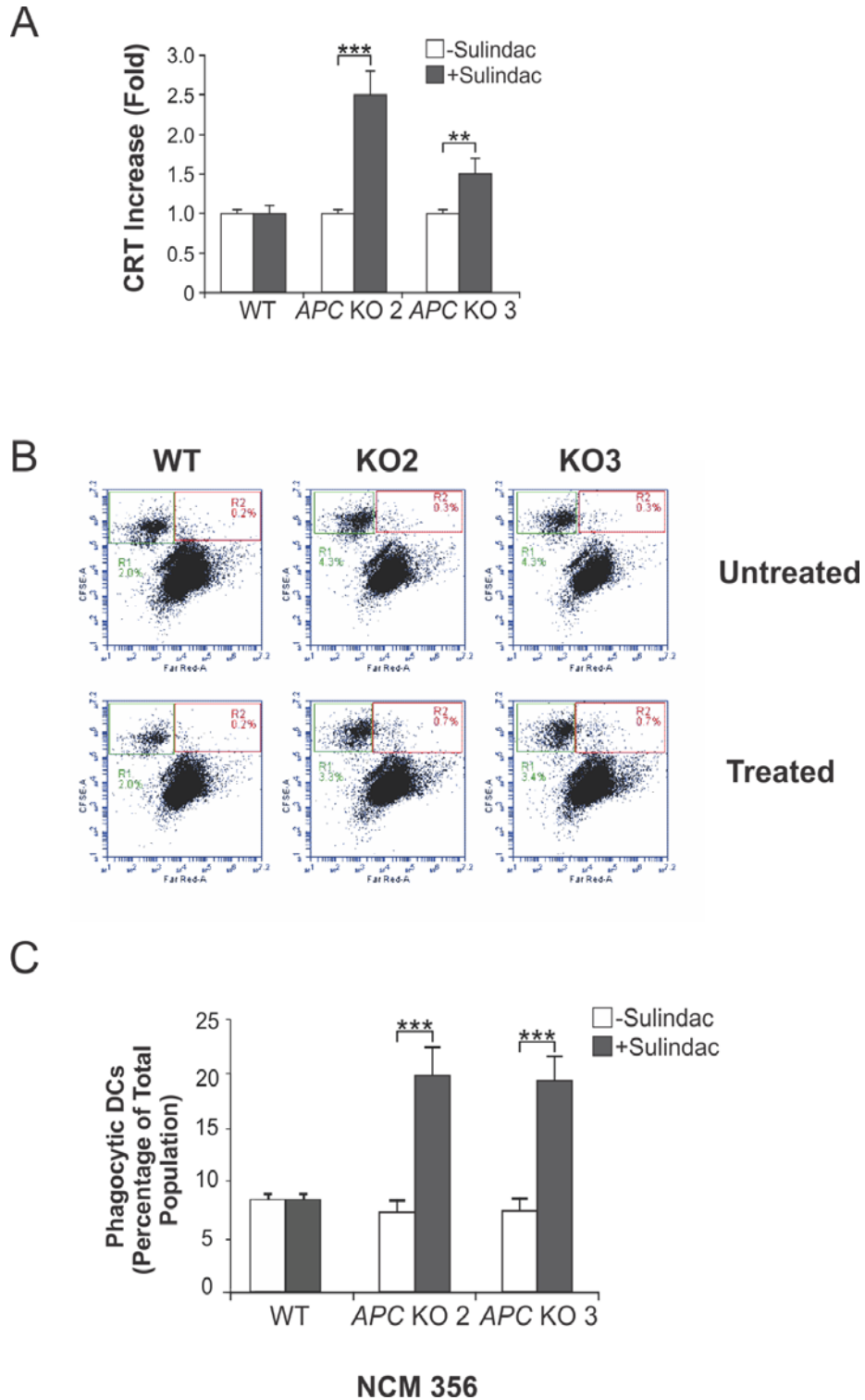


**Figure 39. NSAID Treatment Influences CRT Translocation and DC Phagocytosis upon the Loss of APC in a Normal Epithelial Background.** (A) CRT translocation was examined by immunostaining followed by flow cytometry in two *APC* KO clones and in wild-type NCM 356 cells that were treated for

12 hours with sulindac sulfide (120  $\mu$ M). (B-C) Dendritic cells stained with CFSE were co-cultured for 2 hours with cells stained with Far Red that were previously treated with sulindac for 12 hours. Phagocytosis was examined by the presence of double-stained cells identified via flow cytometry in *APC* KO NCM 356 cells. The red box represents phagocytic DCs, and the green box represents total DCs in (B). Results in (A) and (C) were expressed as means + s.d. of three independent experiments. ANOVA and Tukey's post hoc test were used for statistical analysis.

### **4.3.3 Loss of the Tumor Suppressor *APC* Influences *CD47* Expression**

As mentioned previously, *APC* loss leads to the activation of a critical downstream effector, c-Myc. This transcription factor promotes cell proliferation, survival, and metabolic reprogramming by transcriptionally regulating hundreds of downstream target genes [98]. A recent study also showed that c-Myc regulates the expression of immune checkpoint proteins such as *CD47* that inhibits the innate immune response [99]. *CD47* functions as a “don't eat me” signal, which is the exact opposite of CRT, an “eat me” signal. Therefore, we determined if the loss of *APC* in our system affected the expression of *CD47* (Fig. 40A). This is what was found in a pilot experiment with *APC* KO cells (Fig. 40B). Furthermore, NSAID treatment was able to attenuate this upregulation.

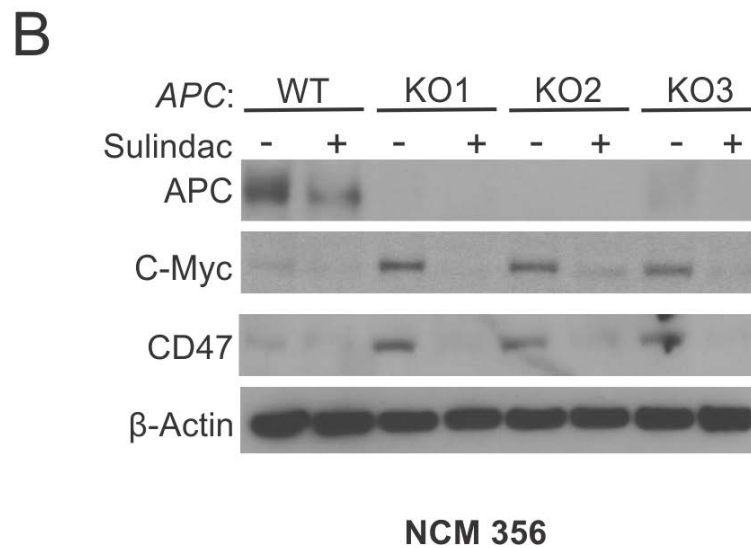
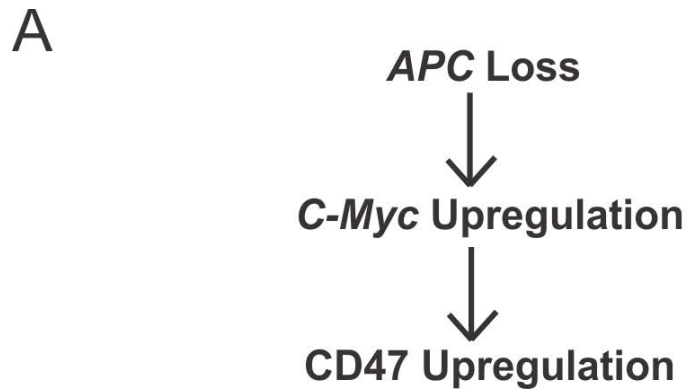


**Figure 40. CD47 Expression is Upregulated in APC KO NCM 356 cells and is Attenuated upon NSAID Treatment.** (A) Proposed model for APC regulation of CD47. (B) Western blot showing changes in CD47 expression in APC KO NCM 356 cells. Cells were treated for 48 hours with 120  $\mu$ M sulindac.

We then proceeded to examine The Cancer Genome Atlas (TCGA) database to look at changes in the gene expression of *CD47* in CRC versus normal cells. As expected, we found that there was a higher gene expression of *CD47* in colon and rectum adenocarcinomas than in normal tissues (Fig. 41).

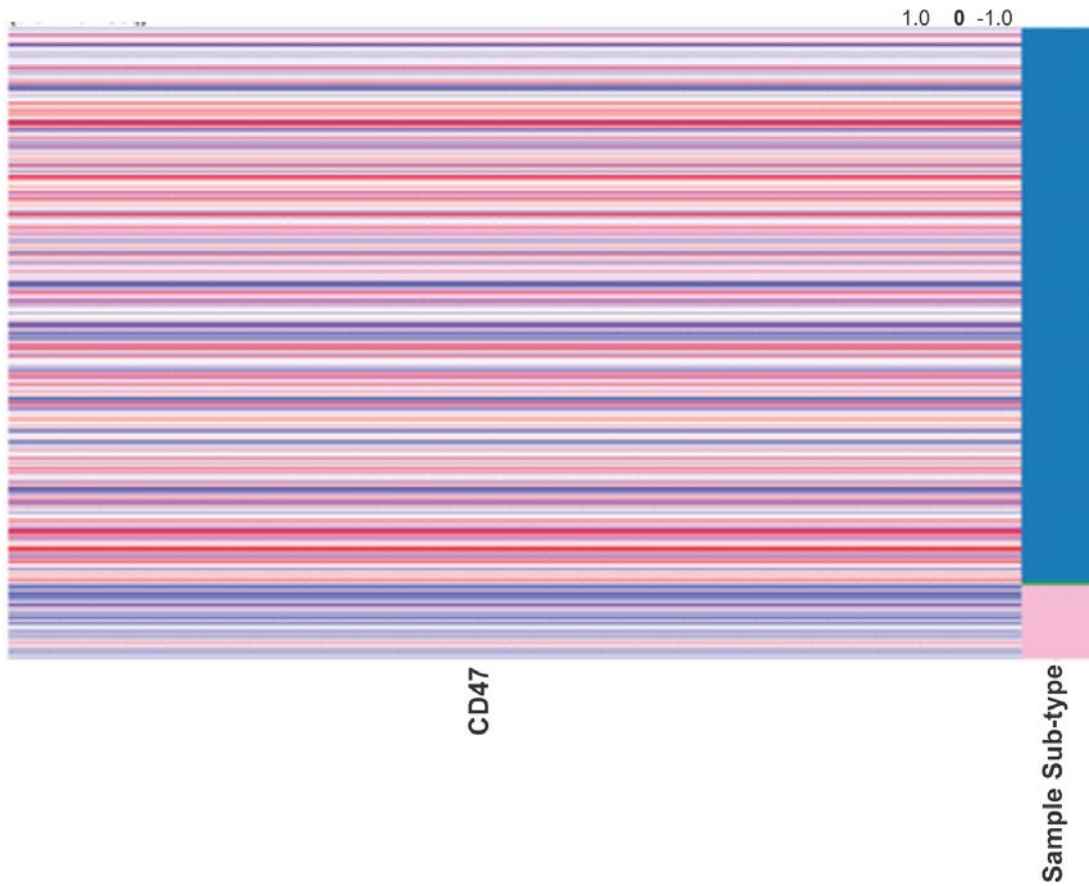


**Figure 41. *CD47* Expression is Elevated in Colorectal Adenocarcinomas vs. Normal Tissue.** Heat map from TCGA database depicting gene expression changes in *CD47* by RNAseq. This was acquired from the Cancer Browser on March 2, 2018. *CD47* expression: **Red - Hot Tumor**, Blue - Cold Tumor; Sample Subtype: **Pink - Normal tissue**, Blue - Adenocarcinoma.

## 4.4 DISCUSSION

Mechanistic studies on CRC prevention have been largely focused on alterations inside tumor cells. However, the immune response has been increasingly appreciated as an essential component of CRC prevention. Along the adenoma to carcinoma model previously mentioned, the immune system plays a role in the actual progression of cancer via immunoediting. Potential tumor cells accumulate neo-antigens or tumor associated antigens (TAAs), which can be recognized by the immune system. The first step (immunosurveillance) is crucial as it is the immune system's first attempt to remove those cells via humoral (B cells) and cell-mediated (CD4/CD8) responses. It is important to make use of this step as it precedes the development of tumor cells that are even more resistant to immune attacks by selection in the equilibrium stage. Therefore, it is significant to study this effect of NSAIDs as a number of studies have shown that these drugs may actually assist in enhancing immunosurveillance [10]. Nonetheless, in all of those studies mentioned, no direct links were made to immunogenic cell death (ICD) as a potential factor in this immune modulation. In this study, we found that both immune modulation and cell death were key components in the chemopreventive effects of the NSAIDs. ER stress is not only linked to death receptor signaling but also ICD, which is cell death that is capable of priming the immune system [29, 83].

Based on our previous work [21, 33], 10 week-old  $APC^{\text{Min/+}}$  mice were chosen for one week of treatment. It was shown that this treatment schedule allowed for a significant drop in polyp numbers so that comparisons could be made amongst the different experimental groups. More importantly, at the completion of this schedule, a sufficient number of polyps remained that could be analyzed for TIL infiltration. Furthermore, this was a good model to look at changes in TIL, as it has been shown that  $APC^{\text{Min/+}}$  mice have an altered T cell balance in

lymphoid organs leading to limited intestinal immune surveillance [100]. In that study, the authors found that  $APC^{Min/+}$  mice had lower levels of CD8+ T cells, as well as lower IFN- $\gamma$  and granzyme B produced by these cells.

We found that NSAID treatment caused an influx of TILs to the adenomas in  $APC^{Min/+}$  mice, and this was attenuated when ER stress, and more so when BID, was inhibited. This highlights the importance of both ER stress and BID to this immune modulation. A study has shown that the induction of ER stress could be a potential mechanism for the influx of TIL, but that was more of a correlative study using patient samples [97]. Our work highlights a causal relationship between ER stress and the presence of TILs. Furthermore, BID has been described as being essential to suppress tumorigenesis on its own [101]. BID expression is a key part of the mechanism of action of chemopreventive agents that act through the death receptor pathway.

The detailed mechanisms by which NSAIDs and other chemopreventive agents restore immunosurveillance through ICD remain to be further elucidated. In this project, we did perform several characteristic experiments for ICD *in vitro*. We initially observed the translocation of CRT to the cell surface, and then the influence of ER stress and BID inhibition on this process. Subsequently, we analyzed DC phagocytosis and the influence of ER stress and BID inhibition. The overarching mechanism of action proposed in this dissertation is very similar to that induced by a type II ICD inducer [29], which specifically targets the ER and upregulates stress-induced apoptosis that is classified as immunogenic. This is unlike type I inducers that target apoptosis by different mechanisms and ER stress is just an off-target effect, which influences the immune system [29].

Furthermore, NSAIDs can regulate other elements of the immune system that are used by abnormal cells to evade its attack. One such example is CD47 which functions as a “don’t eat me” signal and is important to the innate immune system [10]. We have previously shown that the loss of *APC* along the adenoma-carcinoma model results in the upregulation of c-Myc expression [21]. Recent literature has also shown that c-Myc can upregulate the expression of CD47 [99]. Therefore, high c-Myc in CRC could lead to high CD47 expression. Consequently, we examined the TCGA and found that there was an upregulation in the gene expression of *CD47* in colorectal adenocarcinoma tissues. Furthermore, our pilot experiments suggested that CD47 could be an important player in NSAID-mediated chemoprevention. However, more work will have to be done to further examine the specific role of CD47 inhibition in CRC chemoprevention.

Overall, NSAIDs have been shown to play a role in immunomodulation. We found a pivotal role of immunogenic cell death and potentially other mechanisms such as CD47 inhibition in NSAID-induced chemoprevention.

## 5.0 SUMMARY AND FUTURE DIRECTIONS

### 5.1 GENERAL SUMMARY

CRC prevention represents a paradigm for cancer prevention in general, but it faces several significant challenges. Some key issues in CRC prevention, insufficient mechanistic insights in particular, have remained unresolved, despite a large number of published studies. The molecular mechanisms for the specificity of NSAIDs in eliminating emerging tumor cells remain poorly understood. This study was aimed at overcoming this obstacle by further delineating these specific mechanisms of action through analysis of the role of NSAID-induced ER stress and immunomodulation in the suppression of colorectal tumorigenesis.

In chapter two we examined the role of ER stress in chemoprevention. Several papers have shown that NSAIDs can impact the homeostasis of the ER, but further insight is still needed for understanding the role of the ER stress response in chemoprevention. A variety of techniques including protein and mRNA analyses, IHC/IF, and TEM were used to study the induction of ER stress by NSAIDs. We found that NSAIDs clearly induced ER stress associated proteins in a time-dependent manner, which resulted in ultrastructural changes in the RER. However, the mechanisms downstream of ER stress in NSAID-induced apoptosis remained unclear. Our study revealed that DR5 was upregulated following ER stress *in vitro*. Furthermore, we observed a

correlation between ER stress and caspase 8/BID activation in advanced human adenomas from patients taking NSAIDs.

We investigated the mechanism of ER stress-mediated apoptosis induced by NSAIDs by using a variety of *in vitro* and *in vivo* models. HCT 116 cells were used to determine the role of the PERK/EIF2 $\alpha$ /ATF4/CHOP pathway in the induction of DR5 by NSAIDs. Genetic and pharmacological approaches were used to inhibit ER stress response proteins. A model for the gatekeeper alteration in colorectal tumorigenesis was created by KO/KD of *APC* in NCM 356 normal colonic epithelial cells. Our previous study identified a BID-mediated synthetic lethality between NSAID-induced death receptor signaling and the loss of *APC* in normal cells [21]. NSAID treatment was found to most potently induce apoptosis in cells that had acquired oncogenic changes. Using this model, we found that ER stress proteins including ATF4 and CHOP were essential to the NSAID-induced death receptor signaling in the BID-mediated synthetic lethality model.

We then performed *in vivo* analysis by using *APC*<sup>Min/+</sup> mice that carry a heterozygous nonsense mutation in *APC* [50]. Short-term experiments with Salubrinal showed that NSAID-induced ER stress is critical for the induction of apoptosis in intestinal and colonic adenomas in *APC*<sup>Min/+</sup> mice. Long-term experiments demonstrated that ER stress mediated the antitumor effect in these mice. Unfortunately, genetic inhibition of ER stress (in *APC*<sup>Min/+</sup>/*CHOP* KO mice) did not have a similar effect as seen with Salubrinal. This may be due to the complexity of ER stress (timing and threshold) and the dual effects of ER stress in promoting both cell survival and cell death [26].

We further examined the role of immunomodulation in NSAID-mediated chemoprevention by using both *in vitro* and *in vivo* models. We found that NSAID treatment

increased Tumor Infiltrating Lymphocytes (TILs) in the polyps, which was attenuated in mice with ER stress inhibition or *BID* knockout. These results highlighted the importance of ER stress and cell death to the immune modulatory effect of NSAIDs, which prompted us to analyze the induction of ICD by NSAIDs. Results from several *in vitro* ICD assays supported a functional role of ER stress-induced immunomodulation in NSAID-mediated chemoprevention.

In addition, we found that NSAID treatment affected other proteins involved in the immune response such as CD47 [10]. Loss of *APC* induced the upregulation of CD47, which was attenuated in response to NSAID treatment. Furthermore, data from The Cancer Genome Atlas (TCGA) indicated that CD47 is upregulated in colorectal tumors. However, further work needs to be done to fully delineate this pathway in CRC chemoprevention.

Overall, the mechanism of NSAID-induced chemoprevention proposed in this study is summarized below (Fig. 42).

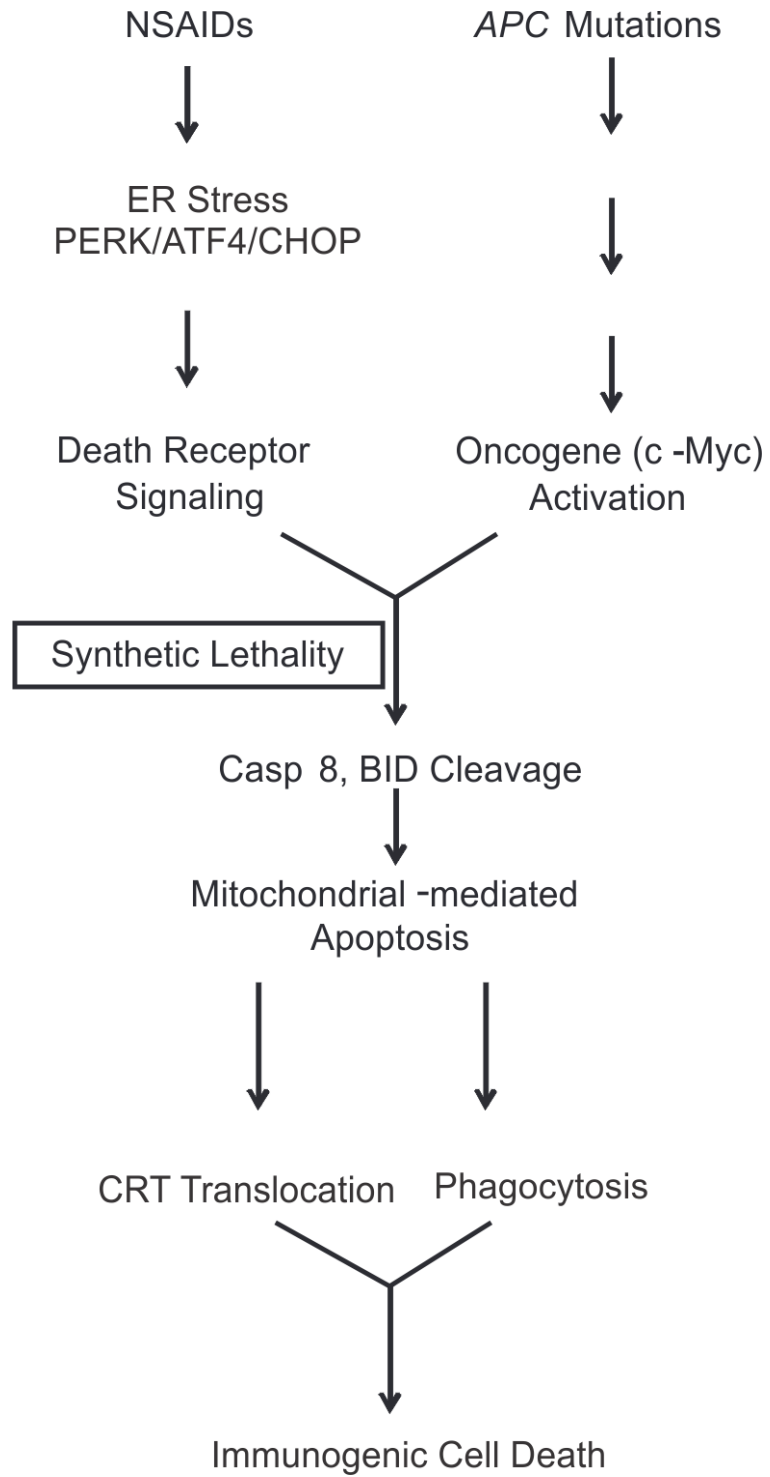


**Figure 42. The Proposed Mechanism of NSAID-Induced Death Seen Upon the Loss of APC in Normal Epithelial Cells.**

## 5.2 FUTURE DIRECTIONS

Based on the data presented, there are several directions that could be further explored. First, the molecular mechanisms upstream and downstream of ER stress need to be further investigated. COX enzymes are well-known targets of NSAIDs in CRC chemoprevention[17]. However, there is still ambiguity on the role of COX inhibition due to observed COX-independent effects of NSAIDs [17].

In collaboration with Dr. Nathan Yates, we used mass spectrometry and the cellular thermal shift assay (CETSA) to examine potential novel binding partners of NSAIDs [102]. Lysates of HCT 116 cells were analyzed by a label-free differential mass spectrometry target identification assay. A total of 11,516 peptides were quantified, corresponding to 1,667 unique proteins. Statistical analysis was used to provide a ranked list of protein candidates (as shown below) which can be further studied (Fig. 43).

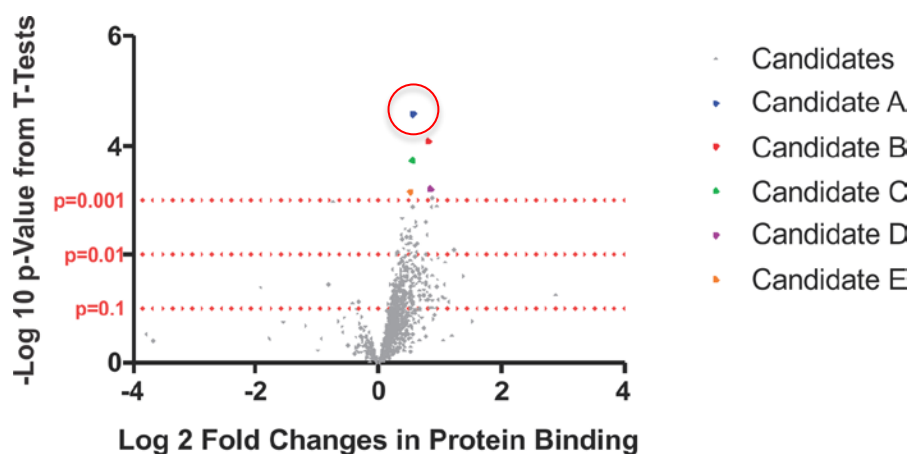


**Figure 43. Identification of Potential NSAID Binding Proteins Upstream of ER Stress by Mass Spectrometry.** Volcano plot showing the top 5 proteins ranked by p-values (t-test) that bind to sulindac sulfide in HCT 116 cell lysate. The red circle highlights the top candidate.

Candidates A and B had the strongest interactions based on the statistics. Our top candidate, A, is a cytosolic enzyme that plays an important role in metabolism [103]. This protein was shown to be upregulated in cancers, and its inhibition could promote apoptosis. Further work will be done to examine the direct impact of NSAIDs on this protein and the influence of inhibiting this enzyme on ER stress and cell death. Candidate B is involved in heme synthesis. However, the relevance of candidate B in our proposed model seems to be significantly less than candidate A.

Further insight is still needed for understanding the functional role of immune modulation. We carried out *in vitro* assays to characterize ICD. The exact mechanism of NSAID-induced ICD will be further examined by using *in vivo* models [84]. Experiments using vaccination models or immuno-deficient mice could be used. We have also conducted a blinded study with patient polyp samples in collaboration with Dr. Reetesh Pai and Dr. Robert Schoen to examine the influence of NSAIDs on TILs. Once the samples that were analyzed are decoded, the results may provide further support for our hypothesis. The number of samples used in this study was significantly greater than that used in our initial analysis. Moreover, we also identified a potential role of CD47 downregulation by NSAIDs. Additional experiments will be conducted to examine the role of this regulation. *APC* KO cells will be used to analyze changes in *CD47* mRNA, cell surface expression, and the binding of c-Myc to the *CD47* promoter upon NSAID treatment. *In vivo* experiments will involve the use of *CD47* KO mice or *CD47* antibodies.

A major obstacle in cancer chemoprevention is the toxicity associated with long-term and regular drug administration. While a handful of anticancer agents have been shown to be effective in CRC chemoprevention, many promising agents could not be applied to CRC

prevention due to their toxicity. On the other hand, immunoprevention, in particular vaccination, potentially offers a safer tumor prevention approach. However, various immune modulating agents have yet to demonstrate efficacy in human clinical studies. Combinations of different classes of anticancer agents represent a promising approach to overcome these limitations and achieve safer and more effective cancer prevention [10]. Initially, we would start with vaccines that have a known preventive effect on CRC, such as those for MUC 1 or CEA [10] and combine them with NSAIDs to see if there is an improved effect. Subsequently, experiments involving combinations of vaccines and even lower dosages of NSAIDs could be tested.

Chemo-immuno based strategies with blocking antibodies are also worth investigating. The recent success of checkpoint inhibition for cancer immunotherapy has generated tremendous enthusiasm for cancer prevention by directly targeting the immune system using immune modulating agents. The information on the efficacy and toxicity profiles of anti-PD-1, anti-PD-L1, and anti-CTLA-4 antibodies is being rapidly accumulated from various clinical studies. It may be possible to utilize these antibodies for CRC immunoprevention in high-risk populations such as those with microsatellite instability (MSI) or Lynch syndrome. The recent findings that PD-1 and CTLA-4 are upregulated to a greater extent in MSI CRCs suggest that these high-risk individuals would benefit from immune checkpoint inhibition [104]. For the purpose of immunoprevention, it is particularly important to define the biomarkers of effectiveness and properly manage potential toxicities. It is anticipated that the ongoing preclinical and clinical studies will soon reveal whether it is feasible to use the immune checkpoint blocking antibodies for cancer immunoprevention.

With many tasks ahead, now is the best time for cancer biologists and immunologists to work together to harness the human immune system to effectively prevent the development of CRCs.

## APPENDIX A

**Table 2. Primers Used in RT-PCR**

Human Primers	Sequence
<i>DR5</i> Forward	5'-AAGACCCTTGTGCTCGTTGT-3'
<i>DR5</i> Reverse	5'AGGTGGACACAATCCCTCTG-3'
<i>CHOP</i> Forward	5'-GGTCCTGTCTTCAGATGAAAATG-3'
<i>CHOP</i> Reverse	5'-CAGCCAAGCCAGAGAAGCA-3'
<i>BiP</i> Forward	5'-CCAAGAGAGGGTTCTTGAATCTCG-3'
<i>BiP</i> Reverse	5'-ATGGGCCAGCCTGGATATACAACA-3'
<i>APC</i> Forward	5'-GGAAGCAGAGAAAGTACTGGA-3'
<i>APC</i> Reverse	5'-CTGAAGTTGAGCGTAATACCA-3'
<i>ATF4</i> Forward	5'-GTTCTCCAGCGACAAGGCTA-3
<i>ATF4</i> Reverse	5'-GTGTCATCCAACGTGGTCAG-3
<i><math>\beta</math>-Actin</i> Forward	5'-GACATTAAGGAGAAGCTGTGCTATGTT-3'
<i><math>\beta</math>-Actin</i> Reverse	5'-GCCTAGAAGCATTGCGGTGGACGA-3'

**Table 3. siRNAs Used in Study**

siRNA	Sequence/Catalogue number	Vendor
<i>APC-157</i>	5'GGAAGUAUUGAAGAUGAAG	Dharmacon
<i>APC-8993</i>	5'GCUGUGAAAUUCACAGUAAUA	Dharmacon
<i>CHOP</i>	5'GCACAGCUAGCUGAAGAGA	Dharmacon
<i>ATF4-89</i>	5'GCCUAGGU UCUUAGAUGA	Dharmacon
<i>ATF3</i>	sc-29757	Santa Cruz
<i>PERK</i>	sc-36213	Santa Cruz

## APPENDIX B

In terms of other related work, we were able to successfully establish Patient Derived Xenograft (PDX) models in the lab for future use by other lab members.

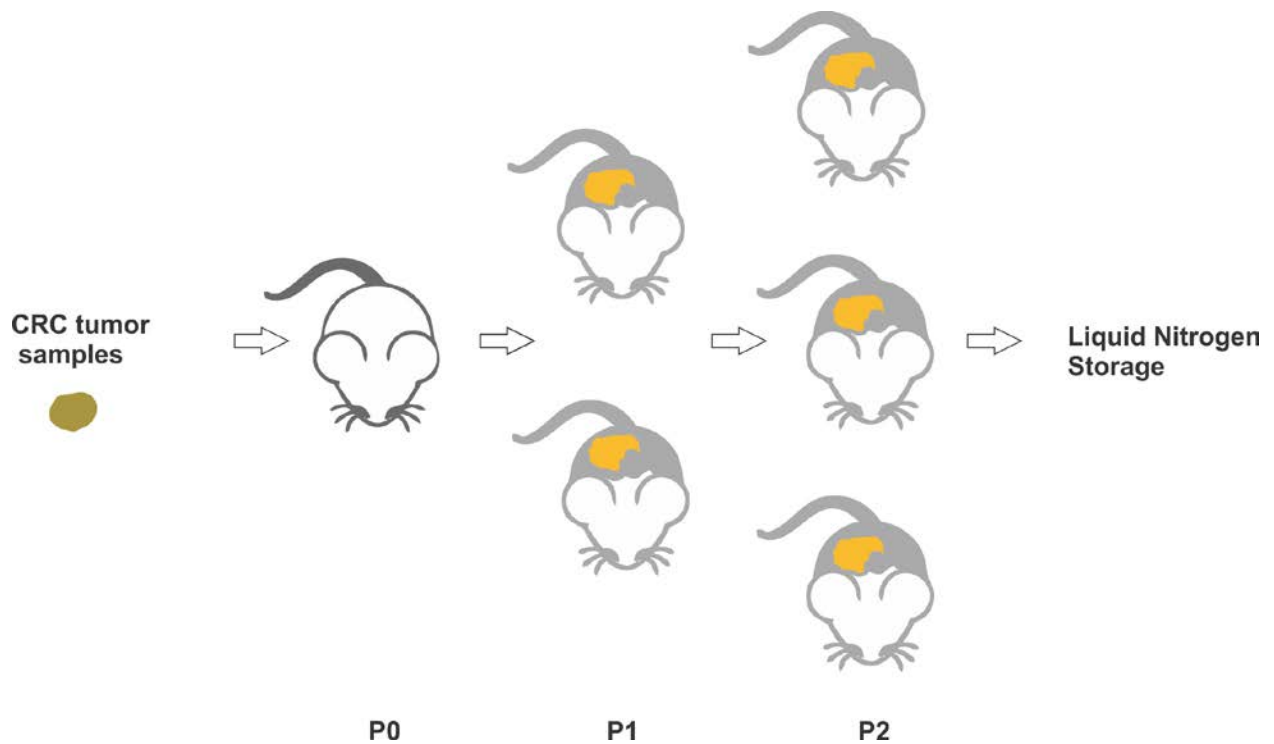


**Figure 44. Establishment of PDX Models with NOD SCID Mice.** P: Passage. This figure is modified from the original artwork by Jackson Laboratory [105].

**Table 4. Log of Lab's Initial PDX Samples**

Date Collected	Passage	Viable tumors in freezing media	Snap frozen	ID
3/9/2016	0	0	10	TP15-S268 36
5/2/2016	1	22	6	TP15-S268 36
5/2/2016	0	5	3	TP16-P28
6/18/2016	1	24	8	TP16-P28
7/12/2016	2	12	6	TP15-S268 36
7/12/2016	0	1	2	TP16-P12
8/10/2016	2	25	6	TP16-P28
8/16/2016	0	6	3	TP16-S47
10/12/2016	1	15	5	TP16-P12

## APPENDIX C

### PERMISSIONS

License Number	4312011237754
License date	Mar 18, 2018
Licensed Content Publisher	Elsevier
Licensed Content Publication	Trends in Cancer
Licensed Content Title	The Unfolded Protein Response in Immunogenic Cell Death and Cancer Immunotherapy
Licensed Content Author	Nicole Rufo,Abhishek D. Garg,Patrizia Agostinis
Licensed Content Date	Sep 1, 2017
Licensed Content Volume	3
Licensed Content Issue	9
Licensed Content Pages	16
Type of Use	reuse in a thesis/dissertation
Portion	figures/tables/illustrations
Number of figures/tables/illustrations	1
Format	electronic
Are you the author of this Elsevier article?	No
Will you be translating?	No
Original figure numbers	Figure 1
Title of your thesis/dissertation	The role of NSAID-induced ER stress and immunomodulation in the suppression of colorectal tumorigenesis
Expected completion date	Apr 2018

**Copyright:** © 2017 Corazzari, Gagliardi, Fimia and Piacentini. This is an open-access article distributed under the terms of the **Creative Commons Attribution License (CC BY)**. The use, distribution or reproduction in other forums is permitted, provided the original author(s) or licensor are credited and that the original publication in this journal is cited, in accordance with accepted academic practice. No use, distribution or reproduction is permitted which does not comply with these terms.



**Title:** Colorectal cancer prevention:  
Immune modulation taking the  
stage

**Author:** Rochelle Fletcher, Yi-Jun  
Wang, Robert E. Schoen, Olivera  
J. Finn, Jian Yu, Lin Zhang

**Publication:** Biochimica et Biophysica Acta  
(BBA) - Reviews on Cancer

**Publisher:** Elsevier

**Date:** Available online 31 January  
2018

LOGIN

If you're a **copyright.com**  
user, you can login to  
RightsLink using your  
copyright.com credentials.  
Already a **RightsLink** user or  
want to [learn more?](#)

© 2018 Elsevier B.V. All rights reserved.

Please note that, as the author of this Elsevier article, you retain the right to include it in a thesis or dissertation, provided it is not published commercially. Permission is not required, but please ensure that you reference the journal as the original source. For more information on this and on your other retained rights, please visit: <https://www.elsevier.com/about/our-business/policies/copyright#Author-rights>

## BIBLIOGRAPHY

1. Siegel, R.L., K.D. Miller, and A. Jemal, *Cancer Statistics, 2017*. CA Cancer J Clin, 2017. **67**(1): p. 7-30.
2. Siegel, R.L., et al., *Colorectal Cancer Incidence Patterns in the United States, 1974-2013*. J Natl Cancer Inst, 2017. **109**(8).
3. Siegel, R.L., K.D. Miller, and A. Jemal, *Colorectal Cancer Mortality Rates in Adults Aged 20 to 54 Years in the United States, 1970-2014*. JAMA, 2017. **318**(6): p. 572-574.
4. Gopal, S., *Moonshot to Malawi*. N Engl J Med, 2016. **374**(17): p. 1604-5.
5. Smith, R.A., et al., *Cancer screening in the United States, 2016: A review of current American Cancer Society guidelines and current issues in cancer screening*. CA Cancer J Clin, 2016. **66**(2): p. 96-114.
6. Vogelstein, B. and K.W. Kinzler, *The genetic basis of human cancer*. 2002, New York: McGraw-Hill Health Professions Division.
7. Vogelstein, B. and K.W. Kinzler, *Cancer genes and the pathways they control*. Nat Med, 2004. **10**(8): p. 789-99.
8. Kinzler, K.W. and B. Vogelstein, *Lessons from Hereditary Colon Cancer*. Cell, 1996. **87**(2): p. 159-170.

9. Wojtowicz, M.E., B.K. Dunn, and A. Umar, *Immunologic approaches to cancer prevention-current status, challenges, and future perspectives*. *Semin Oncol*, 2016. **43**(1): p. 161-72.
10. Fletcher, R., et al., *Colorectal cancer prevention: Immune modulation taking the stage*. *Biochim Biophys Acta*, 2018.
11. Bosetti, C., et al., *Aspirin and cancer risk: a quantitative review to 2011*. *Ann Oncol*, 2012. **23**(6): p. 1403-15.
12. Rao, C.V. and B.S. Reddy, *NSAIDs and chemoprevention*. *Curr Cancer Drug Targets*, 2004. **4**(1): p. 29-42.
13. Ricciardiello, L., D.J. Ahnen, and P.M. Lynch, *Chemoprevention of hereditary colon cancers: time for new strategies*. *Nat Rev Gastroenterol Hepatol*, 2016. **13**(6): p. 352-61.
14. Cooper, K., et al., *Chemoprevention of colorectal cancer: systematic review and economic evaluation*. *Health Technol Assess*, 2010. **14**(32): p. 1-206.
15. Drew, D.A., Y. Cao, and A.T. Chan, *Aspirin and colorectal cancer: the promise of precision chemoprevention*. *Nat Rev Cancer*, 2016. **16**(3): p. 173-86.
16. Keller, J.J. and F.M. Giardiello, *Chemoprevention strategies using NSAIDs and COX-2 inhibitors*. *Cancer Biol Ther*, 2003. **2**(4 Suppl 1): p. S140-9.
17. Gurpinar, E., W.E. Grizzle, and G.A. Piazza, *NSAIDs inhibit tumorigenesis, but how?* *Clin Cancer Res*, 2014. **20**(5): p. 1104-13.
18. Sun, S.Y., N. Hail, and R. Lotan, *Apoptosis as a Novel Target for Cancer Chemoprevention*. *JNCI Journal of the National Cancer Institute*, 2004. **96**(9): p. 662-672.

19. Fulda, S. and K.M. Debatin, *Extrinsic versus intrinsic apoptosis pathways in anticancer chemotherapy*. *Oncogene*, 2006. **25**(34): p. 4798-811.
20. Tait, S.W. and D.R. Green, *Mitochondria and cell signalling*. *J Cell Sci*, 2012. **125**(Pt 4): p. 807-15.
21. Leibowitz, B., et al., *BID mediates selective killing of APC-deficient cells in intestinal tumor suppression by nonsteroidal antiinflammatory drugs*. *PNAS*, 2014. **111**(46): p. 16520–16525
22. Shibata, Y., G.K. Voeltz, and T.A. Rapoport, *Rough sheets and smooth tubules*. *Cell*, 2006. **126**(3): p. 435-9.
23. Osowski, C.M. and F. Urano, *Measuring ER stress and the unfolded protein response using mammalian tissue culture system*. *Methods Enzymol*, 2011. **490**: p. 71-92.
24. Wang, M. and R.J. Kaufman, *The impact of the endoplasmic reticulum protein-folding environment on cancer development*. *Nat Rev Cancer*, 2014. **14**(9): p. 581-97.
25. Corazzari, M., et al., *Endoplasmic Reticulum Stress, Unfolded Protein Response, and Cancer Cell Fate*. *Front Oncol*, 2017. **7**: p. 78.
26. Verfaillie, T., A.D. Garg, and P. Agostinis, *Targeting ER stress induced apoptosis and inflammation in cancer*. *Cancer Lett*, 2013. **332**(2): p. 249-64.
27. Mügge, F.L.B. and A.M. Silva, *Endoplasmic reticulum stress response in the roadway for the effects of non-steroidal anti-inflammatory drugs*. *Endoplasmic Reticulum Stress in Diseases*, 2015. **2**(1).
28. Tsutsumi, S., et al., *Endoplasmic reticulum stress response is involved in nonsteroidal anti-inflammatory drug-induced apoptosis*. *Cell Death Differ*, 2004. **11**(9): p. 1009-16.

29. Rufo, N., A.D. Garg, and P. Agostinis, *The Unfolded Protein Response in Immunogenic Cell Death and Cancer Immunotherapy*. Trends Cancer, 2017. **3**(9): p. 643-658.
30. Keller, J., G. Offerhaus, and M.e.a. Polak, *Rectal epithelial apoptosis in familial adenomatous polyposis patients treated with sulindac*. Gut, 1999. **45**.
31. Mahmoud NN, B.S., Bilinski RT, Martucci C, Chadburn A, Bertagnolli MM, *Apc gene mutation is associated with a dominant-negative effect upon intestinal cell migration*. Cancer research, 1997. **57**.
32. Brown WA, S.S., Malcontenti-Wilson C, Vogliagis D, O'Brien PE. , *Nonsteroidal anti-inflammatory drugs with activity against either cyclooxygenase 1 or cyclooxygenase 2 inhibit colorectal cancer in a DMH rodent model by inducing apoptosis and inhibiting cell proliferation*. Gut, 2001. **48**.
33. Qiu, W., X. Wang, and B.e.a. Leibowitz, *Chemoprevention by nonsteroidal anti-inflammatory drugs eliminates oncogenic intestinal stem cells via SMAC-dependent apoptosis*. PNAS, 2010. **107**(46).
34. Kohli, M., et al., *SMAC/Diablo-dependent apoptosis induced by nonsteroidal antiinflammatory drugs (NSAIDs) in colon cancer cells*. Proc Natl Acad Sci U S A, 2004. **101**(48): p. 16897-902.
35. Wang, P., J. Yu, and L. Zhang, *The nuclear function of p53 is required for PUMA-mediated apoptosis induced by DNA damage*. Proc Natl Acad Sci U S A, 2007. **104**(10): p. 4054-9.
36. Brown, M.F., et al., *Loss of Caspase-3 sensitizes colon cancer cells to genotoxic stress via RIP1-dependent necrosis*. Cell Death Dis, 2015. **6**: p. e1729.

37. Zlotorynski, E., *Apoptosis. DR5 unfolds ER stress*. Nat Rev Mol Cell Biol, 2014. **15**(8): p. 498-9.
38. Heller, D., Fan, T., et al. *In Vitro Cyclooxygenase-2 Protein Expression and Enzymatic Activity in Neoplastic Cells*. J Vet Intern Med, 2007. **21**: p. 1048-1055.
39. Yamaguchi, H. and H.G. Wang, *CHOP is involved in endoplasmic reticulum stress-induced apoptosis by enhancing DR5 expression in human carcinoma cells*. J Biol Chem, 2004. **279**(44): p. 45495-502.
40. Tabas, I. and D. Ron, *Integrating the mechanisms of apoptosis induced by endoplasmic reticulum stress*. Nat Cell Biol, 2011. **13**(3): p. 184-90.
41. Lu, M., et al., *Opposing unfolded-protein-response signals converge on death receptor 5 to control apoptosis*. Science, 2014. **345**(6192).
42. Sun, S.Y., *Chemopreventive agent-induced modulation of death receptors*. Apoptosis, 2005. **10**(6): p. 1203-10.
43. Edagawa, M., et al., *Role of activating transcription factor 3 (ATF3) in endoplasmic reticulum (ER) stress-induced sensitization of p53-deficient human colon cancer cells to tumor necrosis factor (TNF)-related apoptosis-inducing ligand (TRAIL)-mediated apoptosis through up-regulation of death receptor 5 (DR5) by zerumbone and celecoxib*. J Biol Chem, 2014. **289**(31): p. 21544-61.
44. Moyer, M., et al., *Development and Characterization of Normal Colonic Epithelial Cell Lines Derived from Normal Mucosa of Patients with Colon Cancer*. The American Journal of Surgery 1995. **169**.
45. Ran, F.A., et al., *Genome engineering using the CRISPR-Cas9 system*. Nat Protoc, 2013. **8**(11): p. 2281-2308.

46. Yin, X.M., et al., *Bid-deficient mice are resistant to Fas-induced hepatocellular apoptosis*. Nature, 1999. **400**(6747): p. 886-91.
47. Boyce, M., et al., *A Selective Inhibitor of eIF2a Dephosphorylation Protects Cells from ER Stress*. Science, 2005. **307**.
48. Zhang, L., et al., *Chemoprevention of colorectal cancer by targeting APC-deficient cells for apoptosis*. Nature, 2010. **464**(7291): p. 1058-61.
49. Ahmed, D., et al., *Epigenetic and genetic features of 24 colon cancer cell lines*. Oncogenesis, 2013. **2**: p. e71.
50. Roper, J. and K.E. Hung, *Priceless GEMMs: genetically engineered mouse models for colorectal cancer drug development*. Trends Pharmacol Sci, 2012. **33**(8): p. 449-55.
51. Datta, S., et al., *cEBP Homologous Protein Expression in Macrophages Regulates the Magnitude and Duration of IL-6 Expression and Dextran Sodium Sulfate Colitis*. J Interferon Cytokine Res, 2015. **35**(10): p. 785-94.
52. Kensler, T.W., et al., *Transforming Cancer Prevention through Precision Medicine and Immune-oncology*. Cancer Prev Res (Phila), 2016. **9**(1): p. 2-10.
53. Finn, O.J. and P.L. Beatty, *Cancer immunoprevention*. Curr Opin Immunol, 2016. **39**: p. 52-8.
54. Marzbani, E., et al., *The invisible arm of immunity in common cancer chemoprevention agents*. Cancer Prev Res (Phila), 2013. **6**(8): p. 764-73.
55. Umar, A., *Cancer immunoprevention: a new approach to intercept cancer early*. Cancer Prev Res (Phila), 2014. **7**(11): p. 1067-71.

56. Schreiber, R.D., L.J. Old, and M.J. Smyth, *Cancer immunoediting: integrating immunity's roles in cancer suppression and promotion*. Science, 2011. **331**(6024): p. 1565-70.
57. Finn, O.J., *Cancer immunology*. N Engl J Med, 2008. **358**(25): p. 2704-15.
58. Ferrone, C. and G. Dranoff, *Dual roles for immunity in gastrointestinal cancers*. J Clin Oncol, 2010. **28**(26): p. 4045-51.
59. Dunn, G.P., et al., *Cancer immunoediting: from immunosurveillance to tumor escape*. Nat Immunol, 2002. **3**(11): p. 991-8.
60. Roeser, J.C., S.D. Leach, and F. McAllister, *Emerging strategies for cancer immunoprevention*. Oncogene, 2015. **34**(50): p. 6029-39.
61. Cao, Y., et al., *Regular Aspirin Use Associates With Lower Risk of Colorectal Cancers With Low Numbers of Tumor-Infiltrating Lymphocytes*. Gastroenterology, 2016. **151**(5): p. 879-892 e4.
62. Hamada, T., et al., *Aspirin Use and Colorectal Cancer Survival According to Tumor CD274 (Programmed Cell Death 1 Ligand 1) Expression Status*. J Clin Oncol, 2017. **35**(16): p. 1836-1844.
63. Bondurant, K.L., et al., *Interleukin genes and associations with colon and rectal cancer risk and overall survival*. Int J Cancer, 2013. **132**(4): p. 905-15.
64. Slattery, M.L., et al., *JAK/STAT/SOCS-signaling pathway and colon and rectal cancer*. Mol Carcinog, 2013. **52**(2): p. 155-66.
65. Slattery, M.L., et al., *Interferon-signaling pathway: associations with colon and rectal cancer risk and subsequent survival*. Carcinogenesis, 2011. **32**(11): p. 1660-7.

66. Lonnroth, C., et al., *Preoperative treatment with a non-steroidal anti-inflammatory drug (NSAID) increases tumor tissue infiltration of seemingly activated immune cells in colorectal cancer*. *Cancer Immun*, 2008. **8**: p. 5.
67. Wang, D. and R.N. DuBois, *The Role of Prostaglandin E(2) in Tumor-Associated Immunosuppression*. *Trends Mol Med*, 2016. **22**(1): p. 1-3.
68. Arvind, P., et al., *Aspirin and aspirin-like drugs induce HLA-DR expression in HT29 colon cancer cells*. *Int J Oncol*, 1996. **8**(6): p. 1207-11.
69. Bergman, M., et al., *Inflammation and colorectal cancer: does aspirin affect the interaction between cancer and immune cells?* *Inflammation*, 2011. **34**(1): p. 22-8.
70. Yin, T., et al., *Sulindac, a non-steroidal anti-inflammatory drug, mediates breast cancer inhibition as an immune modulator*. *Sci Rep*, 2016. **6**: p. 19534.
71. Prima, V., et al., *COX2/mPGES1/PGE2 pathway regulates PD-L1 expression in tumor-associated macrophages and myeloid-derived suppressor cells*. *Proc Natl Acad Sci U S A*, 2017. **114**(5): p. 1117-1122.
72. Xu, P., et al., *Long-term use of indomethacin leads to poor prognoses through promoting the expression of PD-1 and PD-L2 via TRIF/NF-kappaB pathway and JAK/STAT3 pathway to inhibit TNF-alpha and IFN-gamma in hepatocellular carcinoma*. *Exp Cell Res*, 2015. **337**(1): p. 53-60.
73. Nakanishi, Y., et al., *COX-2 inhibition alters the phenotype of tumor-associated macrophages from M2 to M1 in ApcMin/+ mouse polyps*. *Carcinogenesis*, 2011. **32**(9): p. 1333-9.
74. Kalinski, P., *Regulation of immune responses by prostaglandin E2*. *J Immunol*, 2012. **188**(1): p. 21-8.

75. Fujita, M., et al., *COX-2 blockade suppresses gliomagenesis by inhibiting myeloid-derived suppressor cells*. *Cancer Res*, 2011. **71**(7): p. 2664-74.
76. Dudek, A.M., et al., *Inducers of immunogenic cancer cell death*. *Cytokine Growth Factor Rev*, 2013. **24**(4): p. 319-33.
77. Nagata, S. and M. Tanaka, *Programmed cell death and the immune system*. *Nat Rev Immunol*, 2017.
78. Green, D.R., et al., *Immunogenic and tolerogenic cell death*. *Nat Rev Immunol*, 2009. **9**(5): p. 353-63.
79. Casares, N., et al., *Caspase-dependent immunogenicity of doxorubicin-induced tumor cell death*. *J Exp Med*, 2005. **202**(12): p. 1691-701.
80. Panaretakis, T.e.a., *Mechansims of pre-apoptotic calreticulin exposure in immunogenic cell death*. *The EMBO Journal*, 2008. **28**.
81. Gregory, C., *Apoptosis in Cancer Pathogenesis and Anti-Cancer Therapy*. *Advances in Experimental Medicine and Biology*, 2016.
82. Garg, A.D., et al., *Immunogenic cell death, DAMPs and anticancer therapeutics: an emerging amalgamation*. *Biochim Biophys Acta*, 2010. **1805**(1): p. 53-71.
83. Kepp, O., et al., *Crosstalk between ER stress and immunogenic cell death*. *Cytokine Growth Factor Rev*, 2013. **24**(4): p. 311-8.
84. Kepp, O., et al., *Consensus guidelines for the detection of immunogenic cell death*. *Oncoimmunology*, 2014. **3**(9): p. e955691.
85. Oh, D.e.a., *On the Verge: Immunotherapy for Colorectal Carcinoma*. *Journal of the National Comprehensive Cancer Network*, 2015. **13**(8).
86. Garg, A.D., et al., *Immunogenic cell death*. *Int J Dev Biol*, 2015. **59**(1-3): p. 131-40.

87. Van Vliet, A.R., A.D. Garg, and P. Agostinis, *Coordination of stress, Ca<sup>2+</sup>, and immunogenic signaling pathways by PERK at the endoplasmic reticulum*. Biol Chem, 2016. **397**(7): p. 649-56.
88. Kepp, O.e.a., *Restoration of the immunogenicity of cisplatin-induced cancer cell death by endoplasmic reticulum stress*. Oncogene, 2011. **30**: p. 1147-1158.
89. Kepp, O., et al., *eIF2alpha phosphorylation as a biomarker of immunogenic cell death*. Semin Cancer Biol, 2015. **33**: p. 86-92.
90. Kroemer, G., et al., *Natural and therapy-induced immunosurveillance in breast cancer*. Nat Med, 2015. **21**(10): p. 1128-38.
91. Garg, A.D., et al., *A novel pathway combining calreticulin exposure and ATP secretion in immunogenic cancer cell death*. EMBO J, 2012. **31**(5): p. 1062-79.
92. Obeid, M., et al., *Calreticulin exposure dictates the immunogenicity of cancer cell death*. Nat Med, 2007. **13**(1): p. 54-61.
93. Wang, W.A., J. Groenendyk, and M. Michalak, *Calreticulin signaling in health and disease*. Int J Biochem Cell Biol, 2012. **44**(6): p. 842-6.
94. Tesniere, A., et al., *Immunogenic death of colon cancer cells treated with oxaliplatin*. Oncogene, 2010. **29**(4): p. 482-91.
95. Lopez-Albaitero, A., et al., *Maturation pathways of dendritic cells determine TAP1 and TAP2 levels and cross-presenting function*. J Immunother, 2009. **32**(5): p. 465-73.
96. Pozzi, C., et al., *The EGFR-specific antibody cetuximab combined with chemotherapy triggers immunogenic cell death*. Nat Med, 2016. **22**(6): p. 624-31.

97. Kim, J., et al., *Activation of the PERK-eIF2 $\alpha$  Pathway Is Associated with Tumor-infiltrating Lymphocytes in HER2-Positive Breast Cancer*. *Anticancer Research*, 2016. **36**: p. 2705-2712.
98. Dang, C.V., *MYC on the path to cancer*. *Cell*, 2012. **149**(1): p. 22-35.
99. Casey, S.C., et al., *MYC regulates the antitumor immune response through CD47 and PD-L1*. *Science*, 2016. **352**(6282): p. 227-31.
100. Tanner, S.M., et al., *Altered T-Cell Balance in Lymphoid Organs of a Mouse Model of Colorectal Cancer*. *J Histochem Cytochem*, 2016. **64**(12): p. 753-767.
101. Doerks, T., et al., *Systematic identification of novel protein domain families associated with nuclear functions*. *Genome Res*, 2002. **12**(1): p. 47-56.
102. Mateus, A., T.A. Maatta, and M.M. Savitski, *Thermal proteome profiling: unbiased assessment of protein state through heat-induced stability changes*. *Proteome Sci*, 2016. **15**: p. 13.
103. Zaidi, N., J.V. Swinnen, and K. Smans, *ATP-citrate lyase: a key player in cancer metabolism*. *Cancer Res*, 2012. **72**(15): p. 3709-14.
104. Llosa, N.J., et al., *The vigorous immune microenvironment of microsatellite instable colon cancer is balanced by multiple counter-inhibitory checkpoints*. *Cancer Discov*, 2015. **5**(1): p. 43-51.
105. Yeadon, J., *The Next 'Big Thing' In Cancer Modeling: Patient-Derived Xenografts In Humanized Nsg Mice*. 2016: Jackson Labs.